



TAMPEREEN TEKNILLINEN YLIOPISTO
TAMPERE UNIVERSITY OF TECHNOLOGY

Jani Valtari

**Centralized Architecture of the Electricity Distribution
Substation Automation - Benefits and Possibilities**



Julkaisu 1122 • Publication 1122

Tampere 2013

Tampereen teknillinen yliopisto. Julkaisu 1122
Tampere University of Technology. Publication 1122

Jani Valtari

Centralized Architecture of the Electricity Distribution Substation Automation - Benefits and Possibilities

Thesis for the degree of Doctor of Science in Technology to be presented with due permission for public examination and criticism in Sähköotalo Building, Auditorium S4, at Tampere University of Technology, on the 5th of April 2013, at 12 noon.

Tampereen teknillinen yliopisto - Tampere University of Technology
Tampere 2013

ISBN 978-952-15-3044-9 (printed)
ISBN 978-952-15-3061-6 (PDF)
ISSN 1459-2045

Abstract

Smart grid initiatives around the world show how much the control and protection of distribution networks is expected to change within the next few years. As passive networks with unidirectional power flow evolve into active networks with a variety of different active resources, the requirements for distribution substations will also change, requiring the utilities to take action. Utilities do not want to undertake continuous and costly upgrades of the whole protection system, but there is still a clear need for adapting to new requirements. The need to increase the level of automation in the distribution system has been clearly recognized both on the vendor side and on the utility side.

Various concept-level proposals have been presented in order to address the conflicting requirements for low life-cycle costs and the rapid uptake of new technology. The most traditional approach has been to increase the functionality of the bay-level protection and control IEDs (Intelligent Electronic Devices). This approach has been sufficient, while CPU capacity has been steadily increasing and the price of new technology has remained at a reasonable level. The issue in this approach has been the extensive costs of upgrades. New features have also required substantial changes in the substation's entire secondary system, requiring long maintenance breaks.

This PhD thesis investigates how station-level data processing can be utilized to help in creating a future-proof architecture for the secondary system of a distribution substation. The needed technology is evaluated, and an overall life-cycle cost analysis is performed showing the cost benefit of a centralized architecture. The thesis shows that the larger the substation, the greater the benefits of a centralized architecture. It also shows how great is the impact of increased reliability. The outage costs of a network exceed all the other life-cycle costs of the secondary system, and illustrates how focusing on substation automation is a cost-efficient way to improve the reliability of the network.

The new architecture enables the re-allocation of substation functionality, as both bay-level and station-level data processing is available. This aspect is researched in the thesis, and a clustering method based on fuzzy c-means clustering is proposed for this re-allocation. When the function requires communication, but does not have strict requirements for response times, station-level implementation can be justified. Complex functionality requiring additional CPU performance and anticipated updates in the near future are clear indications of station-level functionality.

In addition to re-organizing the existing functionality, the new architecture also enables the utilization of new features which were not feasible previously. A new measurement method is proposed which emphasizes this aspect by increasing the overall sampling frequency of the substation measurements without increasing the sampling frequency of the individual IEDs. The method is based on Time-Interleaved technology, where the sampling of all the IEDs in the substation is synchronized. However, this synchronization is done in such a way that each IED does not take the measurement at exactly the same time stamp. This is achieved by time-shifting the sampling in the IEDs by a fraction of the sample time. Merging these measurements at the station level creates a single sample stream with a high sampling frequency.

The usefulness of the architecture and the new measurement method is tested with a transient-based fault location method. In earlier studies, transient-based methods have not been used in bay-level IEDs because of the strict requirements for the sampling frequency. However, using the measurement method presented in this thesis, transient-based algorithms can also be used without increasing the sampling frequency of individual IEDs.

Foreword

This doctoral thesis was written for ABB Oy Medium Voltage Products, and finalized within the Smart Grids and Energy Markets (SGEM) research program coordinated by CLEEN Oy, and received funding from the Finnish Funding Agency for Technology and Innovation, Tekes. The research was supervised by Prof. Pekka Verho from Tampere University of Technology, whom I wish to thank for his experienced guidance and excellent advice along my journey. I also wish to thank the pre-examiners of this thesis, Prof. Jero Ahola from Lappeenranta University of Technology and Prof. Vladimir Terzija from The University of Manchester, whose valuable comments improved the quality of this thesis significantly. An important person in this process was also Mr. Adrian Benfield, who did the proofreading, thank you for correcting my English.

I want to thank my line managers, Petri Hovila and Tomas Karlais from ABB Oy and Jatta Jussila-Suokas from CLEEN Oy for supporting and encouraging me and for taking a lot of extra trouble to allow me to write my thesis. Special thanks go to Tapio Hakola, Antti Hakala-Ranta and Dick Kronman from ABB Oy and Prof. Pertti Järventausta from Tampere University of Technology for their valuable professional insights and inspiration - people like you, with long experience yet an enthusiastic focus on the future have encouraged me greatly. I am also grateful to Erkka Kettunen for sharing my interest in this topic and for his valuable contribution in the area of software development. However, the largest debt of gratitude I owe is to my parents and close relatives for all the support I have received during these years, without whom, none of this would have been possible.

Writing this foreword reminds me of the master's thesis I wrote over eight years ago (is it really that long). I remember how easy that was in comparison to this work - merely something to do on the side. The process with this doctoral thesis has been much more challenging - periods of self-doubt and trouble in seeing the big picture

took time to overcome - and I could not have done it without the support of my close friends. Thank you all for that. I particularly want to thank my housemates in The Yellow House in Pispala: Anniina, Johanna, Mintta, Olli, Rene, Tanja and Tuula. The warm atmosphere you created in our home gave me the energy to finalize my thesis. I have recently reread the foreword from my M.Sc. thesis eight years back, and I have noticed that the advice I wrote then, (I do not know if I wrote it then for others or for myself), it is still valid: remember to keep the little child alive ;-)

Contents

Abstract	i
Foreword	iii
List of Figures	xi
Nomenclature	xiii
1 Introduction	1
1.1 The hypothesis and objectives of the thesis	3
1.2 Background of the thesis	4
1.3 Outline of the thesis	5
1.4 The role of the author	6
2 Station Architecture	8
2.1 Background	8
2.1.1 An electricity network	8
2.1.2 The secondary system of the network	11
2.1.3 Network management processes	13
2.2 New drivers and market trends for energy distribution	15
2.2.1 The global situation and climate change	15
2.2.2 The market situation and foreseeable business trends	16
2.3 New requirements for distribution substations	18
2.3.1 Advanced fault management	18
2.3.2 Efficient operation of the network and support for asset management	19
2.3.3 Future-proof technologies, upgradeability	21

2.3.4	Low life-cycle costs	23
2.4	The possible architectures	24
2.4.1	Definition of a substation	24
2.4.2	A proposed architecture and a comparison with other solutions	25
2.4.3	IEC 61850 standard	27
2.5	The cost-efficiency of the possible architectures	31
2.5.1	Life-cycle costing in different scenarios	32
2.5.2	Acquisition costs	33
2.5.3	Acquisition and renewal costs	34
2.5.4	Acquisition, renewal and maintenance costs	36
2.5.5	Failure costs	37
2.5.6	Summary of LCC cost estimates	44
2.5.7	Other benefits of the combined set-up	45
2.6	Details of the proposed architecture	46
2.6.1	Important standards	46
2.6.2	Protection and control IEDs	48
2.6.3	Station computer	48
2.7	Pilot installation of the selected architecture in Noormarkku	50
2.8	Chapter summary	51
3	Station Measurements	53
3.1	Measurement replacement	53
3.2	Measurement merging	54
3.2.1	Introduction	54
3.2.2	Time-Interleaved ADC (TI-ADC)	55
3.3	Increasing sampling frequency at the substation level	56
3.3.1	General concept	56
3.3.2	Voltage measurements	57
3.3.3	Current measurements	57
3.4	Limitations and error analysis	58
3.4.1	TI-ADC model	60
3.4.2	Derivation of the explicit SINAD	62
3.4.3	Derivation of the expected SINAD	62
3.4.4	SINAD values for the substation	64
3.4.5	Time synchronization requirements	68

3.4.6	Special considerations related to TI-ADC	70
3.5	Other existing solutions for increasing the sampling frequency . . .	70
3.6	Chapter Summary	71
4	Station Applications	72
4.1	Functionality in the secondary system of a distribution substation . .	72
4.2	Functionality division	74
4.3	Functionality division criteria	76
4.3.1	Communication requirements	76
4.3.2	Response time	77
4.3.3	Utilization frequency	77
4.3.4	Function immaturity	78
4.4	Functionality division method	78
4.5	Description of the results	83
4.5.1	Unit-level mandatory functions	83
4.5.2	Unit-level optional functions	84
4.5.3	Station-level mandatory functions	84
4.5.4	Station-level optional functions	85
4.6	Chapter summary	86
5	Station Application Example	88
5.1	Earth fault in the distribution network	89
5.1.1	Grounded network	89
5.1.2	Isolated network	90
5.1.3	Compensated network	93
5.1.4	Initial transients	96
5.1.5	Measured fault resistances during earth faults	99
5.2	Earth fault location methods	101
5.2.1	Earth fault location methods based on initial transients . . .	102
5.2.2	Other algorithms for earth fault location	104
5.3	Test results for the impact of sampling frequency on transient-based earth fault location	105
5.3.1	Description of the algorithm	105
5.3.2	Analyzing the simulation results	110
5.4	Chapter summary	120

6 Summary	122
6.1 Contribution of the thesis	123
6.2 Evaluation of the thesis	124
6.3 Future research	125
References	126

List of Figures

1.1	Outline of the thesis.	6
2.1	Typical voltage levels in the electricity network in Finland.	9
2.2	Example topology of a double busbar substation.	10
2.3	Electromechanical, static and numerical relays.	13
2.4	Expected increase in energy consumption (Mtoe = million ton of oil equivalent) and in the share of zero-carbon fuels [IEA, 2009].	16
2.5	Targeted decrease in CO_2 emissions [IEA, 2009].	16
2.6	Present value of a 110 kV network [Jeromin et al., 2009]	21
2.7	Possible Architectures for Distribution Substation Automation.	25
2.8	Two main levels – IED Configurator and System Configurator. Updates possible via IID files[IEC, 2009].	28
2.9	Reference model for the information flow in the configuration process [IEC, 2009].	29
2.10	Modification process [IEC, 2009].	30
2.11	Acquisition costs for different scenarios.	35
2.12	Acquisition and renewal costs for different scenarios.	35
2.13	Acquisition, renewal and maintenance costs for different scenarios.	36
2.14	Total interruption costs.	40
2.15	An example reliability graph of protection	42
2.16	Cost saving with different scenarios.	42
2.17	Overall set-up of a centralized protection and control system.	47
2.18	Separate functionality for centralized protection and monitoring.	50
3.1	Time-Interleaved ADC with M channels [Vogel, 2005].	55
3.2	Timing diagram of time-interleaved ADC with M channels [Vogel, 2005].	56

3.3	Voltage measurements combined from 5 different measurements. . .	58
3.4	Current measurements combined from 5 different measurements. . .	59
3.5	Model of a one-channel ADC [Vogel, 2005].	61
3.6	The effect of gain error in SINAD.	65
3.7	The effect of offset error in SINAD.	66
3.8	The effect of timing error in SINAD.	66
3.9	The combined effect of gain and timing mismatches.	67
3.10	Contours of Figure 3.9.	67
3.11	Contours of Figure 3.9 in THD+N.	68
3.12	The effect on SINAD of increasing the number of ADCs.	69
4.1	Function re-allocation results.	81
4.2	Membership of different functions to different clusters.	82
5.1	An earth fault in a grounded network.	89
5.2	An earth fault in an isolated network.	90
5.3	Voltage vectors during an earth fault.	91
5.4	An equivalent circuit of an isolated network during an earth fault. . .	92
5.5	An earth fault in a compensated network.	93
5.6	An earth fault in a compensated network (vector representation). . .	94
5.7	An equivalent circuit of a compensated network during an earth fault. .	95
5.8	A simulated example, an earth fault in phase 1, transient components visible in phase voltages.	97
5.9	Network model and equivalent circuit used for modeling the charge transient, fault resistance 0Ω	98
5.10	Neutral current in all feeders during an earth fault in one feeder, 6 feeders in the simulated example.	99
5.11	The division of the fault resistances in a compensated network [Hänninen and Lehtonen, 1998].	100
5.12	The division of the fault resistances in a isolated network [Hänninen and Lehtonen, 1998].	101
5.13	Flow chart of the differential equation algorithm and corresponding components.	107
5.14	Simulation model used for testing.	111
5.15	Results with sampling frequency of 16 kHz, $R_f = 10 \Omega$	112

5.16	Results with seven different sample streams, combining to 16 kHz when processed as in Chapter 3, $R_f = 10 \Omega$	112
5.17	Results a sample frequency of $16 \text{ kHz} / 7 = 2.29 \text{ kHz}$, $R_f = 10 \Omega$. . .	113
5.18	Transient frequency and amplitude with $R_f = 10 \Omega$	114
5.19	Results with sampling frequency of 16 kHz, $R_f = 80 \Omega$	115
5.20	Results with seven different sample streams, combining to 16 kHz when processed as in Chapter 3, $R_f = 80 \Omega$	115
5.21	Results a sample frequency of $16 \text{ kHz} / 7 = 2.29 \text{ kHz}$, $R_f = 80 \Omega$. . .	116
5.22	Transient frequency and amplitude with $R_f = 80 \Omega$	117
5.23	Mean errors with different sampling set-ups and fault distances, $f_s =$ 20 kHz.	118
5.24	Mean errors with different sampling set-ups and fault distances, $f_s =$ 16 kHz.	119
5.25	Mean errors with different sampling set-ups and fault distances, $f_s =$ 10 kHz.	119

Nomenclature

ADC	Analogue-to-Digital Converter
AMR	Automatic Meter Reading
CB	Circuit Breaker
CBM	Condition Based Maintenance
CID	Configured IED Description
CIS	Customer Information System
DFT	Discrete Fourier Transform
DG	Distributed Generation
DMS	Distribution Management System
ENS	Energy Not Supplied
FLIR	Fault Location, Isolation and power Restoration
GHG	Greenhouse Gas
GOOSE	Generic Object Oriented Substation Event
GPS	Global Positioning System
HE	High-End
HV	High Voltage
HW	Hardware

ICT Information and Communication Technology

IDA Intelligent Distribution Automation research project

IED Intelligent Electronic Device

IID Instantiated IED Description

LCC Life Cycle Costs

LE Low-End

LN Logical Node

LV Low Voltage

MV Medium Voltage

NCC Network Control Center

NIS Network Information System

RCM Reliability Centered Maintenance

RTU Remote Terminal Unit

SAV Sampled Analogue Value

SCADA Supervisory Control And Data Acquisition

SCD Substation Configuration Description

SCL Substation Configuration Language

SED System Exchange Description

SGEM Smart Grids and Energy Markets research program

SINAD Signal-to-Noise-And-Distortion ratio

SNTP Simple Network Time Protocol

SW Software

THD+N Total Harmonic Distortion with Noise

TI-ADC Time-Interleaved ADC

List of Symbols

A	Amplitude of a signal
C_0	Earth capacitance of power lines
C_{eq}	Equivalent capacitance
C_{pp}	Phase-to-phase capacitance of power lines
f	Fundamental frequency of the network
f_s	Sampling rate
g_l	Deterministic gain of channel l in a TI-ADC set-up
\tilde{g}_l	Random variable for the gain of channel l in a TI-ADC set-up
i_k	Current, instantaneous value at time k
\hat{i}_{Ch}	Amplitude of the charge current transient
$\underline{I_c}$	Current through earth capacitances (phasor)
$\underline{I_f}$	Fault current phasor
$\underline{I_e}$	Fault current phasor
$\underline{I_L}$	Current through the Petersen coil (phasor)
$\underline{I_0}$	Neutral current phasor
C_{LC}	Life cycle costs: Overall costs
C_A	Life cycle costs: Acquisition costs
C_R	Life cycle costs: Renewal costs
C_O	Life cycle costs: Operation costs
C_M	Life cycle costs: Maintenance costs
C_F	Life cycle costs: Failure costs
C_{CR}	Life cycle costs: Replacement costs
C_P	Life cycle costs: Penalty costs
L	Inductance of a Petersen coil
L_{eq}	Equivalent inductance
L_T	Phase inductance of a substation transformer
M	Number of ADCs in a TI-ADC set-up
o_l	Deterministic offset of channel l in a TI-ADC set-up
\tilde{o}_l	Random variable for the offset of channel l in a TI-ADC set-up
P_S^{gr}	Signal power, dependent on gain and timing deviation
P_N^{gr}	Signal error power, dependent on gain and timing deviation
P_N^o	Signal error power, dependent on offset
P_S^{grR}	Expected signal power, dependent on gain and timing deviation

P_N^{grR}	Expected error power, dependent on gain and timing deviation
P_N^{oR}	Expected error power, dependent on offset
r_l	Deterministic relative timing deviation of channel l in a TI-ADC set-up
\tilde{r}_l	Random variable for the relative timing deviation of channel l in a TI-ADC set-up
R_f	Fault resistance during an earth fault
R_{LE}	Leakage resistance of a network
R_p	Resistance in parallel with a Petersen coil
Δt_l	Deterministic absolute timing deviation of channel l in a TI-ADC set-up
T_s	Sampling period
u_k	Voltage, instantaneous value at time k
\underline{U}_0	Neutral voltage phasor
\underline{U}_1	Voltage phasor in phase 1
\underline{U}_2	Voltage phasor in phase 2
\underline{U}_3	Voltage phasor in phase 3
\underline{U}_{0F}	Neutral voltage phasor during an earth fault
\underline{U}_{1F}	Voltage phasor in phase 1 during an earth fault
\underline{U}_{2F}	Voltage phasor in phase 2 during an earth fault
\underline{U}_{3F}	Voltage phasor in phase 3 during an earth fault
μ_g	Expected value of the gain of one ADC/IED in a TI-ADC set-up
μ_o	Expected value of the offset of one ADC/IED in a TI-ADC set-up
σ_g	Standard deviation from the expected gain in a TI-ADC set-up
σ_r	Standard relative timing deviation of a TI-ADC set-up
σ_o	Standard deviation of the offset in a TI-ADC set-up
Ω	Continuous-time angular frequency
ω_N	Angular frequency of the network
ω_C	Angular frequency of the charge transient
ω_0	Angular frequency an input signal, discrete time
Ω_0	Angular frequency an input signal, continuous time

Chapter 1

Introduction

The importance of a continuous supply of electrical energy has steadily increased over the past few decades. There have already been numerous instances in which electricity has been recognized as a critical resource for modern society and nothing indicates any change in this trend [EC, 2008b]. On the contrary, it has been estimated that the consumption of electrical energy will grow twice as much as overall energy consumption [IEA, 2009]. This means that in the future an even bigger proportion of our energy chain will be based on the production, delivery and consumption of electricity.

At the same time, increasing requirements are being placed on the energy sector. One major driver for this is the fight against global warming and the need to cut down on our CO_2 emissions. This calls for new, sustainable, renewable and environmentally-friendly energy sources, such as wind and solar power. Integrating these energy sources into the present energy network is challenging, as these production units are often smaller and more widely distributed than traditional large power plants. This creates bi-directional power flow in distribution networks, which requires new protection and control schemes. To emphasize this, networks with a large share of DG (Distributed Generation) are often called 'active networks' to clearly distinguish them from the more traditional 'passive networks'.

In addition to new energy resources, it is equally important to increase the energy efficiency of the network, as a significant proportion of our energy production is simply lost in various parts of the energy chain. Distributed and renewable energy resources often result in improvements in this regard, too. If the distributed energy production unit is located close to the consumer, there is less need for energy trans-

mission and therefore lower transmission losses during normal operation. However, in general there is no 'single factor' for improving the efficiency of the electricity supply, as the whole chain needs updating - both the 'primary system' that delivers the energy and also the 'secondary system', which monitors, controls and protects the primary system. An important part of this secondary system is the automation equipment located in the distribution substations, and this is the main focus of this thesis. The secondary system in a distribution substation is often referred to as distribution substation automation, which is reflected in the title of this thesis.

Another phenomenon affecting the energy sector is globalization. The drive to optimize the process of supplying electrical power is not only due to environmental factors, but also to financial ones. Competition between electrical supply companies is increasing at all levels. Although the competition between technology providers has long been self-evident, recent changes in government policies mean that the same sense of competition and response to financial imperatives has now spread to the energy producers, too. In Finland, the energy market was opened to competition as long as 1995 [EMV, 1995] and the European Union's target of a single european energy market [EC, 2008b], has further stimulated competition between energy producers.

Despite the severity of the challenges facing the electricity industry, due to the speed of recent technological innovations the number of available solutions has also increased. The exponential growth of ICT (Information and Communication Technology) has made many new solutions available, and has also provided the infrastructure for sharing knowledge about these innovations globally, as soon as new discoveries are made.

So, the new requirements and the corresponding new technical solutions mentioned above have recently spawned a multitude of Smart Grid initiatives around the world. In addition to the predicted overall transformation of the electricity network as a whole, these initiatives also indicate how much the control and protection of the network is expected to change within the next few years. As the passive network with unidirectional power flow evolves into an active network with a variety of distributed generation units, the requirements for distribution substations will also change, forcing the utilities to take action. Utilities do not want to undertake continuous and costly upgrades of the whole protection system, but there is still a clear need to adapt to new requirements. The need to increase the level of automation in the distribution network has been clearly recognized both on the vendor side [Heckel, 2009] and on the utility side [Gorgette et al., 2007]. For distribution substations, this

means increasing the functionality of existing IEDs (Intelligent Electronic Devices) in the substation, or adding entirely new IEDs to the system.

Various concept-level proposals have been presented in order to address the conflicting requirements for low life-cycle costs and the rapid utilization of new technology, and these are briefly introduced in this chapter and again, in more detail, later on in the thesis. The most traditional approach has been to increase the functionality of the bay-level protection and control IEDs. This approach has been sufficient while CPU capacity has been steadily increasing and the price of new technology has remained at a reasonable level. The issue in this approach has been the extensive costs of upgrades. The increased functionality has also required substantial changes to the substations' entire secondary systems, requiring long maintenance breaks or detailed and time-consuming planning for back-up connections.

This doctoral thesis investigates how station-level data processing could be utilized to help create a future-proof architecture for the secondary system of a distribution substation. The main requirements and drivers are described and evaluated, possible technologies are presented, and the proposed architecture is described in more detail with reference to the relevant technologies and standards. Life-cycle cost analyses are also performed on the possible architectures.

Furthermore, the thesis investigates new possibilities for the proposed architecture. The feasibility of new innovations in the measurement chain in the substation is evaluated and a new method for measurement is proposed. Also applications and functions which are currently being implemented in bay-level protection and control IEDs are evaluated and a new scheme of substation functionality allocation is proposed. Finally the overall concept is tested and prototyped, both with simulations and also in practice.

1.1 The hypothesis and objectives of the thesis

The over-riding hypothesis driving the research is that a more centralized architecture for the secondary system of a distribution substation will provide the most future-proof platform for dealing with future requirements, such as active distribution network management or automatic fault management. This hypothesis was approached using both higher concept-level objectives and lower-level, more detailed objectives.

The main concept-level objective was to identify when and in which cases this proposed new architecture is more cost-efficient than the currently dominant one.

Another important target was to specify how this centralized architecture should be utilized, i.e. what functionality in a distribution substation benefits from, or even requires, a more centralized architecture.

In addition to the concept-level objectives, another important objective of the thesis was to discover entirely new and more accurate measurement methods or innovative functions, which could not be implemented without this centralized architecture. The aim was to pinpoint practical examples of new innovative functions for substations, in order to highlight that this new architecture is not just the "same old system with lower life-cycle costs" but also an architecture which enables something entirely new.

1.2 Background of the thesis

The possibilities for centralized functionality at the substation level have been researched at ABB since 2007. Their activities started with the Intelligent Distribution Automation (IDA) project, conducted in cooperation with the Finnish utility company, Fortum, and Tampere University of Technology. The IDA project ended with the pilot installation carried out at the Noormarkku substation in the Fortum distribution network. The author of this thesis joined the IDA project in 2008 and was the project manager when it ended in 2009, and the main results of the project were outlined in [Valtari et al., 2009a].

Research into a centralized architecture for electricity distribution substations continued after the IDA project in the Smart Grids and Energy Markets (SGEM) research program. This was coordinated by CLEEN Oy and received funding from the Finnish Funding Agency for Technology and Innovation, Tekes. The research program covers many aspects of the future Smart Grid, and is planned for the years 2009-2014 with an overall budget of €57 M. The author is currently leading the research activities within the Work Package "New Substation Solutions" under the research theme "Future Infrastructure of Power Systems". The author has also been acting as the overall program manager of SGEM since 2011.

A transient-based earth fault location algorithm was the subject of the author's master's thesis [Valtari, 2004]. The aim of that thesis was to implement and test an algorithm suitable for a bay-level protection and control IED, but this was not achieved. The requirements for the algorithm were too stringent, especially for the sampling frequency of the measurements, and the algorithm was never finalized.

While writing this doctoral thesis, the author has also contributed to other projects supporting the work presented here, such as the supervision of a master's thesis which focused on the end-user engineering process of the environment [Kettunen, 2011]. The author also had a consulting role in a pilot project implementing substation-level fault detection, isolation and restoration functionality [Manner et al., 2011]. Research related to the centralized architecture of substations will continue in the future under the SGEM research program.

1.3 Outline of the thesis

New requirements for the automation of electricity distribution substations and the proposed new automation architecture are presented and evaluated in Chapter 2. This chapter presents the main features of the technology and also performs a life-cycle cost analysis. The measurement chain, and a method for increasing the sampling frequency of substation measurements, are described in Chapter 3. The possibility of using measurements from several bays simultaneously raises new possibilities for the whole measurement chain, and these are described and tested. The new architecture allows for the re-allocation of functionality between the station level and the unit level, and this is evaluated in Chapter 4. An example case utilizing the new measurement method from Chapter 3 and a transient-based earth fault location algorithm is presented in Chapter 5. A summary of the thesis is presented in the concluding Chapter 6.

This thesis is based on five different publications, which together constitute the main results of the thesis. Chapter 2 is based on results from [Valtari et al., 2009a] (republished in [Valtari et al., 2009b]), [Valtari and Verho, 2011a] and [Valtari and Verho, 2011b]. Chapter 3 includes the results from [Valtari and Verho, 2012] while Chapter 4 is derived from [Valtari et al., 2010]. In addition, a patent application has been submitted based on the results of Chapter 3 [Valtari, 2012]. The patent has been allowed and is about to be granted. The function example presented in Chapter 5 has not been published earlier. The basic principles of the algorithm are presented in [Valtari, 2004], but the method is re-tested with a new set-up based on a substation-level implementation.

An outline of the chapters and their relations to publications is presented in Figure 1.1. The logical story line of the thesis is also presented on the left side of the figure.

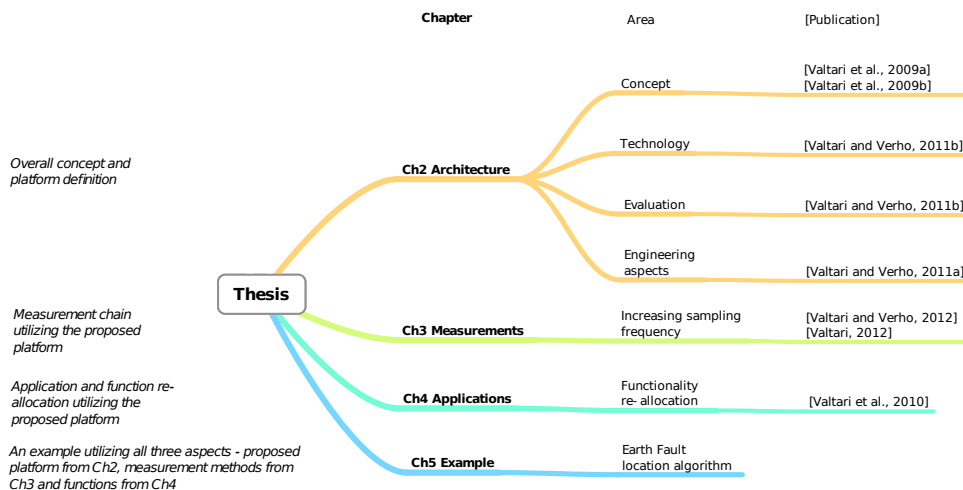


Figure 1.1: Outline of the thesis.

1.4 The role of the author

The initial concept for centralized protection and control presented in Chapter 2 was developed in the early stages of the IDA project by a number of experts: Antti Hakalari, Dick Kronman and Tapio Hakola from ABB Finland; Thomas Werner and Bernhard Deck from ABB Switzerland; and Pekka Vierimaa from Fortum Distribution Finland. The author built on their work by summarizing the ideas and leading the pilot installation in the Fortum-owned substation. After the pilot installation in 2009, the author also took on the leading role in the overall research project. The author performed the life-cycle cost calculations and extended this evaluation to include the engineering processes.

The measurement principle presented in Chapter 3 was created and developed by the author. The example application utilizing the measurement principle presented in Chapter 5 was originally developed by Seppo Hänninen from VTT, but the author made the necessary extensions to the algorithm so that this measurement principle could be used. The simulation model used in section 5.3.2 was developed by Mohammed Abdel-Fattah from Aalto University.

The initial example listing of appropriate station-level functions presented in Chapter 4 was created by Tapio Hakola from ABB Finland at the beginning of the IDA project. The author continued this work and developed the method used for this classification in order to achieve a more comprehensive list for guiding further research activities.

Chapter 2

Station Architecture

After the background, presented in section 2.1, section 2.2 investigates the new drivers and market trends affecting the secondary system of a distribution network. From these drivers and trends, more detailed requirements for the distribution substations are derived in section 2.3. After that, possible architectures and on-going research into the secondary system are presented in section 2.4 and evaluated in section 2.5. Finally, the apparently most suitable architecture is considered in more detail in section 2.6, which also outlines the required technologies and the relevant standards.

2.1 Background

2.1.1 An electricity network

Power generation and consumption often occur at different geographical locations. Although the trend nowadays is towards distributed power production, major power plants are normally situated far away from densely populated areas or large factories. This is not only because the prerequisites for energy generation might be better there, but also because of safety and environmental issues. As a result of this, energy generation and consumption have to be connected together with electricity transmission and distribution networks [Grigsby, 2000].

For economic and safety reasons, the form of electrical energy is different in different parts of the network. The different parts of a network and their typical voltage levels in Finland are presented in Figure 2.1. The energy production end of the chain

is marked with G (Generator) and the consumption end with L (Load).

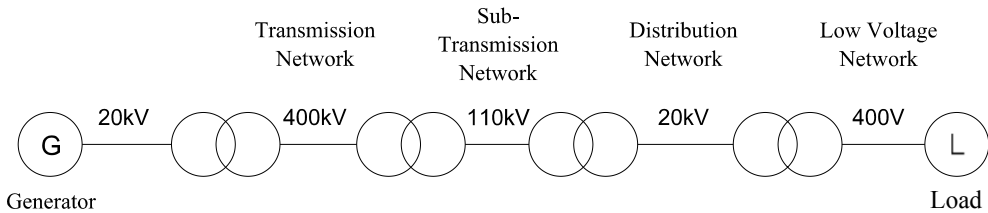


Figure 2.1: Typical voltage levels in the electricity network in Finland.

Energy losses are lower if the voltage is relatively high and the current relatively low. Therefore, the delivery of large quantities of electrical energy can reasonably be handled by HV (High Voltage) networks (400 kV ... 110 kV). This part of a network is called the transmission network. [Elovaara and Laiho, 2004]

The voltage level of the transmission network is too high for electrical devices. The required isolation with high voltages would make such devices too large and expensive. Therefore, the voltage has to be lowered before it can be delivered to customers. Delivery to factories and community centers is normally done with MV (Medium Voltage) networks (20 kV ... 6 kV), and this part of the network is often referred to as the distribution network [Lakervi and Holmes, 1996].

Because manufacturing costs and safety risks are decreased by lowering the voltage, the energy to households is supplied by the LV (Low Voltage) network (in Finland 400 V phase-to-phase, 230 V phase-to-ground) [Elovaara and Laiho, 2004]. These voltage levels are sufficient as long as the required power is relatively low, so that the distribution losses due to the load current do not rise too much.

The different parts of the electricity network require different protection and supervision systems, and the transformation of electrical energy from one voltage level to another also calls for specific devices. All this makes the whole energy distribution system rather complicated and its control is a challenging task.

Distribution substation

The connection point between the distribution and the (sub)transmission network is called a distribution substation. The term 'primary substation' is also often used in the literature [Lakervi and Holmes, 1996], but distribution substation is somewhat more common and is also used in a number of standards [IEEE, 2000]. Therefore,

'distribution substation' is the term that will be used in this thesis. There are other types of substations, such as secondary substations (the connection point between distribution and low voltage networks), transmission substations (between two transmission lines) or collector substations (collecting several distribution lines, e.g. near wind farms).

A distribution substation has the equipment needed for changing the voltage level (power transformers) and also for controlling the topology of the network via CBs (Circuit Breakers), disconnectors and earthing switches. In addition, for the sake of power quality, specific capacitors (if more reactive power generation is needed) or voltage regulators (for keeping the voltage at the required level regardless of the consumption) may be included. This 'primary system' of the distribution substation, i.e. the system which has a direct effect on the transmitted electrical energy, may also contain other components such as generator units or earthing coils (for compensated networks, see Chapter 5) [Lakervi and Holmes, 1996][Lakervi and Partanen, 2008].

Transmission (incoming) feeder lines are connected to distribution (outgoing) feeder lines via a busbar (or several busbars if the substation is large). An example topology for a substation is shown in Figure 2.2, where there are two incoming feeders (and two power transformers) and two outgoing feeders [ABB Ltd., 2000]. The set-up has a double busbar, but only one circuit breaker per feeder (although there are three disconnectors: two between the CB and the busbars and one after the CB).

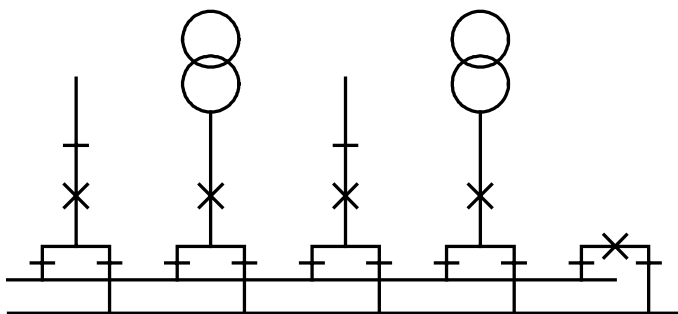


Figure 2.2: Example topology of a double busbar substation.

A separate automation layer is needed in the substation in order to control the equipment in this 'primary system', and this is often referred to as the 'secondary system'. An overview of the secondary system is described in the following section

2.1.2, but the new requirements and future challenges are presented in more detail in section 2.3

2.1.2 The secondary system of the network

The primary system of the substation has generally remained quite stable since the beginning of electrification. New materials and new production technologies have, of course, changed the look and feel of these primary components, but the fundamental structures have remained surprisingly unchanged. The life-span of such equipment is typically between 30 and 50 years [Laine, 2005].

The secondary system, on the other hand, has gone through many revolutionary changes, and this process is expected to accelerate in the future, as described later on in section 2.3. This section describes the historical background and current solutions before looking into new requirements and challenges.

At the very beginning of electrification, the secondary system was virtually non-existent. There were protection relays, but all the control operations were handled by personnel working in the substation. With the development of telecommunication technology, this practice has changed and nowadays all the operations are conducted from a separate NCC (Network Control Center) .

The number of different software systems in NCCs has increased steadily and the integration of these systems is an on-going process. Normal control operations are handled via a SCADA (Supervisory Control And Data Acquisition) system, which in addition to real-time operation possibilities also shows the real-time status of the network topology and performance [Grigsby, 2000].

A system called DMS (Distribution Management System) has been developed to support network operations, and this provides a geographical overview of the network and improved topology management [Grigsby, 2000]. The calculation engine of the DMS performs various calculations related to the network status, such as evaluating the voltage profiles of feeders or locating a fault based on fault currents and the network topology. However, a DMS needs detailed data from the network components, which can be obtained from the NIS (Network Information System). Practically all the utilities in Finland also have a separate CIS (Customer Information System) handling the customer data, often integrated with another system which handles customer calls. [Lakervi and Partanen, 2008]

The installation of AMR (Automatic Meter Reading) meters in customer house-

holds has facilitated a new, extensive source of network status information for the utilities, and the integration of this meter-reading system into the other NCC software systems is currently ongoing in Finland.

The secondary system of distribution substations

Nowadays, communication with a substation is routed through a gateway device called an RTU (Remote Terminal Unit) [Grigsby, 2000]. The term 'Gateway' is also often used for this device, and RTU is in fact a product name of ABB for a particular gateway device. Nevertheless, the general term selected for this thesis is RTU, as that is often used in the literature. All the protection and control IEDs can be accessed via RTUs and all the CBs and disconnectors can be operated via them. Protection and control IEDs are also essential for monitoring the status of the network - both normal state values (measurements) and fault state information (alarms and events).

In addition to RTUs and protection and control IEDs, the secondary system also needs other elements, such as measurement transformers or sensors (voltage and current), battery systems for guaranteeing operation during interruptions in the electricity distribution, telecommunication modems and sometimes, nowadays, even video surveillance cameras. [Lakervi and Partanen, 2008]. However, protection and control IEDs are the core devices in contemporary secondary systems, and these are described in more detail below.

Protection and control IEDs

The earliest protection devices were electromechanical relays, which were utilized at the beginning of the 20th century. Separate devices were needed for every phase and every function, the functions being limited to only simple overcurrent and earth fault protection. These devices were very inaccurate and unreliable in operation. On the other hand, they did not require any external power sources, but could utilize the power from the power lines [Mörsky, 1993] [Lundqvist, 2010].

Static relays became popular during the 1960s, due to the emergence of transistors and electronics. The number of functions increased, and one device was able to handle all three phases (although separate devices were still needed for separate functions). These devices needed their own power supply, but their operation was more reliable and accurate. Even today, almost half of the protection devices in use are static relays [Mörsky, 1993] [Lundqvist, 2010].

The development of integrated circuits and microprocessors (and computers) caused the next revolution in the secondary system at the beginning of the 1980s. The new protection devices which utilized this technology were called numerical relays, and these could handle all the protection and control functions for one feeder within one single device. Self-supervision functionality and support for several communication protocols were introduced at this point, too. Illustrations of these three types of devices are shown in Figure 2.3

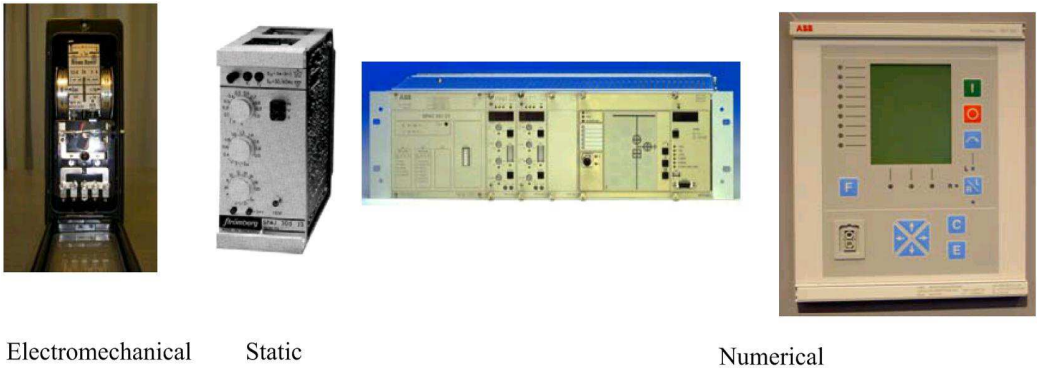


Figure 2.3: Electromechanical, static and numerical relays.

The process of integrating more functionality into single devices (and improving calculation performance) has led to increasingly advanced numerical relays. Because of this increased functionality, the name of the device has changed, and nowadays technology vendors prefer to use the term protection and control terminal or IED, rather than merely a relay. IED is therefore the term used in this thesis.

2.1.3 Network management processes

The previous sections presented the overall physical structure of electricity networks and the main components of a secondary system. This section gives a short introduction to the processes associated with managing the network. The main focus is on those processes which affect the secondary system of a distribution substation - either in terms of the system architecture or simply those processes which require the acquisition of data from the substation.

Network planning means long term strategic planning related to the network topology or to the components used in the network [Grigsby, 2000]. The time frames

involved can span several decades, as the life-span of these components is typically between 30 and 50 years [Laine, 2005]. The network should be planned so that it provides electrical energy to all the customers with a cost-efficient architecture and topology, and with a protection system that fulfills all the safety and power quality regulations [Lakervi and Partanen, 2008]. The plan should also take into account predicted future changes which will affect the network, e.g. changes in legislation, possible technological advances in the near future, increases or decreases in the local population, and also industrial and other intensive energy consumption scenarios. The challenging task in the network planning process is to select an architecture for the distribution system that meets both current and future demands. In addition, the measurement data acquired via the secondary systems at the substations provide valuable information for this process.

Network maintenance encompasses all the actions that are performed to maintain the network, which in practice means servicing, repairing or replacing different network components. These operations should be optimally timed, so that the network performance stays at its target level at all times, while incurring the lowest possible maintenance costs [Lakervi and Partanen, 2008]. Traditionally, maintenance operations have been event-based (reacting to a broken component, corrective maintenance) or time-based (maintenance of a component at a specific maintenance interval, periodic maintenance). However, recently there has been increased focus on CBM (Condition Based Maintenance) and RCM (Reliability Centered Maintenance) [Angel, 2003]. The idea behind CBM is that the actual condition of all the components is monitored constantly, and maintenance operations are triggered when the condition reference value or operation counter exceeds a defined limit. RCM extends the approach of CBM by also taking into account the importance of that particular component to the network, so that maintenance actions and type are defined based on the component's criticality. This means that the components are used for the optimal length of time, but critical components are still maintained before they break down. If a CBM or RCM approach is desired, it is essential to have accurate measurement data available via the secondary system of the distribution substation.

The process of network operation encompasses all the activities related to day-to-day work at the utilities. This involves monitoring and control operations when the network is in a healthy state in order to guarantee a safe power balance (e.g. changes in the network topology due to changes in energy production or consumption), or preparing for other network operations (e.g. back-up connections required for future

maintenance operations on the network). During fault situations, the operation process should provide fast fault location and isolation. The energy should be restored to the healthy part of the network, so that the area affected by the fault is kept at a minimum. For repairing the fault, the process includes controlling the repair personnel and providing them with the necessary information about the fault. Nowadays, an increasingly important part of this process is also communication with the customers. On certain occasions, such as those which trigger major disturbances, many other aspects may become important too, e.g. collaboration with rescue personnel, ambulances and other medical assistance, the media, the police, etc. The process of network operation is immense and it is not possible to cover all possible scenarios in this brief section. Whatever the case, it is the secondary system of the distribution substation that is an important part of the process.

2.2 New drivers and market trends for energy distribution

2.2.1 The global situation and climate change

Climate change is one of the great challenges of the 21st century [IPCC, 2011]. According to IPCC, CO_2 emissions associated with the provision of energy services are a major cause of climate change: “Most of the observed increase in global average temperature since the mid-20th century is very likely due to the observed increase in anthropogenic GHG (greenhouse gas) concentrations.” [IPCC, 2011].

An obvious consequence of this is that CO_2 emissions need to be reduced all around the world. Global conferences have been arranged, and the EU has already declared its targets in its 20-20-20 program. By 2020, the EU is committed to reducing CO_2 emissions by 20%, to increasing the utilization of distributed generation to 20% and to improving energy efficiency by 20% [EC, 2008a].

At the same time, energy consumption is expected to increase, as shown in Figure 2.4 [IEA, 2009]. The expected increase in the use of zero-carbon fuels will also increase the proportion of electrical energy used in total energy consumption. The over-riding aim is to decrease overall CO_2 emissions, as shown in Figure 2.5. This creates a very challenging scenario. How can emissions be reduced when, at the same time, energy production will increase?

Addressing these challenges calls for many different measures, such as moving from petroleum-based transportation to electrical transportation, increasing the share

2.2. New drivers and market trends for energy distribution

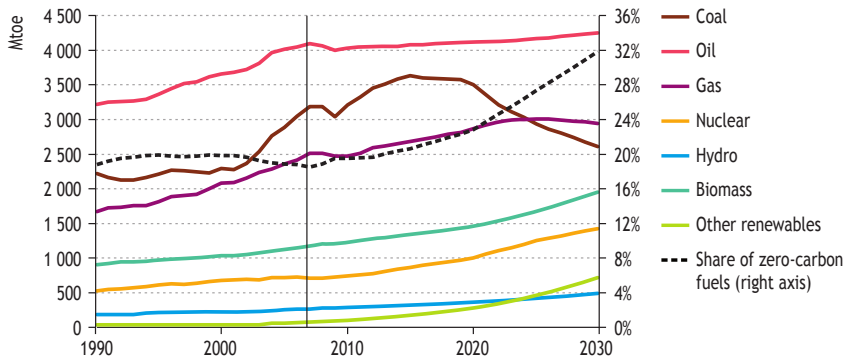


Figure 2.4: Expected increase in energy consumption (Mtoe = million ton of oil equivalent) and in the share of zero-carbon fuels [IEA, 2009].

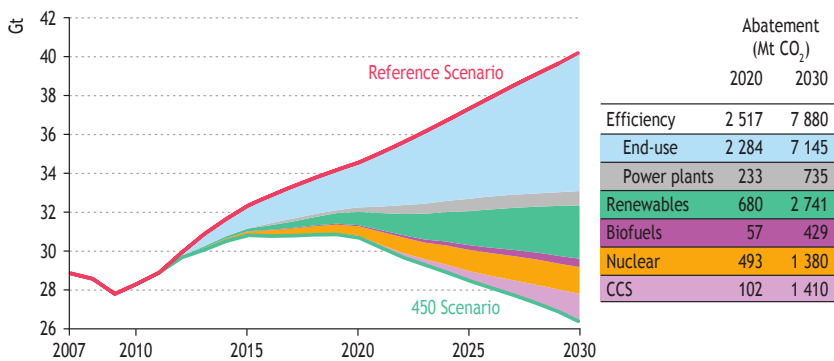


Figure 2.5: Targeted decrease in CO₂ emissions [IEA, 2009].

of renewable and uncontrollable energy production, increasing energy efficiency with controllable consumption and energy storages etc. [IPCC, 2011]. A major burden of this challenge also falls on the electricity networks, which need to be more flexible in order to implement the new actions described above. This challenge has triggered a wealth of smart grid initiatives around the world, and is also one of the drivers behind this thesis.

2.2.2 The market situation and foreseeable business trends

Electricity distribution has traditionally been a business which focuses on long time-frames and has a conservative approach to technological advances. The primary

equipment in the substations has a typical life-span of 30 to 50 years, and upgrades to the secondary equipment have often had to follow almost the same life cycle. However, this industry is now undergoing major changes. Many of these changes come from government legislation, such as the new energy market act which has come into force in Finland [EMV, 1995] and similar legislation which is going on elsewhere in Europe. Energy production and distribution have been separated, and energy production has been opened up to the free market, allowing customers freedom of choice with regard to their energy supplier.

According to the Finnish energy market act, energy distribution in Finland is still a local monopoly, but the business is now closely regulated [EMV, 1995]. The authorities define certain criteria for power quality and for continuity of supply. The legislation defines the permitted 'fair and reasonable' profit levels, and the utility can only affect this by improving the quality of the supply. According to current regulations, customers must be recompensed for interruptions in their electricity supply. Variations in power quality also need to be monitored. In the regulatory model, the emphasis is on the quality of the distributed energy. So, higher quality will generate higher profits for the network operators.

The control of a network is also moving further away from the actual, physical network. Mergers between many companies have created bigger players in the distribution business. In addition, communication network technology has developed rapidly over the past few years, enabling wider communication coverage for network components - for example, the the penetration rate of mobile subscriptions has increased from 20% to 128% (as a proportion of the population) in Europe within the past 14 years [GSMA, 2012]. This has all resulted in an increased demand for the acquisition of data from the larger networks, and also that the data should be pre-processed before it is viewed by the NCC personnel.

In addition to increasing the amount of automation, utilities are streamlining their processes in terms of personnel so that they can focus more on their core business. When a function outside the utility company's core competence cannot be fully automated, it is often outsourced. Such outsourcing is currently prevalent in Finland, where many large utilities have recently outsourced their maintenance and service activities [Fortum, 2010], their communication network operations [ViolaSystems, 2011] and even some network planning tasks, in order to keep the number of personnel in check, despite increases in the size of the network.

2.3 New requirements for distribution substations

This section describes the new requirements for distribution substations in more detail.

2.3.1 Advanced fault management

More accurate and selective network protection

As society becomes increasingly dependent on electricity, the requirements for its uninterrupted distribution have become more stringent. This demand for uninterrupted distribution is also reflected in the legislation of many other countries. Interruptions in electricity distribution need to be recorded for statistical analysis and customers must be compensated for interruptions exceeding a certain duration, which in Finland is currently 12 hours [EMV, 1995].

This must be taken into account in the protection system, so that different types of faults can be accurately detected. Entirely new protection schemes which utilize more measurements than are locally available have been, and are being, researched and proposed. There are many levels to increasing the communication between adjacent protecting nodes. First, there is the horizontal communication within a substation [Apostolov and Vandiver, 2011], and after that there is real-time communication with a remote DG unit, or even a full-scale agent-based protection system [Kauhaniemi et al., 2011]. The results of all these studies indicate the need for protection schemes to take into account a larger area than only one feeder, as is currently the norm.

This also requires enhancements to the protection functions, and new, more accurate protection functions are needed. In addition to protection schemes, many new protection functions have also been researched, and these utilize or require more measurements than are available from one feeder bay. This includes managing new fault types, such as high-impedance earth faults [Tengdin, 1996][Abdel-Fattah and Lehtonen, 2009] [Nikander, 2002].

Fault location and advanced control of distribution networks

Post-fault power restoration and self-healing networks are a common topic in smart grid scenarios [Mekic et al., 2009][Rasmunssen, 2009][Manner et al., 2011]. When a fault appears in the distribution network, it should be automatically located and isolated, and the electricity distribution should automatically be restored to all the

healthy parts of the network. Sometimes, distribution networks also need to be operated in an island mode and controlled from the substation [Oudalov et al., 2011].

In Nordic countries these operations are traditionally conducted from a centralized NCC. However, this places an additional burden on the NCC, which may become a bottleneck for the process, especially during major disturbances. For this reason, much of the ongoing research in this area is targeted at handling these tasks in the substation, so that NCC personnel only need to react when the local automation at the substation has failed in FLIR (Fault Location, Isolation and power Restoration) .

2.3.2 Efficient operation of the network and support for asset management

Automatic adaptation to changes in topology, production and consumption

In addition to fault situations, the network also needs to respond automatically to changes which may occur during normal operation. The number of active resources (DG, energy storages) in the network can vary greatly, and this may require load-shedding functionality at the station level [Apostolov et al., 2007]. Dynamic load-response becomes more critical as the proportion of uncontrollable production increases in the network. Therefore, demand response has recently gained a lot of interest [EC, 2008b] - the load must be controllable if the production is not, especially if no large energy storage facilities are available.

In addition to control operations, changes in topology and active resources also require adaptations to the protection and monitoring functions. The parametrization of the functions needs to be fine-tuned in order to adapt to the network status. Both of these issues require information to be acquired from a larger part of the network than one single bay [Oudalov et al., 2011].

Wide area monitoring, protection and control; Synchronized Measurement Technology utilizing Phasor Measurement Units

The availability of low cost, high precision timing resources, such as GPS (Global Positioning System) has made it possible to acquire phasor measurements from line currents and voltages from a larger network with highly accurate time stamping [O'Brien and Deronja, 2012]. This new synchronized measurement technology utilizing Phasor Measurement Units has gained interest in recent research publications, and many

new applications benefitting from this technology have been proposed, briefly summarized below according to [Terzija et al., 2011].

- Real-time visualization of power systems
- Design of an advanced, early warning system
- Analysis (ex-post) of the causes of system blackouts
- Benchmarking and validation of system models
- Enhancements in state estimation
- Real-time congestion management
- Real-time angular, voltage, and frequency stability
- Improved damping of inter-area oscillations
- Design of adaptive protection and control systems.

Synchronized Measurement Technology allows more accurate status information from the network to be gathered than was previously possible. In order to utilize this data fully, and to facilitate the above-mentioned applications, the electricity distribution substation must be able to receive and process this stream of synchronized measurements.

Condition monitoring and asset management of primary equipment

Smart grids need to optimize the utilization of all the network's resources. This means that all the network components need to be constantly monitored so that their condition is known, and any required maintenance operations can be properly planned. Using condition monitoring information for evaluating future maintenance needs is a common topic in much of the published research. CBM and RCM are a focal point for many utilities. However, these methods can only be properly utilized if data collection and processing is available at the station level [Angel, 2003].

Typically, for both transmission and distribution networks, the cost of the secondary equipment in a substation is marginal when compared to the overall cost of the whole network. An example calculation made for a 110 kV transmission network

shows that the secondary equipment in the substation only accounts for 2% of the total asset value, see Figure 2.6. Similar results have also been obtained for distribution networks in Finland [Matikainen, 2011]. Clearly the cost of the secondary equipment is not the main item affecting the overall cost-efficiency. On the other hand, substation automation does have a significant impact on the reliability of the network. This indicates that focusing on substation automation is a cost-efficient way of improving the reliability of the network.

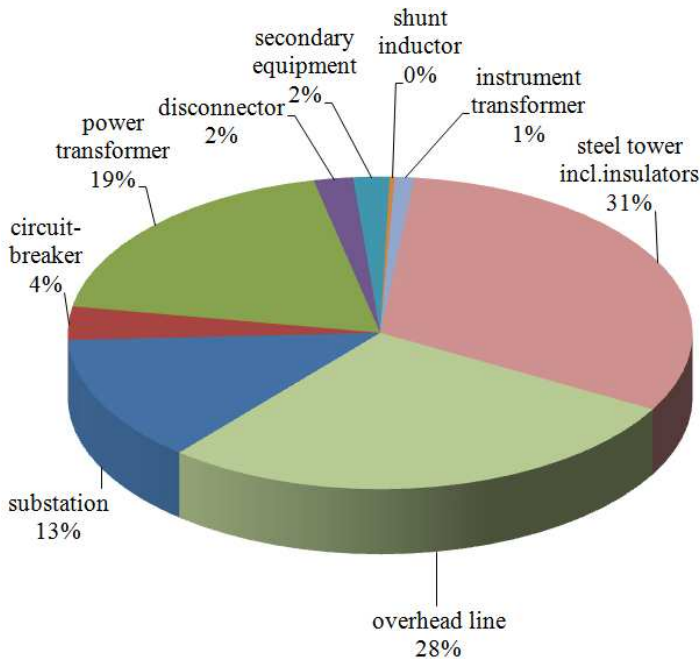


Figure 2.6: Present value of a 110 kV network [Jeromin et al., 2009]

2.3.3 Future-proof technologies, upgradeability

Multi-vendor platform with open interfaces and multiple data streams

As networks get more complex, more data will flow through substations and more interested parties need access to this data. Utilities are increasingly interested in outsourcing parts of their existing services, and this outsourcing to 3rd party service providers requires clear and open SW interfaces to the process data of the substation.

An example of the integration needs of different SW systems is the AMR infrastructure, which in the near future will also be used for the fault diagnostics, an addition to invoicing purposes.

As the functionality in a substation increases, the number of vendors providing functionality to the substation also increases. This means that, in addition to open process data interfaces, open interfaces are also needed for the SW platforms utilizing the data. In the future, the same SW platform may run applications from many vendors, in the same manner as already seen in less critical environments, such as personal computers or mobile phones [Johnson et al., 2010].

Cyber-secure firewall of the distribution network

When enhanced communication is used in the distribution network, cyber-security becomes an essential part of the overall security. A secure product is not in itself sufficient, as potential vulnerabilities may arise from insecure integration into existing infrastructures [Nartman et al., 2009]. While a substation can form a separate, secured island for energy distribution, it must also provide an information firewall for parties communicating with the substation and the associated distribution network.

The requirement for open interfaces described above highlights the importance of information security. In addition to preventing any cyber attacks, it must also protect customer-sensitive information, e.g. related to personal data, invoicing or energy consumption. This is especially challenging in an environment which also performs mission-critical operations.

Upgradeability, engineering and verification processes

Modern IEDs are complex devices and commissioning and updating them is normally handled by skilled personnel from the IED vendor or by a separate service provider. Utilities seldom have their own personnel for extensive engineering work, at least in Finland. There is a clear trend towards increasing the utilization of external service providers. In many cases, utilities have their own designers for determining suitable settings for the protection functions, but for other functional engineering, especially system-level engineering of the substation, their know-how is limited.

The main challenges faced by the utilities are testing and verification. Any new functionality must be tested at the system level, and this normally requires a deep understanding of the devices in use. Test sequences also often mean interruptions

to the supply of electricity or, alternatively, detailed and time-consuming planning of back-up connections. Therefore, the tendency is often to avoid implementing updates if the predicted benefit is low, especially updates that affect engineering at the system level. Furthermore, the functionality of those parts of the system which have not been updated also needs to be tested. This all leads to updates being postponed until the last possible moment, which means that the systems do not benefit from the advanced functionality of modern IEDs. As stated earlier, focusing on substation automation is a cost-efficient way of improving the reliability of the network, but this opportunity is lost if the updating process is too complex and time-consuming.

The lack of generic, system-level engineering tools is often mentioned in technical reports [Castallenos, 2009]. Although, this is not often an issue for the utility companies themselves, as this service is contracted out to other engineering companies, there is an obvious need for a generic tool to serve such companies. Although the aim of standardization is to increase interoperability, very often the IEDs are still selected from a single vendor, simply because this “reduces the possibility of trouble”. In practice, using a number of different vendors often means a number of different tool chains, a number of different philosophies in the engineering process and perhaps even a number of different terms for the same parameter.

2.3.4 Low life-cycle costs

The above sections have described the new requirements for a substation. The speed at which these requirements change is also expected to increase, which makes the life-cycle cost calculations difficult. Currently, the life-span of protection and control IEDs is presumed to be around 15 to 20 years [Lassila et al., 2002], but in many scenarios, new requirements for automation are already expected over the next 5 to 10 years [Gorgette et al., 2007]. Although the utilities do not want to undergo continuous and costly updates and upgrades to the whole protection system, the need to adapt to new requirements is nevertheless clear.

There are many factors which affect the cost-efficiency of the distribution substation and the overall life-cycle costs. The most obvious, but, perhaps the least significant factor in the long run, is the installation cost. Taking only this factor into account would lead to a grossly oversimplified view, as new secondary systems would only appear to decrease the life-cycle costs if the initial installation cost was lower than it had been before.

The costs of maintenance and upgrades to a distribution substation can be of the same order as the original installation costs. As future distribution systems are expected to be more dynamic than static, the possibility of implementing smooth and cheap updates is an important factor affecting the life-cycle costs. Advanced condition monitoring functionality, e.g. focusing on the CB condition or the transformer temperature would also facilitate planning these activities in advance.

More difficult to estimate, but still the factor which may have the greatest impact on the overall costs, is the profit that increased reliability may bring to the distribution network. Currently, utilities in Finland are obliged to pay compensation to customers whenever there is an interruption in the electricity supply exceeding 12 hours [EMV, 1995], and similar conventions are also in operation elsewhere in Europe. Power quality is increasing in importance, and in the foreseeable future the quality of the delivered electrical energy could also carry a price tag.

2.4 The possible architectures

2.4.1 Definition of a substation

The first question to be answered when thinking about new architectures is what exactly constitutes a distribution substation, i.e. how it can be defined? In the International Electrotechnical Vocabulary of IEC 60050 [IEC, 1983] a substation is defined as follows:

The part of a power system, concentrated in a given place, including mainly the terminations of transmission or distribution lines switchgear and housing and which may also include transformers. It generally includes facilities necessary for system security and control (e.g. the protective devices).

The key point in this definition is the change from transmission to distribution – a substation is the connection point between different voltage levels. There is the incoming feeder (normally just one, although there may be a few) from a higher voltage level (the transmission lines) and several outgoing feeders on a lower voltage level (the distribution lines).

One aspect that is emphasized throughout this thesis is the data processing functionality of the substation. A substation is not only an ‘energy hub’, but also an ‘information hub’. As it delivers energy to a large network at a certain voltage level, the substation also monitors and controls the network. The substation is responsible

for keeping the network operational and running safely. Furthermore, many of the control operations emanating from the NCC are focused on the substations.

2.4.2 A proposed architecture and a comparison with other solutions

The question is how to proceed with substation automation so that it is both interoperable and able to utilize new algorithms during the life-span of an IED, without increasing the life-cycle costs or shortening the life-span of the physical device itself. At the same time, utilities want to discourage vendors from creating monolithic secondary systems, which can only be sold and maintained by a single vendor.

Various concept-level proposals for the secondary system of a substation have been proposed which address the conflicting requirements for low life-cycle costs and the speedy utilization of new technology. These are presented later on in this chapter. The most traditional approach has been to increase the functionality of the bay-level protection and control IEDs, as described above in section 2.1.2. This approach has been sufficient while CPU capacity has been steadily increasing and the price of new technology has remained at a reasonable level. The issue in this approach has been the extensive costs of upgrades. New features have also called for substantial changes in the substation's entire secondary system, requiring maintenance breaks or the time-consuming planning of back-up connections. An overview of this set-up, along with the two others, is presented in Figure 2.7, where the set-up is described as 'Decentralized'.

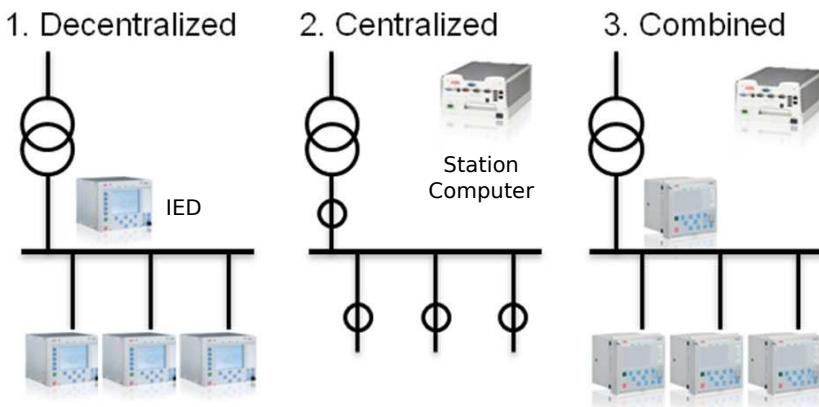


Figure 2.7: Possible Architectures for Distribution Substation Automation.

An alternative approach has been to fully centralize the functionality in a distribution substation [Volberda et al., 2007] [van Riet et al., 2005] (Described in Figure 2.7 as ‘Centralized’). By moving all the functionality to a centralized station computer, the life cycle of the bay-level measurement devices has been greatly extended, up to the lifetime of the primary equipment [Volberda et al., 2007]. Furthermore, the upgrade measures needed to implement new features have been simplified, because only the centralized station computer requires updating. This, however, creates a single point of failure in the substation. When the central station computer is out of operation, the protection for the whole substation is lost. In practice, fully centralized solutions would always need a redundant protection system – either a redundant station computer [Baldinger et al., 2008] or redundant bay-level protection and control IEDs – which would increase the overall costs of the substation secondary system. The same maintenance problem as with a fully decentralized solution also exists. When an upgrade is needed in an environment where all the functionality resides in the same computer, the upgrade affects the whole protection system. Therefore, maintenance breaks and extensive testing are required.

A third approach addresses the challenge by combining these two methods [Valtari et al., 2009a] (described in Figure 2.7 as ‘Combined’). In this approach, only a part of the bay-level functionality is moved to a new substation-level centralized station computer. The functionality is divided so that the most critical and important features, such as earth fault or overcurrent protection, would remain in the bay-level devices, thus ensuring network safety in all situations. This forms the backbone of a network protection system with a long life cycle. The functionality defined for the substation level would consist of value-added applications and other "nice-to-have" features, for which a faster update cycle is both necessary and acceptable. This set-up also has a natural inbuilt back-up scheme, as the bay-level and station-level devices provide a redundant protection system. The measures for updating the central unit are cheaper and safer, allowing the smooth utilization of new functions. One hypothesis of this thesis is that this combined approach will provide the most future-proof platform for the secondary system of an electricity distribution substation, resulting in the lowest overall life-cycle costs.

2.4.3 IEC 61850 standard

The increasing acceptance of the IEC 61850 standard has made it the 'de-facto' foundation on which all architectures must be based. Its increasing importance is also reflected in the title of the standard. In Edition 1, it was still called 'The Standard for Communication networks and systems in substations' [IEC, 2005], but Edition 2 (not yet fully published) uses a broader term 'The Standard for Communication Networks and Systems for Power Utility Automation' [IEC, 2009]. Its use is also spreading beyond substations, which guarantees that it will continue to be used in substations. Therefore, the standard is briefly presented here, as it is a common element in all the alternative architectures.

Station communication (IEC61850-8-1, -9-2)

The introduction and increasing acceptance of the IEC 61850 standard have made fast and standardized Ethernet-based communication more available. First, the station bus (part -8-1 of the standard) allows for the replacement of copper wiring between IEDs on a horizontal level. Secondly, the process bus (part -9-2) makes the digitized measurement information from instrument transformers available in a standardized way for other devices.

The IEC 61850-8-1 station bus utilizing GOOSE messages (Generic Object Oriented Substation Events) is already common in distribution substations, but the IEC 61850-9-2 process bus utilizing SAV messages (Sampled Analogue Value) has so far only been extensively used in transmission applications. The assumption is that the process bus also will become more common in distribution substations in the near future.

Engineering aspects (IEC61850-6)

The recently published second edition of IEC 61850-6 also impacts on the engineering process [IEC, 2009]. The use of SCL (Substation Configuration Language) is now more explicit, and in addition, the roles of different engineering tools are now more accurately defined. Although the "real tool" can play many different roles, the target of the clarification is clear. The division between vendor and/or IED-specific tasks and system-level tasks must be clear before interoperability can be guaranteed. It is not enough that IEDs from different vendors can communicate with each other

via GOOSE messages, if it is not possible to configure the two IEDs with a similar engineering flow. Several different tools at the IED level can be accepted, and this is also often necessary, but it must be possible to perform the system-level configuration with one single system-level tool. These different levels of engineering tools are described in the standard as the IED Configurator and the System Configurator. Their different roles are shown in Figure 2.8.

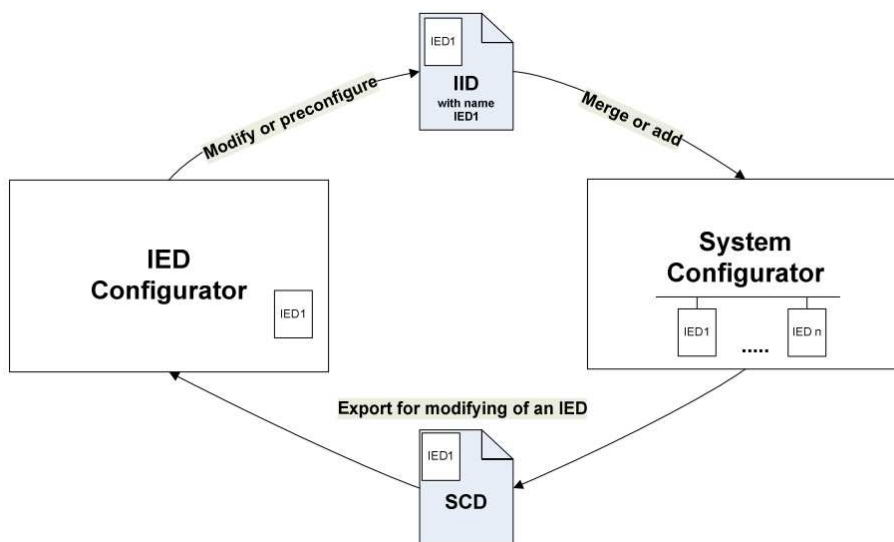


Figure 2.8: Two main levels – IED Configurator and System Configurator. Updates possible via IID files[IEC, 2009].

All engineering data is transferred via SCL files, whose context is indicated in the file extension. SCD (Substation Configuration Description) is the extension for system-level configuration files and CID (Configured IED Description) the extension for IED-level configuration files. A new extension, IID (Instantiated IED Description) was introduced in order to further clarify the IED engineering process, and this is also meant for IED configuration, and thus also shown in Figure 2.8. The difference between CID and IID is that IID does not have any GOOSE engineering information. IID is only IED-specific and does not have any information about other equipment in the substation. IID can be edited entirely in the IED Configurator, whereas CID requires information from the System Configurator. Figure 2.8 also illustrates how updating the configuration of a particular IED is made easier by using the IID file

ecution of a project. Within IID files, the configuration details of an individual IED can be updated without affecting other parts of the substation, thus, for example, reducing the need to “remap” the GOOSE signals every time the IED configuration is changed. The intended modification process with IID files is shown in Figure 2.10.

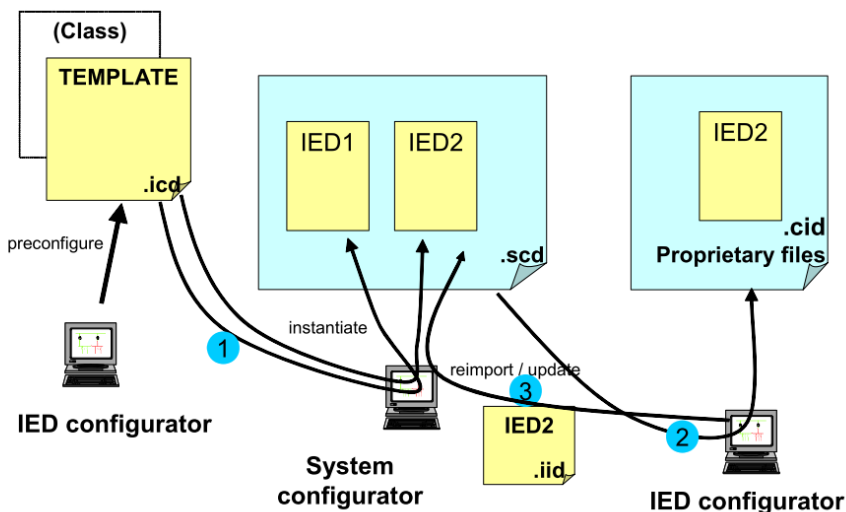


Figure 2.10: Modification process [IEC, 2009].

The implications of IEC 61850-6 Edition 2

How do the clarifications in IEC 61850-6 affect the engineering flow? What is the underlying philosophy and how should vendors address this? The second edition is a natural continuation of other activities defined in the IEC 61850 standard, whose main aim is to increase interoperability, i.e. it should be possible to use two IEDs from different vendors in the same substation without extensive additional work. The actual functionality can, and in practice also should, be different, but using these different functions in the same substation should be possible with reasonable effort. Communication via GOOSE is already possible, but the engineering should now also be possible over a similar tool chain.

The updated standard implies that it should be possible to do system-level engineering with a GOOSE configuration using an external 3rd party tool. This feature not only affects the engineering interface, but also the details of the implementation

of the functionality. The functionality of IEDs should be self-contained in a way that supports multi-vendor solutions. If, for example, advanced functionality is distributed to all the feeder IEDs which need to be configured in order to communicate with each other via GOOSE (aggregated measurement values, intermediate calculations etc.), this does not, strictly speaking, follow the spirit of the standard. It forces the utility to order all its IEDs from the same vendor because otherwise it would not be possible to use the functionality. The standard also implies that one piece of logical functionality should reside in one logical device, which in the standard is also allocated to one physical device.

Of course, with widely-used and already-standardized functions, such as interlocking, this is not an issue – the requirements for the horizontal communication data are well standardized as is the Ethernet frame of the GOOSE message. Sending interlocking information between IEDs of different vendors is feasible, and is actually in use in substations. The problem becomes more apparent with regard to new, advanced functionality, where, for example, it is necessary to share intermediate calculation results between different bays. An example of this functionality is high-impedance earth fault detection, which utilizes measurements from all bays [Abdel-Fattah and Lehtonen, 2009].

2.5 The cost-efficiency of the possible architectures

From the electricity distribution companies' point of view, there are several aspects to cost-efficiency. As previously stated, the most obvious, although least significant part in the long run, is the installation cost. If only this aspect were to be taken into account, it would lead to a highly simplified view of the concept, where centralized protection on a station computer would not be cost-efficient unless the cost saving gained through the reduced functionality of the bay-level IEDs exceeded the expenditure.

The maintenance and upgrade costs of a traditional bay-level protection system for a substation can be of the same order of magnitude as the original installation costs. This is not only due to the investment costs, but also because of the planning work for back-up connections or possible interruptions to the electricity distribution. In this case, the possibility of updating the functionality on a station computer during shorter, or even non-existent power distribution interruptions with the consequent reduced need for secondary testing, generates considerable cost savings and can even

be a decisive factor when planning future maintenance activities. Condition monitoring functionality in a centralized station computer would also help in planning these activities in advance. A more detailed analysis of life-cycle costs is presented below.

2.5.1 Life-cycle costing in different scenarios

According to [IEC, 1997] [Hinow et al., 2008] the overall LCC (Life Cycle Costs) of the equipment in an electricity substation can be broken down into the cost of acquisition C_A , the operation cost C_O and the renewal cost C_R , see (2.1).

$$C_{LC}(t) = C_A(t) + C_O(t) + C_R(t) \quad (2.1)$$

In (2.1) $C_{LC}(t)$ describes the overall life-cycle costs during a time period t . The operation costs can be further divided into maintenance costs C_M (scheduled or condition-based maintenance) and failure costs C_F (unscheduled corrective maintenance), see (2.2).

$$C_O(t) = C_M(t) + C_F(t) \quad (2.2)$$

The failure cost C_F itself is the sum of the component replacement cost C_{CR} and the penalty cost for undelivered energy C_P , see (2.3).

$$C_F(t) = C_{CR}(t) + C_P(t) \quad (2.3)$$

In this section, the estimates for the life-cycle cost of the proposed set-up are compared with other scenarios. Three different scenarios are evaluated:

- A) All functionality is decentralized in IEDs and the IEDs need to be HE (high-end) (HE) relays.
- B) All functionality is centralized within a station computer (two station computers are needed, since a back-up computer is required) and the measurements are retrieved from merging units.
- C) The set-up proposed in this thesis, i.e. a combined solution with a station computer and IEDs. The IEDs can be LE (low-end) relays, since high-end functionality is provided by the station computer

These three scenarios are evaluated with different cost factors: acquisition costs, renewal costs, and maintenance costs. In addition, failure costs are calculated for the different fault cases. The main purpose is not to derive full life-cycle cost calculations

for each scenario, but to indicate the areas where the life-cycle costs differ between scenarios. The calculations are done for a 40-year period, in which the value of many of the cost components will change, e.g. the interest rate on investments, the acquisition cost of the equipment, the customer outage costs, the consumer price index and the value of money in general. These changes are not taken into account in the calculations, since they have a similar effect on all the scenarios and it can be assumed that they will not result in any additional differences between the scenarios.

The cost components also include factors which are impossible to fully estimate accurately over a 40-year period. An example of this is the acquisition costs of the equipment presented in the next section. It is impossible to estimate the price of the substation automation equipment over 40 years accurately. This is particularly true if the concepts behind this thesis become a reality, i.e. if the substation automation architecture moves towards a more centralized architecture. Such a fundamental change in automation architecture will also eventually change the pricing structure of IED vendors, and may well bring about new competition in this business area. Therefore the analysis is performed based on the current cost structure, without making any presumptions about future price developments.

2.5.2 Acquisition costs

In order to obtain acquisition costs, it is necessary to make rough estimates of unit prices (both for acquisition and renewal) and of the expected intervals for renewal, and these are shown in Table 2.1. The prices are based on a survey made for the Finnish Energy Market Authorities [Pahkala et al., 2010], which is aimed at assessing reasonable pricing for electricity distribution and transmission network services. As indicated above, the analysis is performed based on the current cost structure, without making any presumptions about future price developments. In the survey, the protection and automation devices for one feeder (including planning, installation and wiring) had the unit price of €5900, and the basic automation infrastructure (including planning, RTU, communication modems and installations) had a unit price of €13,900.

As the prices were average total prices, some additional estimations were needed. Enquiries to IED vendors resulted in using the total automation price of one feeder for the HE relay, and half of that for the LE relay. The most difficult item to evaluate was the station computer, as it is an item which is not yet on the market. In order

Table 2.1: Price and Renewal Interval for Different Equipment

	Acquisition / k€	Renewal / k€	Ren.Interval / a
High-end relays	6	6	15
Low-end relays	3	3	20
Merging units	1	1	20
Station computer	20	3	2
Back-up computer	20	20	20

not to give too positive a picture of the centralized set-up, an estimate of two times the price of the RTU (assumed to be €10,000 out of total of €13,900) was used, as shown in Table 2.1. The life-span of the IEDs is estimated to be 15-20 years [Lassila et al., 2002], of which two alternatives the shorter 15-year period was selected for the HE relay and the longer 20-year one for the LE relay. Furthermore, no separate prices were given for merging units, so an estimate of one third of the price of the LE relay was used to describe the limited functionality of a merging unit. The life cycle was assumed to be the same as with LE relays, because for both items the life cycle of the electronics is the limiting factor.

The renewal price is the same as the acquisition price for all the items except the station computer. The station computer is expected to be updated more frequently, and in these cases most of the renewal actions consist only of software updates. In a fully centralized set-up, the second station computer is only needed for back-up functionality, and therefore the same update interval is estimated as for the low-end relays.

When using the unit prices from Table 2.1, acquisition costs for different scenarios are as shown in Figure 2.11. Based on Figure 2.11 one can conclude that using only bay-level high-end relays is the most cost-effective solution in most of the cases. When a substation has more than seven feeders, the combined set-up is the most cost-effective. When the number of feeders exceeds 10, having a fully centralized set-up yields the lowest acquisition costs.

2.5.3 Acquisition and renewal costs

If the renewal costs are also taken into account, the situation changes. High-end relays have a shorter life cycle, since all the functionality required for the substation needs to be realized through the IEDs. This means a faster upgrade cycle has to be

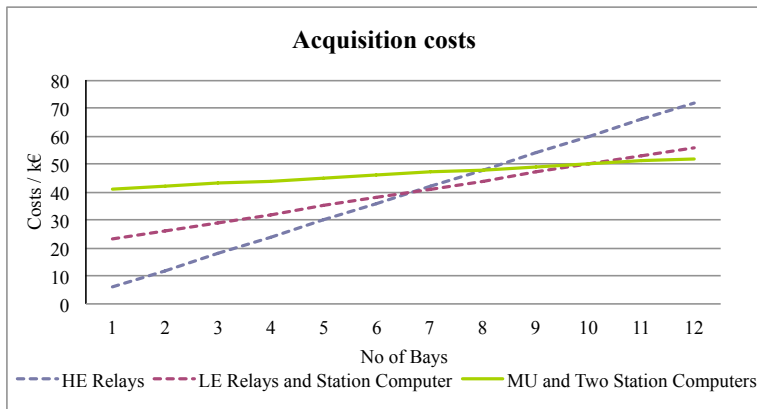


Figure 2.11: Acquisition costs for different scenarios.

applied than in the other scenarios (15 years). The life cycle of the low-end relays and the back-up station computer is estimated to be the same (20 years). The life cycle of the station computer is set to as low as two years, in order to capture the dynamic nature of any future substation. On the other hand, these upgrades are mainly SW updates, which mean inexpensive renewals. Using these parameters, the overall costs for a 40-year period would be as shown in Figure 2.12.

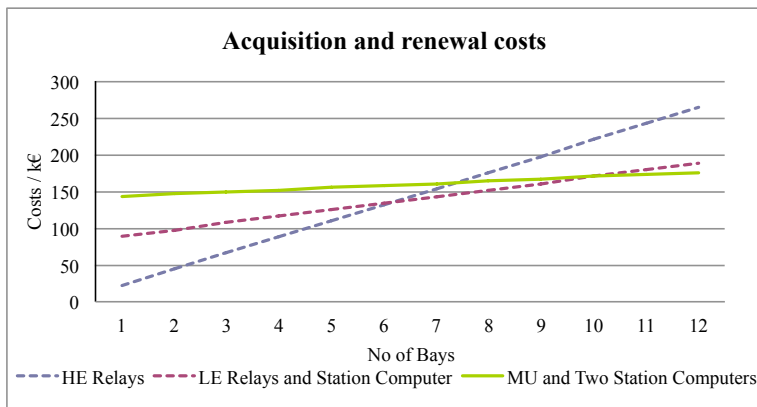


Figure 2.12: Acquisition and renewal costs for different scenarios.

This addition already makes the scenario with a station computer and low-end relays more cost-effective, when the substation has only six feeders.

2.5.4 Acquisition, renewal and maintenance costs

The next item to be included in the life-cycle cost is the scheduled maintenance. The secondary system always needs scheduled testing, regardless of the scenario. These maintenance activities are not taken into account individually, but instead only those activities that differ between the scenarios are calculated, such as the maintenance activities during the renewal. The previous calculations have only taken into account the cost of equipment during the renewal. However, a renewal also requires the utilities to take other actions not directly related to the equipment, such as project planning, gathering quotations, vendor selection, planning temporary network topologies during the renewal, the execution of switching operations for back-up connections, etc. Accurate statistics for these costs were not available, but according to estimates from Finnish utilities, these operations require roughly one and a half man-months per substation, which in Finland amounts to approx. €15k in additional costs.

These maintenance costs have the same interval as the primary protection of the station, which in this example means 15 years for a fully decentralized set-up and 20 years for both of the centralized set-ups. Taking these additions into account, the costs for the secondary system are as shown in Figure 2.13.

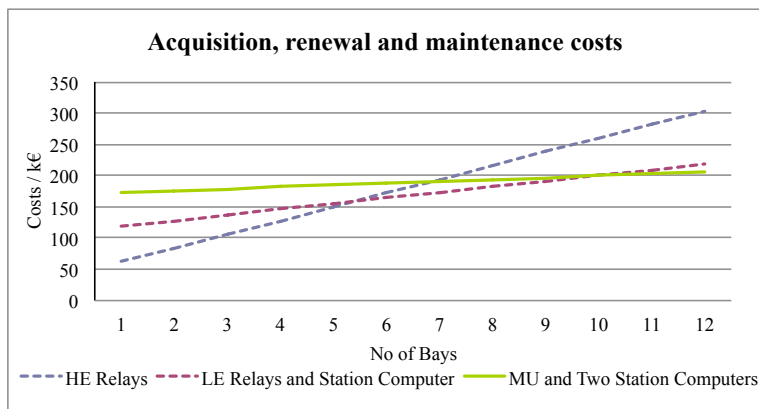


Figure 2.13: Acquisition, renewal and maintenance costs for different scenarios.

This addition makes the centralized set-up even more economically viable, in that a centralized set-up can be justified even for a substation with only five feeders.

Case example: maintenance cost of the main transformer

In addition to the maintenance costs of the secondary system itself, the functionality in the substation also affects the maintenance costs of other substation components. As mentioned in section 2.3, a substation's functionality needs to support the utilities' asset management procedures. Asset management as a whole is a large topic, so instead of a full analysis, one example case for a substation main transformer is presented.

The main transformer of a substation is the single most expensive component of the substation, with 19% asset value share of the whole network [Jeromin et al., 2009]. According to [Pahkala et al., 2010] the cost varies from €246 k (for a 6 MVA transformer) to €900 k (for a 100 MVA transformer) with main transformers from 110kV to 10/20kV. Because of these costs, condition monitoring of the transformer is an important aspect of asset management. For example, the rated temperature of the transformer must not be exceeded, because that would shorten the lifetime of the transformer, leading to premature maintenance. On the other hand, too large a safety margin would mean that the transformer would be oversized. If the improved functionality in the protection and automation system were to allow, say, the use of a 16 MVA transformer instead of a 20 MVA one, this would instantly yield a saving of €40 k in the investment phase. Furthermore, an improvement in automation can result in postponing the replacement of the transformer, due to, for example, the lower operation temperature of the transformer, which would yield yet further savings.

2.5.5 Failure costs

Although it is more difficult to estimate, the factor which can have the largest impact on the overall costs is the cost saving gained by increasing the reliability of the distribution network. When the substation automation functionality is up-to-date, it can be assumed that the overall performance will be better than it was before the update, i.e. the protection would be more selective (less unwanted trips), the fault situations would be cleared faster, the areas affected by the faults would be smaller, and the maintenance requirements would be more accurately known, etc.

However, this factor is very difficult to estimate. What is the reliability of a 10-year old secondary system, compared to a 1-year old system? How often does the secondary system malfunction? Furthermore, what would the answer to these two questions be in 10 years time? For distribution networks in particular, there are no

accurate statistics for these factors as the utilities have not had the resources to collect and analyze the statistics on secondary system failures. The financial consequences of faulty operation can also vary greatly. One unwanted trip on an outgoing feeder might not have any real effect on the ENS (Energy Not Supplied). On the other hand, one missing operation on the outgoing feeder protection can trigger the protection on the incoming feeder, causing an interruption to the whole substation.

To better understand the costs of a failure, an assessment of the average outage times in Finnish distribution networks has to be carried out. The financial consequences can then be evaluated based on these average values, and according to specific cases of use.

Customer outage costs in Finland

The importance of an uninterrupted electricity supply has increased steadily over the years, and is well illustrated by the estimated customer outage costs. Over the past 10 years these costs have doubled, or in some cases even tripled [Partanen et al., 2006]. Nevertheless, it would be wrong to assume that this trend will continue in exactly the same way. Recent studies have shown that it looks more likely that the differences between the different customer groups will grow. For many consumers, an uninterruptible electricity supply is not critical, and therefore the increase in customer outage costs can be expected to stay within reasonable bounds. On the other hand, in specific industry and service areas the outage costs may increase considerably. The most recent results from the evaluation of customer outage costs in Finland for different customer groups are shown in Table 2.2 (at 2005 prices) [Partanen et al., 2006]. The weighted average values in Table 2.2 are the ones used in the Finnish regulation model [EMV, 2011] (also at 2005 prices). The consumer price index maintained by the Official Statistics of Finland (OSF) indicates an increase of 13.6% for the values in Table 2.2 in terms of 2011 prices [OSF, 2011], but for the sake of clarity, this is not taken into account in these example cases.

Table 2.2: Customer Outage Costs in Finland for Different Customer Groups [Partanen et al., 2006] [EMV, 2011]

	Unplanned		Planned	
	€/kW	€/kWh	€/kW	€/kWh
Households	0.36	4.29	0.19	2.21
Agriculture	0.45	9.38	0.23	4.80
Industry	3.52	24.45	1.38	11.47
Public	1.89	15.08	1.33	7.35
Services	2.65	29.89	0.22	22.82
Weighted average	1.1	11.00	0.5	6.8

Average outage times in Finnish distribution networks

The Finnish Energy Industries authority (Energiateollisuus ry, ET) publishes interruption statistics every year. The results from the past six years and the calculated average values are shown in Table 2.3 [Energiateollisuus, 2005-2010], and include both long interruptions (permanent faults) and short interruptions (faults cleared by auto-reclosing).

Table 2.3: Amount of customer outages in Finland 2005-2010 [Energiateollisuus, 2005-2010]

	2005	2006	2007	2008	2009	2010	Average
Time (h)							
Short Interruptions (h)	0,12	0,05	0,05	0,06	0,11	0,07	0,08
Long Interruptions (h)	2,36	1,57	1,15	1,56	0,92	3,22	1,80
Planned Interruptions (h)	0,48	0,31	0,3	0,31	0,3	0,36	0,34
All Interruptions (h)	2,96	1,93	1,5	1,94	1,3	3,61	2,21
Amount (pcs)							
Short Interruptions (pcs)	10,02	3,54	4,45	4,94	3,89	5,98	5,47
Long Interruptions (pcs)	3,52	1,92	1,66	1,8	1,32	2,45	2,11
Planned Interruptions (pcs)	0,55	0,25	0,26	0,22	0,24	0,31	0,31
All Interruptions (pcs)	15,19	5,71	6,38	6,96	5,43	8,72	8,07

2.5. The cost-efficiency of the possible architectures

Using the average outage values from Table 2.3 and the weighted average values from Table 2.2, the overall outage costs for a 40-year period are as shown in Figure 2.14, assuming that the outage costs and interruption times remain similar during that period. In these calculations, 0.81 MW was used for the power of one feeder, i.e. the average power of feeders in Finland, this also being calculated from the statistics of ET. When this chart is compared to the other costs calculated in Figure 2.13, we can see the proportion of outage costs in comparison with the overall costs. An interesting way to view to these charts is to calculate the ratio between the costs, i.e. only 2.4% of all the interruption costs equals all the costs of the 'High-End relays'-scenario shown in Figure 2.13. Remember that the aim of this calculation was not to derive exact cost shares, but to indicate how much larger the outage costs are in comparison to the other costs.

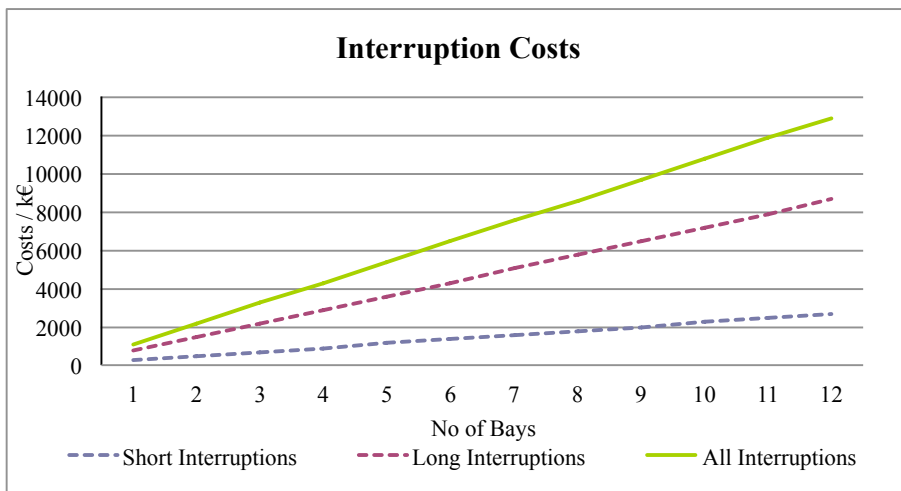


Figure 2.14: Total interruption costs.

The reliability of the protection system

An attempt was made to estimate the cost of protection failures in Norway [Kjølle et al., 2005]. The paper presents the key results gained from a study of incorrect operation of protection and control systems at voltage levels of 1-420 kV in Norway, consisting mainly of incorrect and missing operations. The statistics for the period 1999-2003 show that incorrect or unwanted operation is a major fault type,

and that the relative number of faults and their contribution to the ENS increases as the voltage level rises. The study estimated that of all the ENS due to faults in the distribution network, approximately 5% were due to failures in the protection system, and approximately 1.5% of all the operations were faulty. 46% of all the failures were unwanted operations and 6% were missing operations; the remaining 48% of failures were not accurately specified. Unfortunately, the detailed results for the distribution networks were insufficient, and only gave an overview of the percentage of faulty operations.

The outage statistics of ET include some analyses of the causes of the fault, but unfortunately those statistics are also limited [Energiateollisuus, 2005-2010]. Between the years 2005 and 2010, on average over 11% of all faults were due to faulty construction or faulty operations. However, no detailed division into faulty relay operations was provided. Furthermore, on average as much as 22.5% of the faults were attributed to 'unknown cause'.

Because of these deficiencies in the statistics, it was not possible to carry out an accurate evaluation of the cost of faulty relay behavior. Instead, a few scenarios were evaluated in order to show the cost impact under different assumptions. The first reference point was set to this moment; a certain percentage of all interruptions at a given moment are unnecessary and faulty. Then, assuming that the reliability of the protection system will improve in the future, a reliability graph was created, as shown in Figure 2.15.

In Figure 2.15, the reliability for year zero was set as the reference point. The blue line in the figure represents the estimated maximum achievable reliability. In this case, it is assumed that after 15 years the reliability of the protection will be higher than it is today. The red line in the figure represents the change in the reliability of the decentralized set-up. After installation, the reliability starts decreasing for several reasons, e.g. the equipment is aging or the parameterization becomes outdated due to changes in the network. This is shown in the figure as a decline, based on the assumption that without upgrade measures a larger proportion of all operations would be faulty after 15 years. The aim of Figure 2.15 is to illustrate the benefits of a centralized set-up. The functionality is constantly near the state-of-the-art level due to frequent updates, but the maintenance costs are kept at a minimum.

How much the reliability might improve within 15 years (and how much the reliability of the decentralized set-up might decrease) is not known, due to insufficient statistics. This is also the reason that there are no numeric values on the Y axis in

2.5. The cost-efficiency of the possible architectures

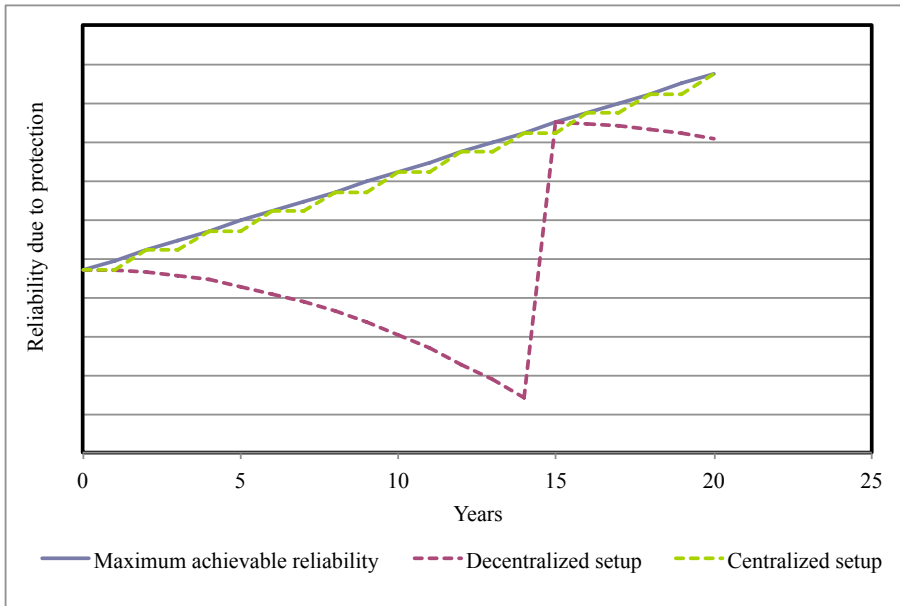


Figure 2.15: An example reliability graph of protection

Figure 2.15. Instead, different scenarios were evaluated, and the results of this are shown in Figure 2.16.

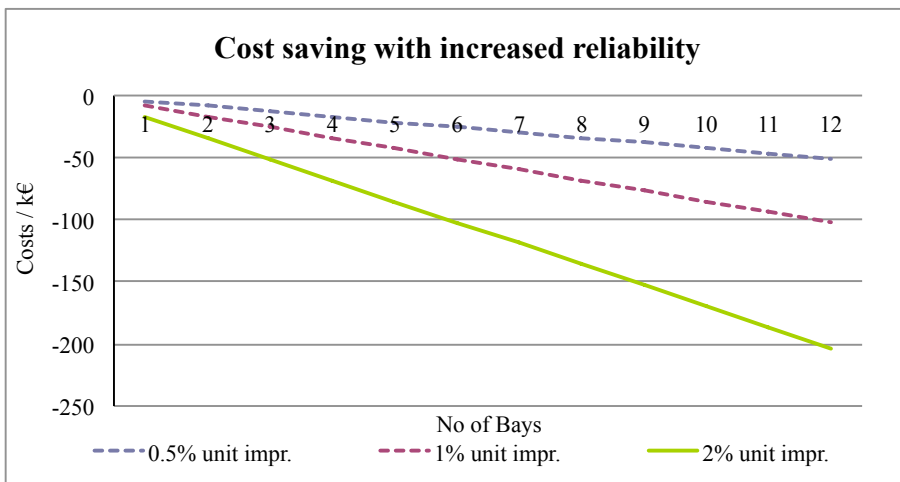


Figure 2.16: Cost saving with different scenarios.

The curves in Figure 2.16 represent three different scenarios. The zero level in the figure indicates the reference case, in which the reliability of the protection devices remains the same during the whole 40-year period. The '0.5% unit impr.' scenario means that after 15 years there are 0.5% fewer unnecessary trips per unit. In other words, if the amount of unnecessary trips were 5% today, after 40 years it would be 4.5%. Similarly '1% unit impr.' describes a scenario with 1% unit improvement, and '2% unit impr.' a 2% unit improvement. The cost saving in this last scenario would already be on a par with all the other costs shown in Figure 2.13.

Case example 1: Unnecessary tripping of one feeder

The first example case to be evaluated was the cost of an interruption in one feeder. The outage costs were calculated for when one feeder experiences an unnecessary trip and customers have an interruption in the energy supply due to a malfunction in the protection. The results for one single interruption with different outage times and for different customer groups are shown in Table 2.4. The first five cases assume that all the customers of the particular feeder belong to the same customer group, and the last, the 6th case, is a weighted average feeder [EMV, 2011].

Table 2.4: Cost of one interruption in one feeder (in k€)

Case	Customer group	Outage cost (k€)			
		1min	6 min	60 min	120 min
1	Households	0,35	0,64	3,78	7,27
2	Agriculture	0,49	1,13	7,99	15,62
3	Industry	3,19	4,85	22,74	42,63
4	Public	1,74	2,76	13,80	26,06
5	Services	2,56	4,59	26,46	50,76
6	Weighted Average	1,04	1,79	9,84	18,78

Table 2.4 illustrates the differences between different customer groups. If one feeder line contains only household customers, the outage costs are negligible, but the cost for industrial customers is from five to nine times higher.

Case example 2: Missing trip in one feeder, causing an unnecessary trip for the whole substation

The second example deals with a missing operation. If the protection in one feeder fails, and the back-up protection in the incoming feeder trips instead, all the other healthy feeders experience an unnecessary trip. According to ET statistics [Energia-teollisuus, 2005-2010] the average size of a Finnish substation is ten feeders, which means that nine of them would be tripped unnecessarily. The outage costs in this case are shown in Table 2.5, again with six different cases.

Table 2.5: Cost of one interruption in the whole substation (in k€)

Case	Outage time(min)	Outage cost (k€)			
		1	6	60	120
1	Households	3,16	5,77	34,03	65,43
2	Agriculture	4,44	10,16	71,94	140,58
3	Industry	28,74	43,65	204,69	383,63
4	Public	15,67	24,87	124,19	234,55
5	Services	23,04	41,27	238,14	245,88
6	Weighted Average	9,39	16,10	88,55	169,05

The total costs derived for different scenarios in Figure 2.13 were in the range of €200 - 250 k for a substation with 10 feeders. One single 60 minute outage in a substation with only industrial customers would cost the same. On the other hand, a substation in a residential area could experience six similar events before the other costs in Figure 2.13 were exceeded.

2.5.6 Summary of LCC cost estimates

The currently prevalent approach of using only bay-level IEDs will only be economically justifiable in the future in very small substations. In contrast, according to the estimates presented earlier in this chapter, a substation with more than five feeder bays should utilize centralized station computers. The calculations presented here very much depend on the initial costs given in Table 2.1. Depending on the initial cost estimates, the size of a substation for which the centralized set-up becomes more cost-effective can vary. Nevertheless, it is clear that the larger the substation, the more likely a centralized station computer will decrease life-cycle costs.

However, as stated earlier, the costs incurred through failure in the delivery of electricity are much higher than all other the costs combined, at least in Finland with the outage costs that apply to Finnish networks (presented in Table 2.2). This confirms the main idea behind this thesis, i.e. investing in substation automation is a cost-efficient way of improving the reliability of the network. Of course, this applies to all the evaluated architectures, and not just to the set-up proposed here, which is based on a centralized station computer.

2.5.7 Other benefits of the combined set-up

As shown earlier, upgrading functionality in IEDs is a problematic task. It demands updates to the whole protection system of the substation. Updates are expensive, not only because of new installations and new equipment, but also because of the required manual engineering, commissioning and testing work. If the functionality utilizes measurements from more than one bay, an implementation at the IED level is only possible when all the IEDs are from the same vendor.

According to the IEC 61850 standard, and also from the engineering point of view, it is beneficial that system-level engineering and functionality do not have unnecessary IED-level vendor-specific features, such as algorithm-level communication based on intermediate calculations. This also means that unnecessary GOOSE engineering at the substation level should be avoided. In addition to the extra engineering work, testing and commissioning in such environments is a complex task, not to mention the documentation and maintenance issues. When the new functionality can be encapsulated within one logical device, the amount of system-level communication engineering is reduced. Testing, maintenance and documentation at the system level is also reduced compared with a situation where the functionality includes system-level communication engineering.

The architecture proposed in this thesis, which is based on centralized station-level protection devices and the IEC 61850-9-2 process bus, provides a framework for these new logical devices. When all the measurements are available at the station level via the IEC61850-9-2, it is feasible to implement new functionality by hooking in to the process data via the process bus. Ideally, system-level configuration can be avoided entirely. One example of such a station function which is already on the market is the high impedance earth fault protection. There are solutions which require measurements (and separate wiring) to all the feeder bays in order to guarantee de-

tection of high-impedance earth faults [Tengdin, 1996][Abdel-Fattah and Lehtonen, 2009] [Nikander, 2002].

This approach reduces the complexity of bay-level IEDs and the bay-level IED engineering tools. Functionality can be divided into logical devices, which is also the target of the standard. These logical devices could then be acquired from different vendors and added to the substation as they all share the same interface – measurement data via SAV messages as defined in IEC 61850-9-2 and other communication via GOOSE messages as defined in IEC61850-8-1.

The engineering flow could be adjusted so that functional engineering would be directed via the IID files introduced by IEC 61850-6 Edition 2. When a function resides in one IED/Computer/Logical device, it can be updated and tested without affecting the system-level configuration. Functionality requiring changes to the full system configuration should be avoided as it incurs high costs during the upgrade and commissioning.

In practice, this approach moves some of the implementation from the GOOSE signals to the logical device's internal logic. This implementation can be vendor-specific, whereas GOOSE should not be. The proposed architecture enables new advanced functionality to be added as a single module at the station level – such a module could be either new equipment or even a new module in a centralized SW platform, as envisioned by the Swedish utility, Vattenfall [Johnson et al., 2010].

2.6 Details of the proposed architecture

This section describes the elements of the architecture investigated in this thesis, and referred to in earlier sections as the 'combined set-up'. This set-up is based on centralized protection and control functionality, which complements but does not replace the functionality of the bay-level protection and control IEDs. The overall structure of the proposed architecture is presented in Figure 2.17.

2.6.1 Important standards

IEC 61850 modeling and station communication

As already described in section 2.4.3, nowadays IEC 61850 has become the 'de-facto' standard. The recent additions and clarifications, which are also mentioned in the same section, have made it clear that future IEDs need to fully support IEC 61850. In

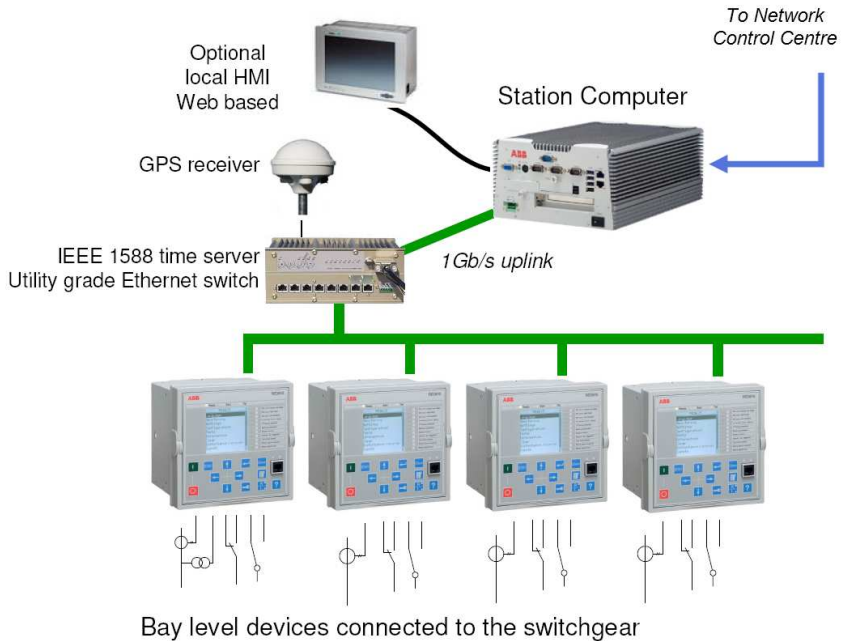


Figure 2.17: Overall set-up of a centralized protection and control system.

most respects this is already the case, and does not need any further comment. One aspect not yet used in distribution automation is the process bus specified by IEC 61850-9-2, yet for the reasons presented in this thesis, in the future it is more than likely that this process bus will be used.

IEEE 1588 time synchronization

With Ethernet-based technology it is possible to achieve software-based time synchronization with an accuracy of 1 ms quite easily, and without any help from HW. This is also what the IEC 61850 standard refers to as the basic time synchronization accuracy class (T1) [IEC, 2005].

An older and more common protocol is the SNTP (Simple Network Time Protocol), which is suitable for local substation synchronization in relatively small systems Ferrari et al. [2011]. However, if the SNTP server is behind multiple Ethernet nodes, the latency increases, which reduces the accuracy of the time synchronization. Therefore, SNTP is not an ideal solution for system-wide implementation. Normally

a GPS or equivalent time synchronization resource is required in every substation.

IEEE 1588 [IEEE, 2009] deals with these issues and makes it possible to achieve a time synchronization accuracy of 1 μ s. This is required if an IEC 61850 process bus is used. IEEE 1588 provides a cost-efficient and accurate method for system-wide time synchronization, where the network devices are able to correct the node delays into time synchronization frames. The application notes from technology vendors promise even greater accuracy of 10 ns [Texas Instruments Inc., 2007].

2.6.2 Protection and control IEDs

Using this concept, the protection and control IEDs are still seen as important components of the secondary system. They handle the time-critical basic protection functions, and they also communicate with a centralized station computer. The main idea is that the protection and control IEDs are 'freed' to perform their original and mission-critical operations. By removing the non-critical functions from the bay-level devices the life cycle of the devices can be maintained at the current level. Traditionally, the life-span of these devices has been 15-20 years [Lassila et al., 2002], largely due to the lifetime of the electronics used in the device. The aim is to retain the same life-span and to avoid the need for early updates for application or functional reasons. A more detailed description of the 'time-critical basic protection' functionality which would still be needed in bay-level devices will be presented in Chapter 4.

One important feature of the bay-level devices is that they support the relevant and most important standards, so that it is feasible to integrate new devices and/or functions later on. These standards have been presented earlier in this chapter, and for the architecture investigated in this thesis the most important ones are IEC 61850 and IEEE 1588.

2.6.3 Station computer

In the proposed architecture, the centralized station computer handles all the advanced functionality. As the primary protection is covered by bay-level IEDs, the functionality in the station computer can be updated at will without affecting the safety of the network, allowing fast and smooth updates.

Another important factor is that with small (less than 5 feeders) substations, the

most economically viable solution is to use only bay-level devices. The concept proposed here allows this, and the centralized station computer can also be added later, provided that the bay-level devices that are used support the required standards. This means that future updates can be installed without the need to renew the whole secondary system, and cost-efficient migration scenarios can be utilized, guaranteeing optimal utilization of investments made today.

Unlike the IEDs, the station computer is not directly connected to the measurement devices. The IEDs handle the measurements and send them on to the station computer (as well as using the measurements themselves for protection purposes). When these measurements (and other relevant data, such as control commands and status information) are sent according to IEC 61850, it is purely Ethernet-based. This is an important benefit, as it enables the use of standard industrial PC technology as a base, and provides for better economies of scale than the dedicated designs for embedded systems which are currently utilized in protection and control IEDs.

The functionality in the station computer can be broadly divided into two categories. First, there is the protection and control functionality, which needs real-time process data and directly affects network safety. This functionality has strict requirements for reliability and cyber security.

The second category is offline functionality, which can operate based on historical information. This functionality only indirectly affects the network's safety via, e.g. the condition monitoring and fault analysis functions. In this functionality, open interfaces can be provided for 3rd party functions, and multi-vendor SW platforms are possible. This categorization is presented in Figure 2.18. Here, the 'Data Storage' describes the data to which external partners may have access, and a database symbol highlights the fact that the data does not directly affect the control and protection of the network.

It should be noted that, currently, protection and control devices hold many functions with different 'functional life cycles'. Many basic protection functions can be expected to remain the same throughout the life cycle of the IED, whereas, say, a new fault location algorithm may be superseded by a new improved version as early as the following year. The aim of this concept is to locate those functions that have different life cycles in different places, thus retaining a long life cycle for the IEDs while simultaneously allowing a shorter life cycle for the station computer. This approach will be studied further in Chapter 4.

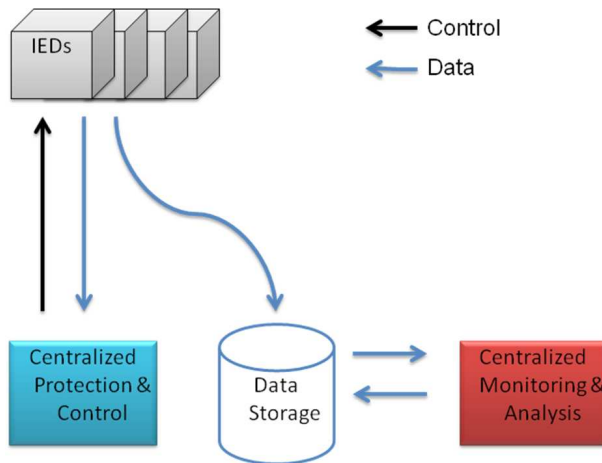


Figure 2.18: Separate functionality for centralized protection and monitoring.

2.7 Pilot installation of the selected architecture in Noormarkku

A pilot installation was implemented in the substation located at Noormarkku village in Finland. This was done in cooperation with Fortum and ABB in 2008, during the IDA project mentioned in section 1.2. The purpose was to have a 'proof-of-concept' type of pilot, which would show that time-critical protection functionality can be achieved with the architecture proposed in this thesis. The pilot installation consisted of the following items:

- Bay-level protection and control IEDs supporting both the station bus defined in IEC 61850-8-1, and the process bus defined in IEC 61850-9-2, but not supporting IEEE 1588. There were 8 feeder bays in the pilot installation.
- One station computer, utilizing standard PC technology and supporting IEC 61850-8-1, IEC 61850-9-2 and also IEEE 1588
- IEEE 1588 time synchronization master
- The required wirings from voltage and current transformers to the bay-level devices

- Communication between the station computer and the bay-level devices realized with optical fibers

The functionality in the station computer consisted of overcurrent protection, and also control logics for the CBs with interlocking functionality. The time synchronization was not fully tested, as the bay-level devices did not support IEEE 1588. Furthermore, the devices were installed next to the existing protection relays. i.e. the trip signal from the IEDs used in the pilot was not connected to the trip circuit. What the pilot clearly showed was that the proposed architecture can be implemented with the existing technology. During the 1-month pilot period there were no real fault cases, so it was not possible to verify the system's operation during fault situations. The project ended after the piloting period.

2.8 Chapter summary

Because of the increasing use of distributed generation, and other active resources, distribution substations require more intelligence. As the significance of these “Smart Grid impacts” is not yet known, the secondary system needs a faster upgrade cycle than it has done previously. Any future architecture for the automation of a distribution substation needs to enable this without increasing the life-cycle costs. To address these life-cycle cost challenges, the architecture proposed here utilizes a centralized station computer and new communication and time synchronization standards.

The currently prevalent approach of using only bay-level IEDs will only be economically justifiable in the future for substations with a maximum of five feeders. In contrast, the calculations presented in this thesis show that a substation with more than five feeder bays should already utilize centralized station computers. However, the costs of undelivered electricity outweigh all the other costs combined, at least in Finland with the outage costs calculated for Finnish networks. This further emphasizes the importance of upgradeability for the substation automation system.

Both centralized substation functionality and the second edition of IEC61850-6 support a more modular view of the secondary system. This modularity should be utilized, because the possibility of upgrading functionality without affecting the system-level communication engineering reduces the cost of an upgrade and increases the cost-efficiency of the distribution network, thanks to the optimal and fast deployment of new state-of-the-art functionality.

The calculations presented here very much depend on the initial costs given in Table 2.1, and especially on the estimates for the reliability of the protection system. More detailed results cannot be provided without further research into the reliability of the protection system. Depending on the given values, the size of a substation for which the centralized set-up becomes more cost-effective can vary. However, the main point is clear, i.e. the larger the substation, the more likely it is that a centralized station computer will reduce the life-cycle costs.

The requirements presented in section 2.3 may also compel the implementation of faster renewal cycles on the decentralized set-up than the estimated 15 years, making the benefits of centralization even more persuasive.

Chapter 3

Station Measurements

This chapter shows how station-level measurements can be used to achieve additional measurement accuracy. Chapter 2 mainly focused on showing how the existing protection system could be implemented in a more cost-efficient way with a different architecture. This chapter takes another approach. It seeks out what more can be done with the proposed substation automation architecture, i.e. what features can be implemented in the proposed architecture which can not be implemented with the currently dominant architecture, utilizing only bay-level IEDs.

3.1 Measurement replacement

When all the current measurements are locally available, a missing current measurement can be calculated with the help of Kirchhoff's current law. This can be useful if, for example, one of the measurement transformers is out of order and measurements are not available.

Another option is to save costs by removing unnecessary measurement transformers or sensors entirely, and sharing the measurement data from another IED. Normally, with current measurements, this is not feasible, as for safety reasons each feeder must have its own current measurements available. But for voltage measurements this is a possible option - phase voltages measured from the busbar could be delivered to all the feeder bays with IEC 61850-9-2, which would yield cost savings as only one measurement chain would be needed [Starck et al., 2012].

However, in this thesis these issues are not studied further, and instead, the main

focus is on measurement merging, i.e. what can be achieved by merging the measurement streams from different devices.

3.2 Measurement merging

3.2.1 Introduction

Modern protection and control IEDs in a distribution network have a fairly moderate sampling frequency, typically in the range of 1- 2 kHz [ABB Ltd, 2010]. This is because most of the functionality in the IED is based on phasor measurements, calculated from the nominal frequency components of the phase currents and voltages. A higher sampling frequency does not bring any benefits when calculating the components of current and voltage measurement signals with a nominal frequency of 50 Hz or 60 Hz.

Much research has been done regarding transients in power systems. Whenever a change occurs in the status of the network, e.g. due to a fault, there is also always a transient phenomenon involved. The generated transients normally have a higher frequency than the system frequency, between 100 Hz and several kHz [Lehtonen and Hakola, 1996]. According to the Nyquist-Shannon sampling theorem, a 1 kHz signal should be detectable with a 2 kHz sampling rate [Phadke and Thorp, 1990], but this is not fully applicable for transients. The transients last for just a few milliseconds and therefore the number of data points is low, especially if the sampling frequency is low.

Methods based on transient measurement have rarely been used in IEDs. The additional unit costs of the IEDs with higher sampling frequencies (and the additional CPU performance it requires) have been considered too high compared with the benefits they can provide. Furthermore, there has not been great customer demand for transient-based methods, as in most cases, the standard measuring methods based on fundamental frequency components have been sufficient.

This thesis introduces a method for increasing the sampling frequency of current and voltage measurements in an artificial way, by processing multiple measurements on a lower sampling frequency.

3.2.2 Time-Interleaved ADC (TI-ADC)

Acquiring high sampling frequency with low cost ADCs (Analogue-to-Digital Converters) is a constant target in signal processing [Vogel, 2005]. Time-interleaved technology approaches this target by using multiple ADCs, which have the same sampling frequency but different sampling phases. The architecture is shown in Figure 3.1 [Vogel, 2005], where each ADC has a sampling frequency of f_s / M , where M is the number of ADCs and f_s is the sampling frequency of the combination. The timing diagram of the system is shown in Figure 3.2, where the sampling period of the combination is T_s , but the sampling period of an individual ADC is $M T_s$.

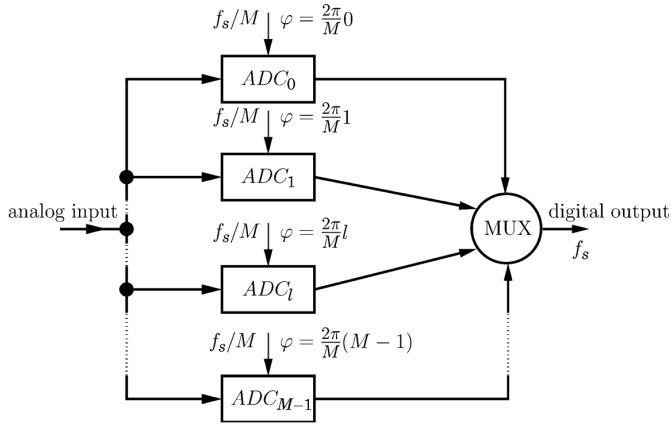


Figure 3.1: Time-Interleaved ADC with M channels [Vogel, 2005].

The concept itself is not new [Black and Hodges, 1980], but technological challenges have limited the number of actual implementations to just a few. The main issue is that any mismatch between the individual ADCs introduces spurious components into the spectrum, thus degrading the SINAD (Signal-to-Noise-And-Distortion ratio)[Vogel, 2005]. These mismatches consist of differences in gain, offset and timing, where timing refers to the deterministic deviation between the ideal and the real sampling time, resulting from an inaccurate synchronization of the ADCs. Stochastic timing deviation from each ideal sampling point is a separate error source, often referred to as the timing jitter.

Both the individual and combined effects of these mismatches have been extensively studied in various scientific publications [Vogel, 2005] [Soudan and Farrell,

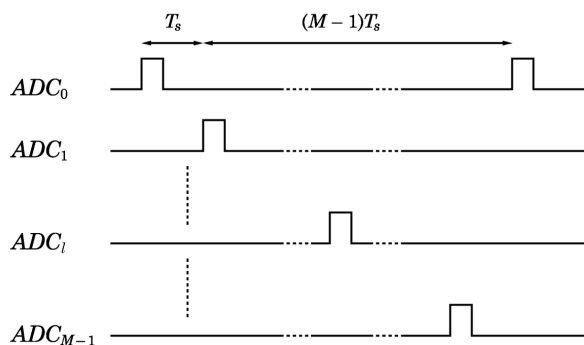


Figure 3.2: Timing diagram of time-interleaved ADC with M channels [Vogel, 2005].

2008]. Several different compensation methods have also been investigated for correcting these errors, also presented in [Vogel, 2005]. A more detailed error analysis suitable for protection and control IEDs is presented later on in this thesis.

The advancements in substation automation presented earlier offer the option of utilizing the TI-ADC concept in distribution substations, and this is explained in more detail below.

3.3 Increasing sampling frequency at the substation level

3.3.1 General concept

The concept presented here is based on a synchronized sampling of all IEDs. But the synchronization is not done in such a way that each ADC performs the measurement at exactly the same time stamp. The synchronization is done by time shifting the sampling in the IEDs by a fraction of the sample time.

If, say, five IEDs with a 2 kHz sampling frequency measure the same phase voltage, the IEDs are synchronized so that samples from the same time actually have a time difference of $1 \text{ s} / 2000 / 5 = 100 \mu\text{s}$. This means that, over a period of one second, one would get 10,000 samples, all of which have different time stamps, instead of 10,000 samples from only 2000 different time stamps (5 separate samples from each time stamp). The effect this has on the time synchronization of the IED will be presented later on, in section 3.4.5. The method is not dependent on a continuous external time synchronization signal (e.g. via GPS), but the requirement is that the

IEDs are locally synchronized to each other.

So in theory, the sampling frequency can be increased to the sampling frequency of one IED times the number of IEDs in the substation. In practice, the case is not quite that good, since the sample stream of each IED passes through an anti-alias filter which reduces the bandwidth of the resulting sample stream. This aspect will be discussed in more detail in the following sections.

The method, known as Time-Interleaved ADC, has been used in ADC design, but only within one measurement unit. All the ADCs have been located on the same PCB (Printed Circuit Board), and thus, viewed from outside the combination appears as one single ADC. Currently the applications of the concept have focused on telecommunications and software radio [Soudan and Farrell, 2008]. The concept has not so far been used in this context, i.e. within a substation and between separate IEDs. Other methods for artificially increasing the sampling frequency by using multiple lower frequency measurements are presented later on, in section 3.5.

3.3.2 Voltage measurements

Voltage measurements are simpler since the same voltage is measured in each bay. As the same quantity is available in each IED, the samples can simply be merged as shown in Figure 3.3, which presents an example substation with five feeders, one incoming and four outgoing.

Currently, the most common case is that each feeder only measures the neutral voltage (for directional protection functions), so only the sampling frequency of that quantity can be increased. But it is more than likely that full three-phase voltage measurements in each bay will become more common, as new cheaper sensor technologies emerge and as the scope of DG increases. When there is DG in the network, it may also feed a fault current and maintain line voltage even after a circuit breaker has been opened (in fact, this functionality may even be desired during an intended island operation). Therefore, measuring phase voltages behind the circuit breaker (CB) of each feeder may soon be an actual requirement.

3.3.3 Current measurements

The same procedure is not possible with current measurements, since each current is only measured once. However, as long as measurements are available from each feeder, this limitation can be partly avoided using Kirchhoff's current law.

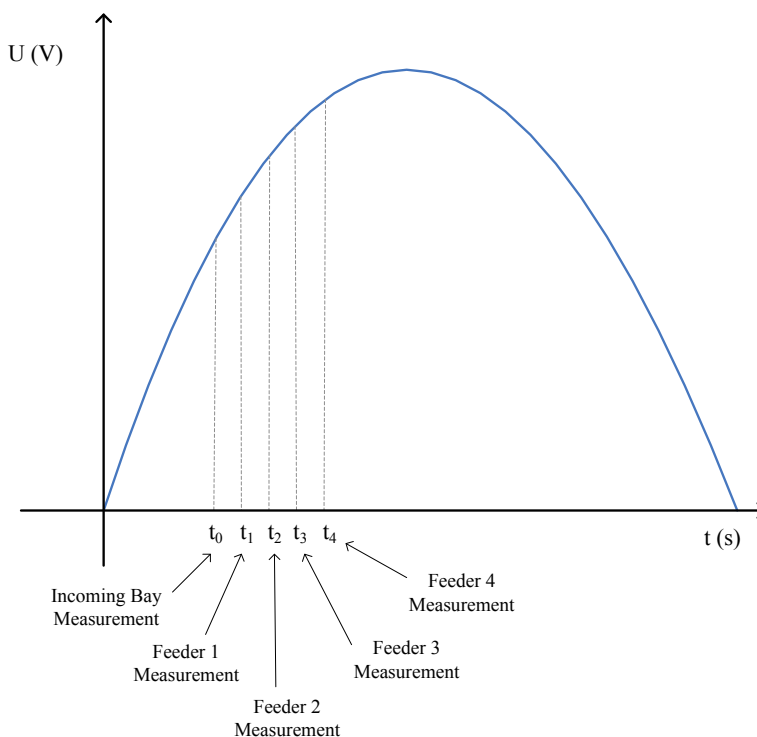


Figure 3.3: Voltage measurements combined from 5 different measurements.

The method tested here uses linear interpolation for calculating virtual measurement points between actual measurements. With this procedure, there is one actual physical measurement and several virtual interpolated ones from each time stamp. If the sum of all the samples is zero at any given instant, the residual error caused by the interpolation can be added to the interpolated values. The procedure is presented in Figure 3.4, in a substation with five feeders: one incoming and four outgoing.

3.4 Limitations and error analysis

Even if, in theory, 5 IEDs with a 2 kHz sampling frequency could produce a 10 kHz sample stream, in practice it is not that good. Each measurement chain, even with identical IEDs and sensors, has a unique measurement error, which is hard to fully eliminate before the signal is used by the applications. If, for example, one IED has a small scaling error or offset error in the measurement, it creates an additional

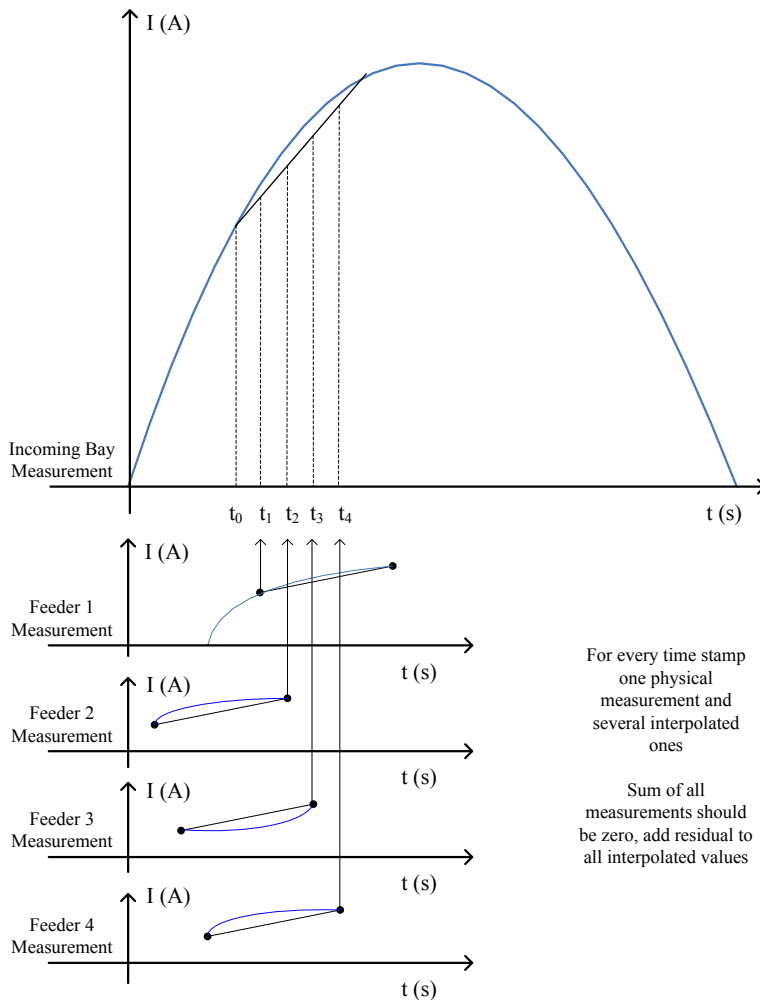


Figure 3.4: Current measurements combined from 5 different measurements.

frequency component equal to the sampling frequency (2 kHz in this example), and if this can't be compensated for, it needs to be filtered out with a low-pass filter.

Normally, the sample stream also passes through an anti-aliasing filter in the IED before it is transmitted. With 2 kHz sampling, the cut-off frequency of the filter is less than 1 kHz, which means that frequencies higher than that cannot be reproduced, even if multiple sample streams are available. For the transient analysis this is not a major issue, as the frequency of the dominant charge transient is normally less than 1 kHz. The problem with transient-based methods is not the Nyquist-Shannon

theorem, but the small number of data points. If it were possible to receive samples from the IED before anti-aliasing, or after a separate anti-aliasing filter with a higher cut-off frequency, then in theory, the frequency band of the signal could be increased, but this has not yet been tested.

For a better understanding of these limitations, calculations need to be done to assess the effect of different mismatches. The following error analysis is largely based on [Vogel, 2005], and the equations below use the following notation:

A = amplitude of the input signal

ω_0 = angular frequency of the input signal, discrete time

Ω_0 = angular frequency of the input signal, continuous time

M = number of ADCs/IEDs

μ_g = expected value of the gain of one ADC/IED

μ_o = expected value of the offset of one ADC/IED

σ_g = standard deviation from the expected gain

σ_r = standard relative timing deviation of the TI-ADC set-up

σ_o = standard deviation of the offset

The different measurement ADCs/IEDs are assumed to be of same type, which means the same design of the measurement electronics, and the same anti-alias filters. The mismatches are indicated with σ_g , σ_r and σ_o , and they can be caused either by differences in the anti-alias filter, differences in the other measurement electronics, or both.

3.4.1 TI-ADC model

The calculations were performed based on the simplified model shown in Figure 3.5, which describes one channel, l , in a multi-channel TI-ADC. In Figure 3.5, the input signal $x(t)$ is time-shifted by Δt_l , amplified by g_l , added to an offset o_l and sampled with a sampling period of $M T_s$ and a constant time shift of lT_s .

With this model, the sampled output of a one-channel ADC is as shown in (3.1), where $\delta(t)$ is the Dirac delta function.

$$y_l(t) = \sum_{k=-\infty}^{\infty} (g_l x(t - \Delta t_l) + o_l) \delta(t - kMT_s - lT_s) \quad (3.1)$$

If these parameters were identical for all channels, no mismatch errors would occur. In practice this can never happen, and for further analysis the Fourier transform

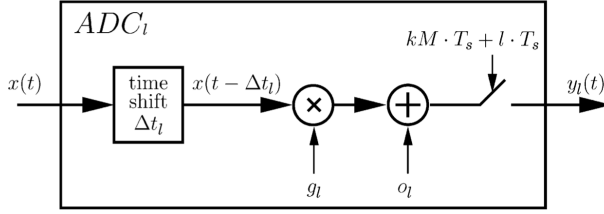


Figure 3.5: Model of a one-channel ADC [Vogel, 2005].

of (3.1) for a sinusoidal input signal $x(t) = A \sin(\Omega_0 t)$ and with $\omega_0 = \Omega_0 T_s$, is presented in (3.2) and (3.3).

$$\begin{aligned}
 Y(j\Omega) = \frac{2\pi}{T_s} \sum_{k=-\infty}^{\infty} \left[\alpha[k] \delta \left(\Omega - \Omega_0 - k \frac{\Omega_S}{M} \right) \right. \\
 \left. - \alpha^*[M - k] \delta \left(\Omega + \Omega_0 - k \frac{\Omega_S}{M} \right) \right. \\
 \left. + \beta[k] \delta \left(\Omega - k \frac{\Omega_S}{M} \right) \right] \quad (3.2)
 \end{aligned}$$

where

$$\begin{aligned}
 \alpha[k] &= \frac{A}{j2M} \sum_{l=0}^{M-1} g_l e^{-j\omega_0 r_l} e^{-jkl \frac{2\pi}{M}} \\
 \beta[k] &= \frac{1}{M} \sum_{l=0}^{M-1} o_l e^{-jkl \frac{2\pi}{M}} \quad (3.3)
 \end{aligned}$$

The symbol $*$ in (3.2) denotes the complex conjugate, and Ω_S indicates the overall sampling frequency of the setup. When looking at points where $\delta(t) = 0$, it is noticeable that some additional spurious peaks are centered at $(\pm\Omega_0 + k\Omega_S/M)$ in the case of gain and timing mismatches, whereas others are centered at $(k\Omega_S/M)$ in the case of offset mismatches. Both the coefficient sets $\alpha[k]$ and $\beta[k]$ are discrete Fourier transforms (DFTs) of their corresponding channel parameters [Vogel, 2005].

3.4.2 Derivation of the explicit SINAD

This section shows the formula for the SINAD, when the explicit values for the gain/offset/timing errors are known.

SINAD is as shown in (3.4).

$$SINAD = 10 \log_{10} \left(\frac{P_S}{P_N} \right) = 10 \log_{10} \left(\frac{P_S^{gr}}{P_N^{gr} + P_N^o} \right) \quad (3.4)$$

In (3.4) the following notation is used:

P_S^{gr} = Signal power, dependent on gain and timing deviation

P_N^{gr} = Signal error power, dependent on gain and timing deviation

P_N^o = Signal error power, dependent on offset

The sub-calculations of this equation are shown in (3.5):

$$\begin{aligned} P_S^{gr} &= 2|\alpha[0]|^2 = \frac{A^2}{2} \left| \frac{1}{M} \sum_{l=0}^{M-1} g_l e^{-j\omega_0 r_l} \right|^2 \\ P_N^o &= \sum_{k=0}^{M-1} |\beta[k]|^2 = \frac{1}{M} \sum_{l=0}^{M-1} |o_l|^2 = \overline{|o|^2} \\ P_N^{gr} &= 2 \sum_{k=0}^{M-1} |\alpha[k]|^2 - 2|\alpha[0]|^2 \\ &= \frac{A^2}{2M} \sum_{l=0}^{M-1} |g_l e^{-j\omega_0 r_l}|^2 - 2|\alpha[0]|^2 = \frac{A^2}{2M} \sum_{l=0}^{M-1} g_l^2 - 2|\alpha[0]|^2 = \frac{A^2}{2} \overline{g^2} - 2|\alpha[0]|^2 \end{aligned} \quad (3.5)$$

This leads to (3.6) [Vogel, 2005].

$$\begin{aligned} SINAD &= 10 \log_{10}(2|\alpha[0]|^2) - 10 \log_{10} \left(2 \sum_{k=1}^{M-1} |\alpha[k]|^2 + \sum_{k=0}^{M-1} |\beta[k]|^2 \right) \\ &= 10 \log_{10} \left(\frac{P_S^{gr}}{\frac{A^2}{2} \overline{g^2} - P_S^{gr} + P_N^o} \right) \end{aligned} \quad (3.6)$$

3.4.3 Derivation of the expected SINAD

This section shows the formula for the SINAD, when in stead of explicit values, the probability distribution of these same errors is known.

SINAD is as shown in (3.7), where E describes the expected value of the random variable and tilde ($\tilde{\cdot}$) the random variable itself.

$$\begin{aligned} SINAD &= 10 \log_{10} \left(\frac{E\{P_S\}}{E\{P_N\}} \right) = 10 \log_{10} \left(\frac{E\{P_S^{grR}\}}{E\{P_N^{grR}\} + E\{P_N^{oR}\}} \right) \\ &= 10 \log_{10} \left(\frac{E\{P_S^{grR}\}}{E\{\frac{A^2}{2}\tilde{g}^2 - P_S^{grR}\} + E\{P_N^{oR}\}} \right) \end{aligned} \quad (3.7)$$

In (3.7) the following notation is used:

P_S^{grR} = Expected signal power, dependent on gain and timing deviation

P_N^{grR} = Expected error power, dependent on gain and timing deviation

P_N^{oR} = Expected error power, dependent on offset

The sub-calculations of (3.7) are shown in (3.8).

$$\begin{aligned} E\{P_S^{grR}\} &= \frac{A^2}{2} \left| \frac{1}{M} \sum_{l=0}^{M-1} \tilde{g}_l e^{-j\omega_0 \tilde{r}_l} \right|^2 \\ &= \frac{A^2}{2M^2} \sum_{l=0}^{M-1} \sum_{m=0}^{M-1} E\{\tilde{g}_l \tilde{g}_m e^{-j\omega_0 \tilde{r}_l} e^{j\omega_0 \tilde{r}_m}\} \\ &= \frac{A^2}{2M} (\mu_g^2 ((M-1)|\Phi_r(\omega_0)|^2 + 1) + \sigma_g^2) \\ E\{\frac{A^2}{2}\tilde{g}^2 - P_S^{grR}\} &= \frac{A^2}{2M} (M-1) (\mu_g^2 (1 - |\Phi_r(\omega_0)|^2) + \sigma_g^2) \\ E\{P_N^{oR}\} &= \frac{1}{M} \sum_{l=0}^{M-1} E\{|\tilde{o}_l|^2\} = (\mu_o^2 + \sigma_o^2) \end{aligned} \quad (3.8)$$

In (3.8), $\Phi_r(\omega_0)$ is the characteristic function of the random variable \tilde{r} , and if Gaussian distribution is expected, it is as shown in (3.9).

$$|\Phi_r(\omega_0)|^2 = \left| \int f_{\tilde{r}}(x) e^{j\omega_0 x} dx \right|^2 = e^{-\omega_0^2 \sigma_r^2} \quad (3.9)$$

Then the overall SINAD is as shown in (3.10), when the expected value of offset μ_o is zero [Vogel, 2005].

$$\begin{aligned}
 SINAD = & 10 \log_{10} \left(\frac{A^2}{2M} (\mu_g^2 ((M-1)e^{-\omega_0^2 \sigma_r^2} + 1) + \sigma_g^2) \right) \\
 & - 10 \log_{10} \left(\frac{A^2}{2M} (M-1) (\mu_g^2 (1 - e^{-\omega_0^2 \sigma_r^2}) + \sigma_g^2) + \sigma_o^2 \right)
 \end{aligned} \tag{3.10}$$

3.4.4 SINAD values for the substation

(3.10) was initially constructed for ADC design, where the accuracy requirements are considered from the point of view of a TI-ADC set-up, rather than for individual ADCs. As in substation automation the individual ADC of an IED still plays an important role, modifying the equation in that direction makes the results more descriptive. The standard relative timing deviation in (3.10) is presented as a fraction of the sample time of the TI-ADC set-up. A more descriptive approach is to use the fraction of the sample time of an individual ADC, see (3.11).

$$\sigma_r = M\sigma_{r1} \tag{3.11}$$

where σ_{r1} indicates the standard relative timing deviation of an individual ADC. For example, a 1 μ s deviation with a sample frequency of 1 kHz per device (sample time 1 ms) means a value = 0.001, regardless of the number of ADCs used. Furthermore, when investigating the effect of multiple measurements, instead of angular frequency ω_0 , it is better to use a frequency relative to the sampling frequency of one IED, see (3.12).

$$\omega_0 = 2\pi \frac{a_0}{M} \tag{3.12}$$

In (3.12) a_0 indicates the input signal frequency relative to the sampling frequency of one IED, e.g. a 1 kHz signal with a 2 kHz sampling frequency means $a_0 = 0.5$. With these additions SINAD can be calculated with (3.13).

$$\begin{aligned}
 SINAD = & 10 \log_{10} \left(\frac{A^2}{2M} (\mu_g^2 ((M-1)e^{-4\pi^2 a_0^2 \sigma_{r1}^2} + 1) + \sigma_g^2) \right) \\
 & - 10 \log_{10} \left(\frac{A^2}{2M} (M-1) (\mu_g^2 (1 - e^{-4\pi^2 a_0^2 \sigma_{r1}^2}) + \sigma_g^2) + \sigma_o^2 \right)
 \end{aligned} \tag{3.13}$$

The effect of individual components can be derived from (3.13) by setting the other deviations to zero, for example, the effect of the timing deviation is clearly

visible when both the gain and the offset deviation are set to zero. Such formulas, simplified from (3.10), are presented in [Vogel, 2005], and the same simplifications can be made to (3.13), the graphical results of which are presented in Figures 3.6, 3.7 and 3.8. In these figures, $M = 8$, $\mu_g = 1$ and $a_0 = 0.5$.

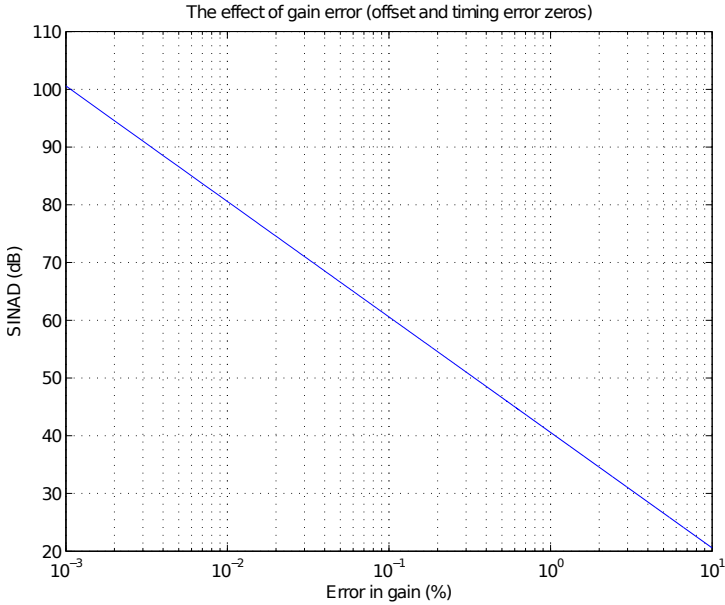


Figure 3.6: The effect of gain error in SINAD.

Figures 3.6, 3.7 and 3.8 provide the maximum possible SINAD, if the error in one element is known. If the timing error were 1% of the sample time of one IED, the maximum possible SINAD as shown in Figure 3.8 is around 30 dB, no matter how identical the measurement chains are in other respects. In the measurement chain of an IED, the offset error is normally negligible, and its effect can be ignored. The most interesting issue, therefore, is the combined effect of gain and timing mismatches, and these are presented in Figures 3.9 and 3.10. As before, $M = 8$, $\mu_g = 1$ and $a_0 = 0.5$ in the figures.

The combined effect is clearly visible in Figure 3.10. If, for example, the gain accuracy in the IEDs is 0.5%, the best possible SINAD value in the TI-ADC set-up is around 45 dB, and requires timing accuracy to be 0.1%. With a 2 kHz sampling frequency per IED this means around 0.5 μs accuracy.

Another view of the accuracy of the TI-ADC concept is to look at the percentage

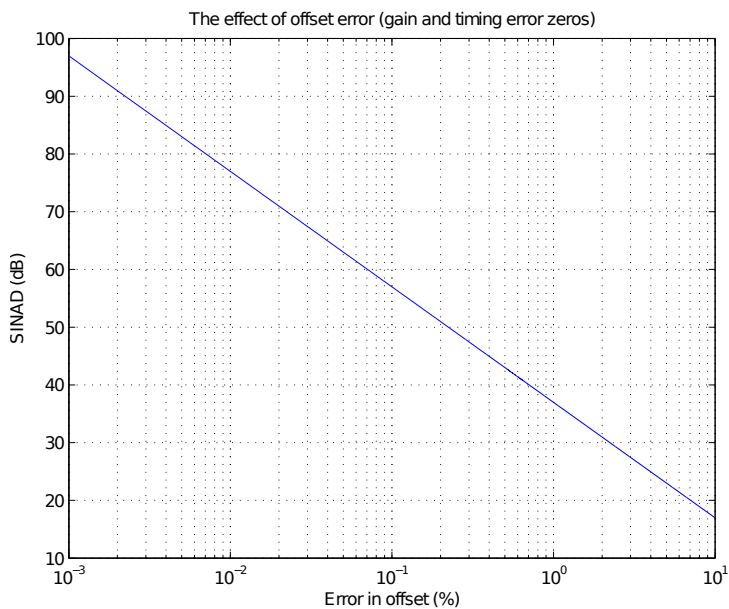


Figure 3.7: The effect of offset error in SINAD.

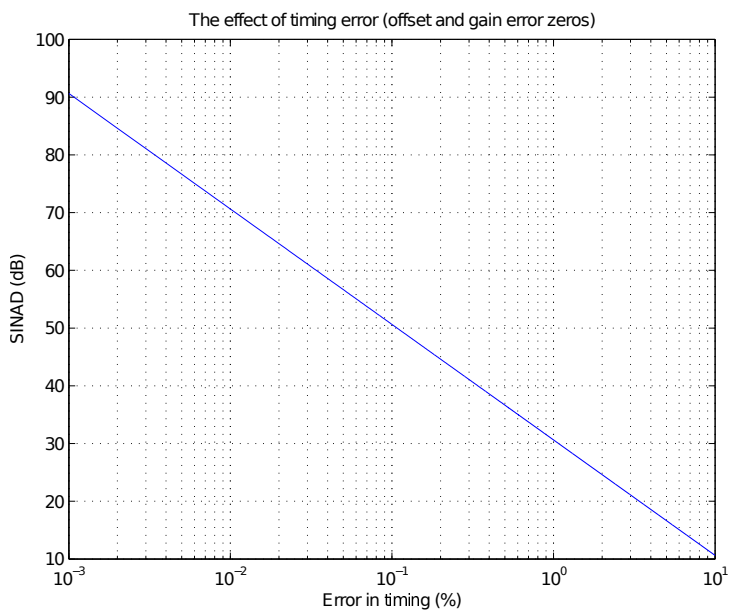


Figure 3.8: The effect of timing error in SINAD.

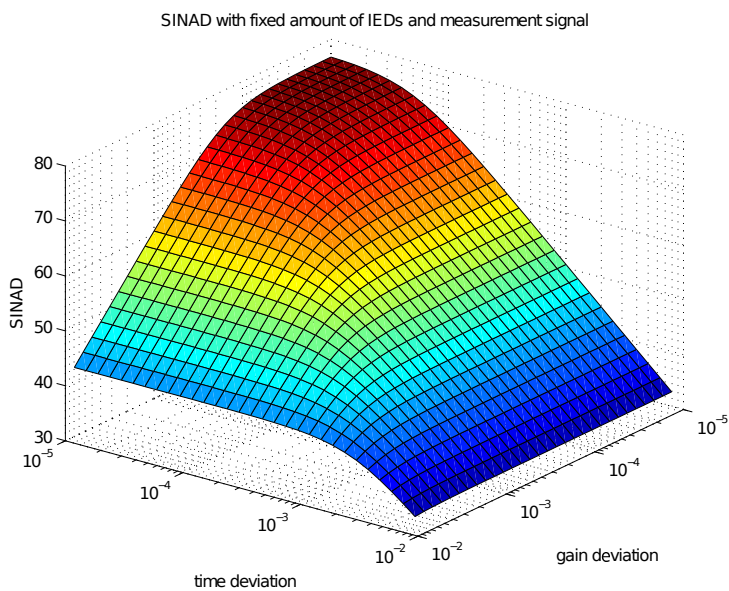


Figure 3.9: The combined effect of gain and timing mismatches.

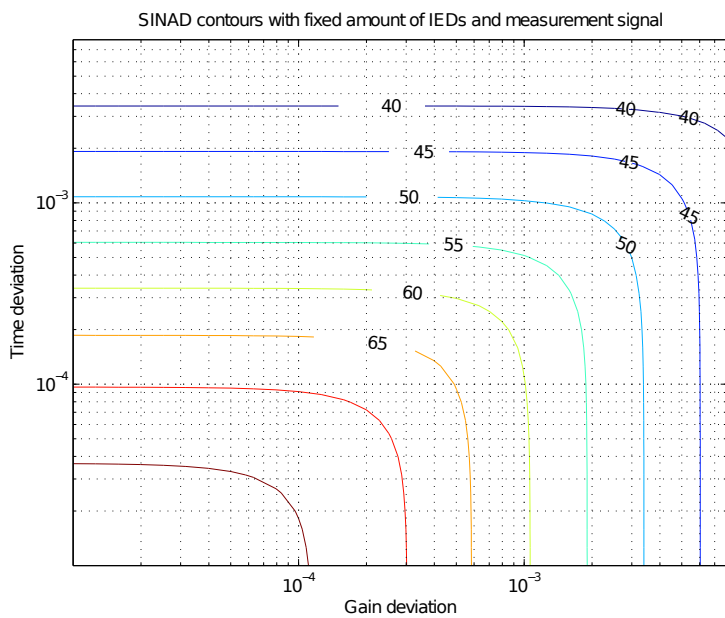


Figure 3.10: Contours of Figure 3.9.

value of the Total Harmonic Distortion with Noise (THD+N), which is often viewed in stead of SINAD. Similar contours as in Figure 3.10 are shown in Figure 3.11.

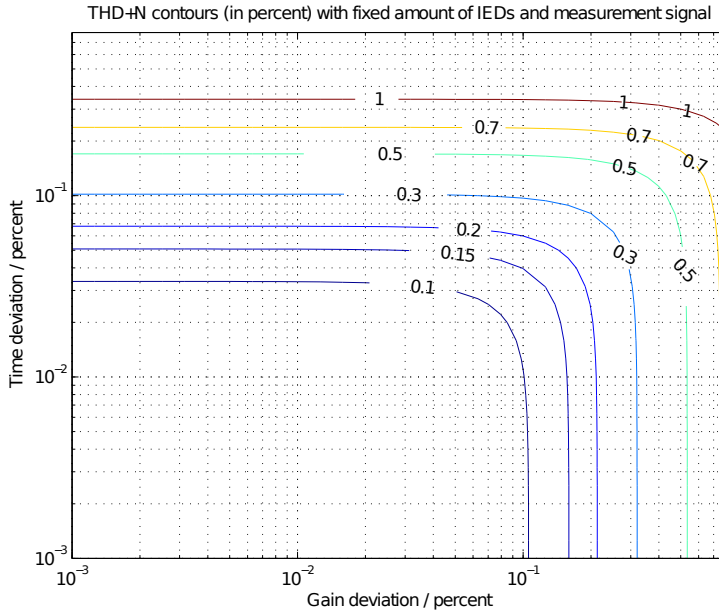


Figure 3.11: Contours of Figure 3.9 in THD+N.

One example from an IED manufacturer shows, that the measurement accuracy of the IEDs is around 0.5% ABB Ltd. [2009], which is in the same range as is achievable with the TI-ADC set-up as shown in Figure 3.11. One further issue is the effect of additional IEDs. What happens to the accuracy when the number of IEDs increases, as shown in Figure 3.12? In this figure, $\sigma_g = 0.005$, $\sigma_{r1} = 0.001$, $\sigma_o = 0$ and $\mu_g = 1$.

SINAD does deteriorate slightly when the number of ADCs increases, but not greatly. This indicates that the signal quality would remain at the same level, which is the most important issue with transient-based algorithms. Power system transients last only for a few milliseconds, e.g. during an earth fault [Lehtonen and Hakola, 1996], so the main point is that the number of data points can be increased without having any major effect on the SINAD value.

3.4.5 Time synchronization requirements

According to the calculations presented above, the timing mismatch of samples should not exceed 0.1% of the sample time, as long as the gain accuracy is around 0.5%,

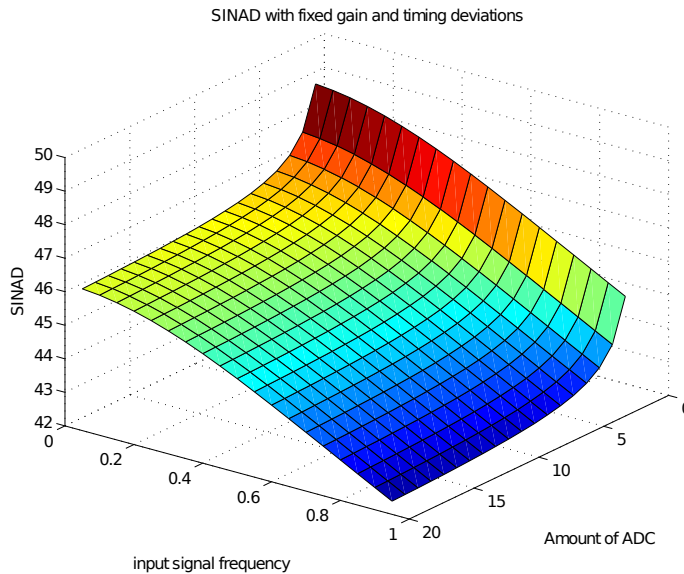


Figure 3.12: The effect on SINAD of increasing the number of ADCs.

which is the measurement accuracy stated in the IED manufacturers manuals [ABB Ltd., 2009]. Interestingly, other research based on different assumptions came to the same conclusion of a 0.1% timing accuracy requirement. If the individual ADC has 16 bit sampling, timing accuracies less than 0.1% degrade the SINAD considerably [Soudan and Farrell, 2008]. With a sampling frequency of 2 kHz the sample time is 0.5 ms, which provides time accuracy requirements of $0.5 \mu\text{s}$ with 0.1% accuracy. As indicated earlier in this thesis, the IEEE 1588 time synchronization protocol fulfills these requirements, so it can be used for the synchronization of IEDs. In addition, there are the two following requirements:

- The IED synchronization must also affect ADC sampling times.
- The IED must have an adjustable time offset for ADC synchronization. When the ADC of one IED is running in sync with the synchronization master (offset = 0), the other IEDs must have an offset time with multiples of $(1/M/f_s)$ where M is the number of IEDs and f_s is the sampling frequency. For example, if 5 IEDs with 2 kHz sampling frequency are synchronized from the same synchronization master, one IED must have a timing offset of $1 / 5 / 2000 = 100 \mu\text{s}$, and the other offset times are $200 \mu\text{s}$, $300 \mu\text{s}$ and $400 \mu\text{s}$.

3.4.6 Special considerations related to TI-ADC

Many research results related to TI-ADC can be directly applied to the concept proposed in this thesis. A few special items related to substation automation, however, must be given special consideration. Firstly, the number of ADCs is expected to stay constant in a TI-ADC set-up, which might not be the case in a substation. In particular, if the measurement sensor is behind a circuit breaker, a change in network topology, e.g. due to a fault, can remove one IED from the measurement chain. Because of this, centralized logics must be implemented in the substation, which would take this factor into account. If one IED measurement is missing, new timing offset values must be calculated and provided to the IEDs, in order for the TI-ADC arrangement to be able to resume operation with $(M-1)$ measurements. As indicated earlier, this does not much affect the SINAD of the measurement signal, but the number of data points for transient analysis is reduced. It should also be noted that if a functionality were to require measurements from the same moment (e.g. comparing phasor values from the measurements from different feeder bays), the calculated timing offset value must also be provided to these functions in order for them to operate properly.

Another consideration is that the existing compensation strategies for TI-ADC mismatches focus on analyzing the combined high-frequency signal, e.g. an offset mismatch is visible in the signal as a signal component, which has the same frequency as the sampling frequency of one ADC [Vogel, 2005]. In a substation, however, the measurement signal of one IED is needed for protection purposes, and thus it has already undergone extensive signal processing, such as calculating nominal frequency 50Hz or 60Hz components and higher order power system harmonics [ABB Ltd., 2009]. The gain mismatch can be eliminated through comparison of the fundamental frequency phasors of the different IEDs. The same elimination method is also useful in other respects, as it simultaneously provides a new way to supervise measurement circuits, which is an important issue for the secondary system of a substation. This aspect is a topic for future research, but is not investigated further in this thesis.

3.5 Other existing solutions for increasing the sampling frequency

Different sparse sampling methods have also been investigated, especially for power quality monitoring. The need for acquiring information from higher order harmonics

with cheap equipment is a common one. The doctoral thesis of Pekka Koponen [Koponen, 2002] addresses this issue too, and proposes multiple sampling, but with different sampling frequencies of the same signal (e.g. 2 kHz and 3 kHz).

Using the same sampling frequency with shifted time intervals seems to be a concept which has not been tested earlier. One reason for this is that processing several sample streams simultaneously in a substation was not feasible earlier. On the other hand, a similar concept would also work offline with normal bay-level IEDs, by using disturbance records downloaded after faults have occurred.

3.6 Chapter Summary

The concept presented in this thesis makes it possible to increase the sampling frequency of current and voltage measurements at the substation level. When the transient frequency is below the cut-off frequency of the anti-aliasing frequency of one IED, combining the measurements from the IEDs of several bays increases the number of measurement data points from the transient period.

The accuracy of time synchronization has a significant impact on the overall measurement accuracy in the proposed method. Furthermore, particularly with transients, the analogue front end of each IED must have the same characteristics and similar frequency response. However, these factors shouldn't limit the use of the method, as the IEEE 1588 time synchronization specifies a time accuracy which is sufficient for the method presented in this thesis. In addition, the need to calibrate the measurement chain of each IED as accurately as possible is not confined to the use of this method.

This concept is further tested with an example functionality for transient-based earth fault location in Chapter 5. Testing the method further with other transient-based methods, such as intermittent earth fault detection or power quality measurements, is a topic for future research.

Chapter 4

Station Applications

As was pointed out in Chapter 2, the proposed architecture allows the functionality to be allocated in a new way. Not all the functions which currently reside in the bay-level protection and control IEDs need be located there any longer, since the proposed concept enables certain functions to be implemented at the station level. This chapter evaluates how this functionality should be re-allocated, i.e. which functions should remain at the bay level and which functions should be moved to the station level. An example case study, targeted at Finnish electricity distribution networks, is used as the basis for this evaluation because the functionality needed in a substation is always case-specific.

4.1 Functionality in the secondary system of a distribution substation

The first issue to consider is what set of functions needs to be re-allocated in this case. How are they to be selected? With the existing functionality, the issue is easier, as one can simply collect a representative set of various functions based on the product guides of the IED vendors, and make the selections from there.

However, with new functions not yet available in the IEDs, the process is more difficult, as there is no definitive list of the future functions. Although functional areas may have already been identified, as discussed in section 2.3, the names and number of the particular functions might not yet be known. Nevertheless, the items which were regarded as most important were selected and added to the function set.

The list of functions to be re-allocated in this chapter is based on the LN (Logical

4.1. Functionality in the secondary system of a distribution substation

Node) classes defined in IEC 61850-7-4 [IEC, 2005], as this encompasses all the main function classes in modern IEDs. Only the Protection (P), Protection related (R), and Control (C) categories of the LN classes were selected, as these are the main point of interest. Some changes to the LN list were made based on a review of the results from the IED vendors, and some LNs were removed because they were redundant (e.g. the Directional Element LN PDIR was removed as the protection logic is normally modeled with PTOC, and nearly all the LNs related to the disturbance recorder were removed as RDRE LN already describes the main functionality). In addition, the PTOC LN used for many different protection functions was split into several different functions. The derived list was extended with currently ongoing research topics, and is summarized in Table 4.1. Furthermore, the related ANSI numbering according to [IEEE, 2008] is presented when applicable.

Table 4.1: Functions selected for re-allocation

Abbr	ANSI	Function
PDIF	87	Differential protection (busbar)
PDIS	21	Distance protection (first zone)
PHIZ	64	Ground detector, high-impedance earth fault protection
PIOC	50	Instantaneous overcurrent protection
PSDE	67N	Sensitive directional earth fault protection (intermittent earth fault)
PTEF	67N	Transient earth fault protection
PTOC	51	Time overcurrent protection, overcurrent
EFPTOC	51	Time overcurrent protection, non-directional earth fault (double earth fault)
DEFPTOC	51	Time overcurrent protection, directional earth fault
DISPTOC	51	Time overcurrent protection, phase discontinuity
PTOF	81	Overfrequency protection
PTOV	59	Overvoltage protection
PTTR	49	Thermal overload
PTUC	37	Undercurrent protection
PTUV	27	Undervoltage protection
PTUF	81	Underfrequency protection
RDRE		Disturbance recorder
RBRF	50BF	Breaker failure
RFLO		Fault locator
RREC	79	Auto-reclosing

continued on the next page

4.2. Functionality division

<i>continued from the previous page</i>		
Abbr	ANSI	Function
CILO	3	Interlocking
CBCSWI		Switch controller (CB)
DISCSWI		Switch controller (DIS)
flir		Post-fault network restoration, and dynamic reconfiguration of network topology, self-healing networks (IEC61850: separate logical devices including several control LNs)
cbm		Condition monitoring, Asset Management, CBM/RCM (IEC61850: additions made to IEC 61850 after Edition 1, e.g. CB condition monitoring LN SCBR)
dgoper		island operation, LOM, FRT (IEC61850: separate logical devices including several control LNs)
loadshed		load-shedding (IEC61850: separate logical devices including several control LNs)
adapt		Automatic recalculation of protection parameters based on topology and DG changes, adaptation of protection (IEC61850: Generic process control LN defined, GAPC)
selfsup		Station-level self-supervision (IEC61850: IED-level self-supervision modeled with LN SSYS)
cybersec		Cyber-security (IEC61850: Generic security LN defined, GSAL)
reporting		Statistics, regulation reports (IEC61850: Simple statistics report LN available, MSTA. More extensive reports not available)

The abbreviations in Table 4.1 are LN class names with their functionality defined in the IEC 61850, in capital letters. To separate different PTOC functions from each other, different prefixes are used for different functions. Ongoing research topics not accurately defined in IEC 61850 are abbreviated with lowercase letters for ease of identification. In these cases, possible ways of modeling these applications in IEC 61850 are shown in the table in parentheses. These abbreviations are used later on in this chapter when summarizing the results.

4.2 Functionality division

Function re-allocation is approached from two different perspectives. The first division is based on importance. First, there are the mandatory functions, such as primary protection and control. These functions are critical for the operation of the network, and are therefore normally always present when a suitable protection device is available. These functions also normally need back-up functionality, in case the primary

function fails to operate.

At other end of this 'importance' axis are the optional functions, such as monitoring and analysis applications. They are not vital for the safe operation of the network, but they affect its cost-efficiency. If these functions fail, fault situations might last longer (e.g. through incorrect fault location) or they might occur more frequently (e.g. due to insufficient condition monitoring resulting in flawed estimates of maintenance needs). Inadequate monitoring functionality can also impact on profits due to non-optimal utilization of the network resources. Normally, these functions do not need to be backed up.

The other division is based on the location of the function. In the evaluated architecture, functions can be located either at the unit level, or the station level. In the currently dominant secondary architecture only unit-level devices are available. On the other hand, in a totally centralized solution there is only one location available - the station level. The need to position functions on the station-unit axis only exists in the combined approach investigated in this thesis.

These two ways of dividing the functions create four different categories, which are presented below in Table 4.2. The four categories have different requirements – and different execution environments are suitable for different categories. In general, unit-level functions should have longer life cycles than station-level functions, and mandatory functions place stricter requirements on the operating system running the functions. There are more unit-level devices, and they are more closely connected to the electricity distribution process, which causes longer and more costly maintenance breaks.

Table 4.2: Functional categories

	Unit level	Station level
Optional functions	Unit level optional	Station level optional
Mandatory functions	Unit level mandatory	Station level mandatory

Careful attention should be paid to these categories when designing the functional content of the secondary system of a distribution substation. If a function is implemented in the wrong category/environment it can impose updates to the automation equipment earlier than would otherwise be needed.

4.3 Functionality division criteria

Finding an optimal set-up for distribution automation is a complex issue. Even when the scope of the functionality is limited to the distribution substations, it is still a difficult problem. The criteria generally regarded as being most important are presented below.

4.3.1 Communication requirements

The most obvious indication of station-level functionality is the communication requirement. If the functionality requires horizontal and/or vertical communication, in other words, if information needs to be exchanged between several units, it is best to implement the functionality at the station level. Whatever the case, the function will not operate properly if there are communication problems, so implementing the function at the station level will not make the system less reliable than it would be if this functionality were to be implemented at the unit level.

In general, data should be processed at the lowest level possible so that fast and reliable response can be guaranteed. This 'lowest level' depends on the functional requirements and the available computational and communication capabilities. An apposite example of this approach can be found in the human nervous system. When fast response is needed (e.g. when a human touches a hot surface), an immediate command is issued at the spinal cord. Sending the signal from the sensors to the brain and processing it there would create unnecessary delay when the appropriate reaction is unambiguous (i.e. to remove the hand from the hot surface). When more information is needed from other senses, (e.g. the surface is not very hot and it is better to look at it first), the information needs to be gathered in the brain and processed there.

The functions listed in Table 4.1 were evaluated based on the communication requirements. The method selected for this case evaluation was to use the number of nodes communicating with each other. For 'all nodes in the substation' a value of 10 was used, because this represents the average size of a Finnish substation (10 feeders). If several different solutions exist for the function, (both stand-alone algorithms as well as algorithms requiring communication), an average value of 5 was used.

4.3.2 Response time

The desired response time for the function indicates whether the function should reside at the unit level or the station level. In general, the faster the function should operate, the closer it should be to the process. Another way to express this is to say that functionality can be centralized to the extent that communication delays do not add too much latency and uncertainty to the operation. Functions requiring shorter response times are more often unit-level mandatory functions, whereas those functions which do not require such a short response time, or have no response time requirement, point toward either optional or station-level functionality, or both. The distinction between 'short' and 'long' response times is application-specific.

The time limits for the response of the different functions can be gathered from research papers or from the utility requirements. For this thesis, information was gathered by interviewing protection experts from various Finnish utilities (Fortum, Vattenfall and Helsinki Energy) and asking for their default operation time settings for various functions. The average default operation times gathered from these interviews were used to define the expected speed of operation.

4.3.3 Utilization frequency

Utilization frequency means how often these functions are used in the real-time operation of the distribution network. One approach to measuring utilization frequency is to use the statistics gathered from disturbances in the power system. When a particular fault situation is common in a distribution network, protection against it becomes essential and makes the function mandatory. According to the outage statistics for Finnish distribution networks [Energiateollisuus, 2005-2010], over 80% of the faults in electricity distribution networks occur in medium voltage networks. Of these faults, nearly 50% are short-circuit faults, and nearly 40% are earth faults.

Another approach to defining the utilization frequency is to refer to technical specifications of the IEDs, and this was the approach selected in this thesis. Those functions which are almost always present in protection and control IEDs are mandatory, whereas those functions which are only included in high-end IEDs are usually optional. To this end, a total of 124 different feeder protection IEDs from a number of different vendors (ABB, Alstom, Arcteq, Areva, Basler Electric, CEE, Cooper Industries, General Electric, Mikro, Nari-relays Electric Co., Protecta, Reyrolle, Roccon, SEL, Schneider Electric, Siemens, Sprecher, Thytronic, Toshiba, VAMP and

Woodward) were evaluated in terms of their available functions.

4.3.4 Function immaturity

Function immaturity indicates how often a function can be expected to be upgraded. If the function is stable and is expected to have a long life cycle, it is reasonable to locate it at the unit level where updates are more costly than at the station level. If, on the other hand, there is extensive research going on in that area, or changes are expected in the requirements for the function, either through legislation or from the business environment, the function should be located at the station level, where updating is easier.

The method used in this case was to categorize the functions according to the technology generation from which they were first introduced, i.e. from electro-mechanical relays, static relays or numerical relays. The source of information used here was the historical timeline of the relays from ABB, derived from [Lundqvist, 2010]. This described the milestones of one relay manufacturer and gives an overall view of the progress of the industry, showing the decade in which a particular functionality was first introduced. In addition, functions proposed in recent research articles were allocated to this decade to illustrate the fact that development is still going on.

4.4 Functionality division method

It is difficult to express the four above-mentioned criteria accurately in a numerical form. Furthermore, the aim of the exercise, i.e. the re-allocation of the available functions, cannot be explicitly defined, as in practice their implementation always depends on the requirements of the substation in question. For these reasons, the tool most appropriate for such an analysis is fuzzy logic [Klir and Yuan, 1995]. This provides a means for handling inaccurate or ambiguous data and using them for further analysis. First, the fuzzy logic rule-set for function allocation had to be defined, which is described below.

- If the function requires communication, does not have strict response-time requirements and is not very mature, it belongs to the station-level functions. Otherwise, it belongs to the unit-level functions

- If the function has strict response-time requirements and high utilization frequency, it is a mandatory function. Otherwise it is an optional function.

After defining the rule-set, the required data must be put into a numerical form. The methods used were those mentioned above, in section 4.3, and they are summarized below:

- Communication: number of communicating nodes
- Response time: average response times used by Finnish utilities
- Utilization frequency: number of evaluated relays having the functionality
- Function maturity: decade in which the functionality was first introduced

Of course, there are other ways for defining numerical values for the defined criteria. However, these were the methods found suitable for this case study, which focuses on Finnish electricity distribution networks, and the resulting numerical values are presented in Table 4.3.

Function	Communication	Response time	Utilization frequency	Function maturity
PDIF	10	13ms	7	1940
PDIS	1	20ms	10	1940
PHIZ	5	55s	16	1960
PIOC	1	133ms	120	1900
PSDE	5	2.5s	24	1940
PTEF	1	270ms	13	1970
PTOC	1	700ms	116	1910
PTOF	1	5s	55	1920
EFPTOC	5	300ms	124	1910
DEFPTOC	5	400ms	68	1920
DISPTOC	5	55s	44	1960
PTOV	1	3.25s	57	1920
PTTR	1	30s	73	1910
PTUC	1	10s	36	1920
PTUF	1	5s	55	1920
PTUV	1	6s	61	1920
RDRE	5	60s	103	1980
RBRF	1	100ms	103	1960
<i>continued on the next page</i>				

4.4. Functionality division method

<i>continued from the previous page</i>				
Function	Communication	Response time	Utilization frequency	Function maturity
RFLO	5	60s	29	1980
RREC	1	300ms	73	1920
CILO	10	1s	56	1920
CBCSWI	1	50ms	94	1900
DISCSWI	1	1s	13	1900
flir	10	60s	1	2000
cbm	5	15min	59	2000
dgoper	10	700ms	1	2000
loadshed	10	5s	7	2000
adapt	10	15min	1	2010
selfsup	5	700ms	10	2000
cybersec	1	700ms	30	2000
reporting	5	15min	10	2010

Table 4.3: Numeric values for each function

It was not possible to directly calculate the average response times for the selected active research topics ('flir', 'cbm', 'dgoper', 'loadshed', 'adapt', 'selfsup', 'cybersec' and 'reporting' in Table 4.3), since their use in Finnish utilities is currently rare. Instead, the related response times from existing functions were used. The research topics abbreviated to 'dgoper', 'selfsup' and 'cybersec' affect the primary, time-critical protection functionality, so in these cases the response time for PTOC was used. A power imbalance situation requiring load-shedding functionality is normally detected from frequency variations, so in this case the response time of PTUF was used. With functions affecting fault management (RREC, RFLO and flir) the total operating time of the auto-recloser was used (normally, in Finland, two shots are used with the auto-recloser; the average time for the second shot being 60 seconds). With the other reporting and monitoring related functions, an average time of 15min was used, which is currently the granularity in the nordic energy market.

These numeric values cannot be processed as raw figures. Instead, they need to be normalized to a value between 0 and 1. In fuzzy logic, this process is normally called fuzzification. This normalization allows different criteria to be combined and facilitates the unit/station and mandatory/optional categorization targeted in this research. Logarithmic values were used with the response times, in order to better differentiate between very short and very long response times. After normalization, the source data was categorized as shown in Table 4.4.

Table 4.4: Normalization rules applied to different criteria

Criteria	Value 0	Value 1
Communication	Local measurements are enough	Communicating with all nodes in the substation
Response time	Shortest of all	Longest of all
Utilization frequency	Not present in any IED	Present in all IEDs
Function immaturity	Used in relays since beginning of 1900	New function, under active development

The resulting membership values of station-level functions and optional functions are presented in Figure 4.1.

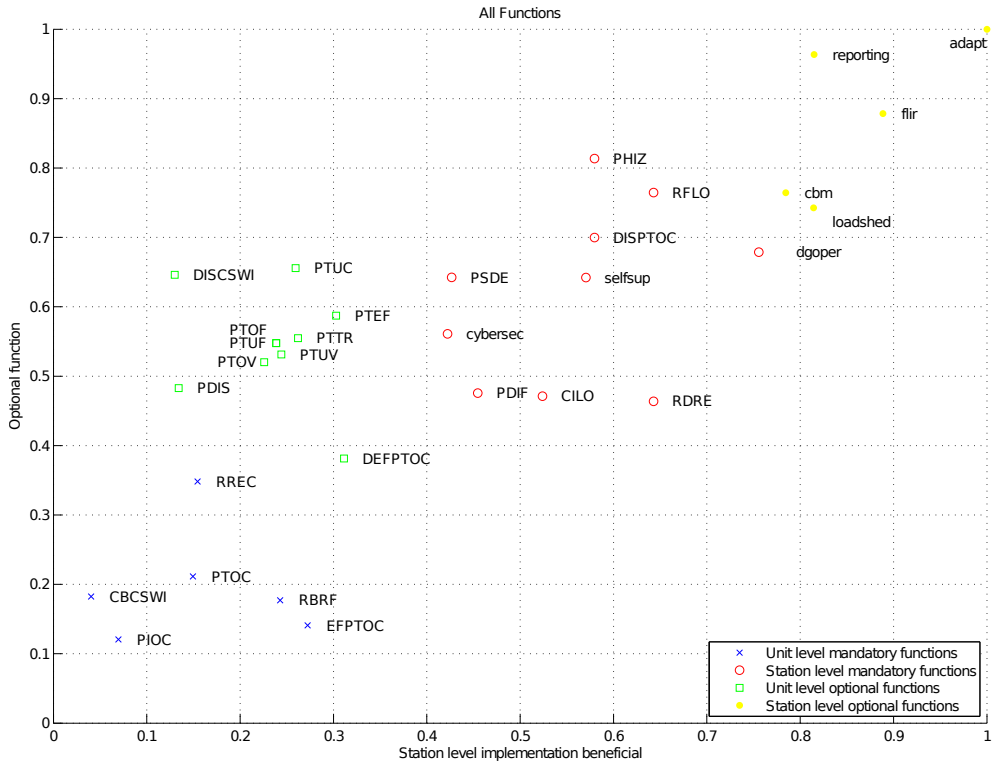


Figure 4.1: Function re-allocation results.

In Figure 4.1, the X-axis presents the membership of a station-level function group. A value of 100% (value 1.0) means that the function clearly belongs to the station level, and a value of 0% (value 0.0) means that the function clearly belongs to

4.4. Functionality division method

the unit level. Similarly, the Y-axis presents the membership of Optional functions; 100% indicates an optional function and 0% a mandatory function. An average of the individual criteria values was used as the AND-operator of the rule-set. The figure shows that there is a clear correlation between the two viewpoints. i.e station-level functions are more often also optional functions.

A fuzzy c-means clustering method [Miyamoto et al., 2008] was used to identify the center points for each of the four main categories used in this example. Having selected the number of clusters to be four, the identified cluster centers with their related effect-areas in the defined xy-plane are illustrated in Figure 4.2.

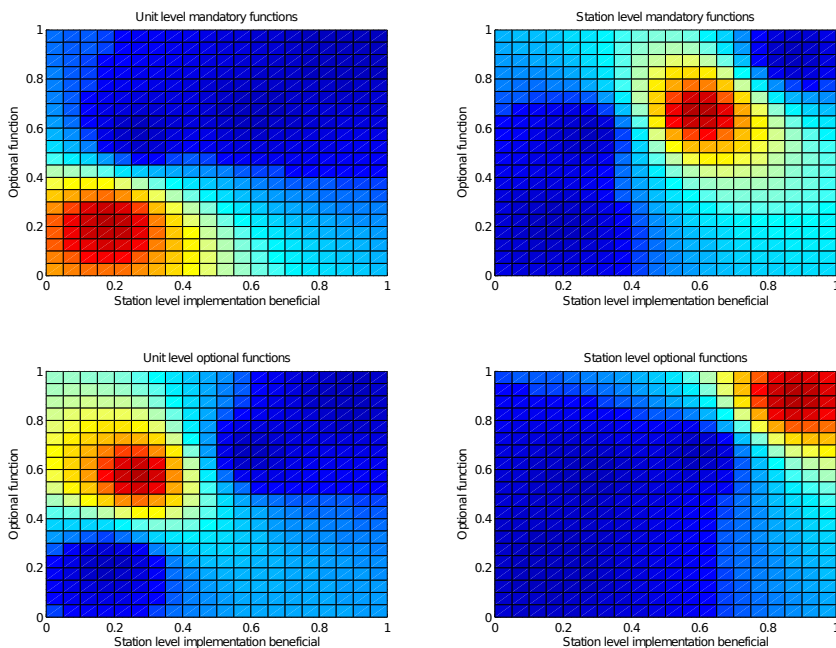


Figure 4.2: Membership of different functions to different clusters.

The final step in this fuzzy logic operation is the defuzzification - allocating functions to one and only one category based on their fuzzy membership values. This was done by calculating the degree of membership that each function had to each category, and selecting the category in which the membership had the highest value. The derived results are also presented in Figure 4.1, where a different marker represents a different category.

It must be noted that the clusters for 'Unit-level optional' and 'Station-level mandatory' are very close to each other, so depending on the case and on the available architecture, some functions can reside in either of those two categories. Another way to look at the situation is that when only a small number of functions belonging to either the 'Unit-level optional' or 'Station-level mandatory' categories are needed in a particular substation, the most cost-efficient solution would be to allocate them all to the bay level, and leave the station-level equipment out entirely. But when the requirements for the substation increase and station-level secondary equipment is needed, it could be beneficial to also include 'Unit-level optional' functions in the station level, and keep the unit level as simple as possible (and with as long a life cycle as possible).

4.5 Description of the results

4.5.1 Unit-level mandatory functions

This category is the most traditional category in substations. The functionality in this category should be selected so that the most important features of the unit are secured at all stages. These functions should not rely on external communication, so that safety is guaranteed even if communication is lost. For smaller stations with less stringent requirements, this category might be the only one needed. This category alone should fulfill the most critical requirements. The functions belonging to this category are presented in Figure 4.1, and briefly described below.

- Protection
 - Overcurrent protection, instantaneous and delayed (PIOC, PTOC)
 - Earth fault protection: Non-directional (EFPTOC)
- Control
 - Circuit breaker control and operation (CBCSWI)
 - Auto-recloser (RREC)
- Supervision
 - Breaker failure protection (RBRF)

4.5.2 Unit-level optional functions

Because optional functionality is rarely essential for network safety, this category is not always needed at the unit level, although an extensive library of these functions is available in modern protection and control IEDs. This includes functions which do improve the protection by, for example making it more selective or more accurate, but the network safety in general can also be guaranteed with only mandatory functions. This may also include functions which are mandatory for a limited number of special cases, but are not always mandatory.

The functions belonging to the unit-level optional functions category are presented in Figure 4.1 and briefly described below.

- Protection
 - Over/under frequency and voltage protection (PTOF, PTUF, PTOV, PTUV)
 - Over/under power protection, thermal overload protections (PTTR)
 - Earth fault protection: Directional (DEFPTOC)
 - Transient earth fault protection (PTEF)
 - Distance protection (PDIS)
 - Undercurrent protection (PTUC)

- Control
 - Disconnecter operation (DISCSWI)

4.5.3 Station-level mandatory functions

Currently, this category is not normally present at all in substations. All such functionality resides at the unit level (feeder bays, transformers, generators, etc.) and the station-level equipment is only used as a gateway for accessing these unit-level IEDs. The drawback with this approach is the update cycle, as has already been mentioned.

The purpose of this category is to complement the functions at the unit level, rather than to replace them. When the unit-level protection can operate without the station-level protection, station-level functionality can be updated without interruptions. This will also extend the life cycle of the unit-level functions, as most of the update measures are carried out at the station level.

The functions belonging to station-level mandatory functions are presented in Figure 4.1, and briefly described below.

- Protection
 - Differential protection - bus bar (PDIF)
 - Sensitive directional earth fault protection - intermittent faults (PSDE)
 - Phase discontinuity protection (DISPTOC)
 - Protection against faults with low fault current magnitude: e.g. high impedance earth faults [Tengdin, 1996] [Nikander, 2002] (PHIZ)
 - Islanding operation and Loss-of-Mains protection when islanding is not allowed [Rintamäki and Kauhaniemi, 2009] (dgoper)
- Control
 - Interlocking (CILO)
- Other
 - Fault locator (RFLO)
 - Disturbance recorder (RDRE)
 - Cyber security aspects [Nartman et al., 2009] (cybersec)
 - Station-level self-supervision (selfsup)

As noted earlier, this category is very close to the 'unit-level optional' functions category and in situations where both unit- and station-level devices are available many protection functions from that category could also be allocated to this category.

4.5.4 Station-level optional functions

The functions belonging to station-level optional functions are presented in Figure 4.1, and consist mainly of functions which are not essential for the safety of the substation, but important for increasing the efficiency of the network and fast reaction to fault situations. This category also contains functions which are not yet mandatory, but can be expected to be mandatory soon. These functions address issues which are not yet common in the network (at least not in Finland), but which will gain in importance if the future challenges outlined in section 2.3 become a reality. These items are listed briefly below, and have been explained in more detail in section 2.3.

- Post-fault power restoration [Mekic et al., 2009] and self-healing networks in general [Rasmunssen, 2009][Manner et al., 2011] (flir)
- Load shedding [Apostolov et al., 2007] (loadshed)
- Automatic recalculation of protection parameters based on topology and DG changes, adaptation of protection [Oudalov et al., 2011] (adapt)
- Advanced condition monitoring and Asset management support, CBM/RCM [Angel, 2003] (cbm)
- Reporting support (reporting)

4.6 Chapter summary

The functional division presented here focuses on increasing the life cycle of the substation automation system by utilizing station-level data processing. Initially, the station-level functionality criteria are defined. When the function requires communication, but does not have strict requirements for response times, station-level implementation can be justified. Complex functionality requiring additional CPU performance and anticipated updates in the near future are also clear indications for station-level functionality. Based on the defined criteria, an example case of both existing functionality and current research topics was divided between the unit level and the station level.

The difficulty in the method is the numerical representation of the criteria, which are also case-specific, depending on the substation and the network. Furthermore, new algorithms can change the location of a particular function entirely (e.g. the introduction of a new, more accurate method, which may need more communication than traditional methods). Numerical values for, e.g. 'communication requirement' or 'function maturity' are very difficult to determine. For this reason, fuzzy logic methods and fuzzy c-means clustering were used, which provide a suitable toolset for handling these types of attributes. The focus of this chapter is more on the method than on the final categorization. In this thesis, the method was applied to Finnish electricity distribution substations. When similar categorization is needed for a particular substation and/or application area, a new list of functions can be defined with new numeric values for the criteria. With this updated data, new categorizations can be obtained using the method presented here.

A future addition to this method would be a definition of the financial benefit of each function, such as the effect of the function on life-cycle costs. This could be added as an additional criterion, with a rule 'if a function has high financial benefit, it is mandatory', but it could also be added as a third axis to the derived plane. This would help in visualizing the implementation roadmap for adding new functionality to a substation, highlighting those functions with the highest financial benefit, and showing them in the appropriate category. The challenge in this is in evaluating the financial benefit of each function. The life-cycle cost evaluations in section 2.5.5 have already shown the problem of insufficient statistics, the relevant different fault cases, and their root causes. Therefore, a more detailed analysis of fault cases and their root causes is also a future research topic. If the more detailed fault analysis proposed in the summary part of Chapter 2 could be conducted, the same data could be used here, connecting the results from Chapters 2 and 4 together more completely.

Chapter 5

Station Application Example

This chapter presents an example case which utilizes all the main aspects of the thesis. The centralized architecture presented in Chapter 2 is tested with a new function proposed for the station level in Chapter 4. In order to gain as much benefit from the new architecture as possible, the measurement method presented in Chapter 3 is utilized in order to increase the sampling frequency of the measurements.

An earth fault occurs when one or several phases become galvanically connected to the ground. It is very common in MV distribution networks, where almost half of the faults are single-phase earth faults. Early indication and location of these faults is important, since it can prevent new faults from developing from the original one. If a single-phase earth fault is not detected, it can develop into a two-phase earth fault and/or a short circuit, and can be hazardous to people.

All this makes the reliable detection and location of earth faults a very important feature of the secondary system of the distribution network, as was indicated in the list presented in the previous chapter. In Chapter 4, FLIR functionality (Fault Location, Isolation and Power Restoration) was identified as a functionality that would benefit from the centralized architecture. One such algorithm has already been evaluated [Valtari, 2004], but this yielded insufficient results. Due to the possibility of increasing the sampling frequency for the current and voltage measurements with the method presented in Chapter 3, this algorithm is worthy of reassessment, and this is done in this chapter.

5.1 Earth fault in the distribution network

5.1.1 Grounded network

If the neutral point of the network is connected to the ground, the network is grounded. Figure 5.1 presents an equivalent circuit to the earth fault in a grounded three-phase network:

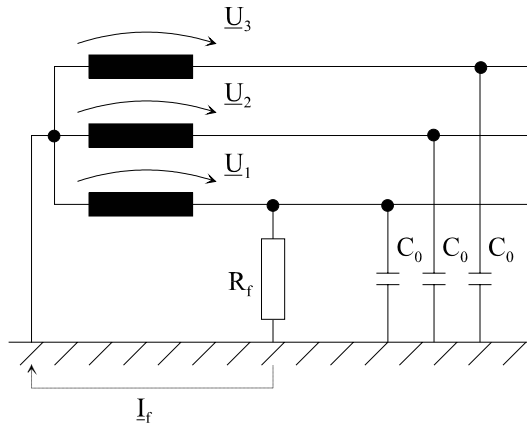


Figure 5.1: An earth fault in a grounded network.

The inductances shown in the figure represent the windings of a voltage transformer (only secondary coils in the figure). The phase voltages are marked with \underline{U}_1 , \underline{U}_2 and \underline{U}_3 , and the earth capacitances with C_0 . The resistance R_f connected to one of the phases represents an earth fault, and the fault current flowing through the star point of the network is marked with \underline{I}_f . The current flowing through the earth capacitances can be regarded as negligible in comparison with the current through the star point.

Detecting and locating earth faults in grounded networks is fairly easy, since the fault current during the fault is always large. When the potential of the neutral point is fixed to the earth potential, the voltage across the fault resistance will remain equal to phase-to-earth voltage. This keeps the fault current high and the faulted part of the network has to be disconnected for safety reasons. In principle, this fault corresponds to a normal short circuit between two phases.

Earth faults in grounded networks are usually detected with overcurrent relays, and the distance can be estimated from their magnitude of the fault current. Grounded

networks are practically nonexistent in Finland due to the grounding conditions, although they are relatively common in few other countries such as in the UK.

5.1.2 Isolated network

When the neutral point of the network is not connected, but left floating, the network is isolated. In Finland, most of the MV networks are isolated, largely due to the low conductivity of the ground [Lehtonen and Hakola, 1996]. The Figure 5.2 shows an earth fault in an isolated network:

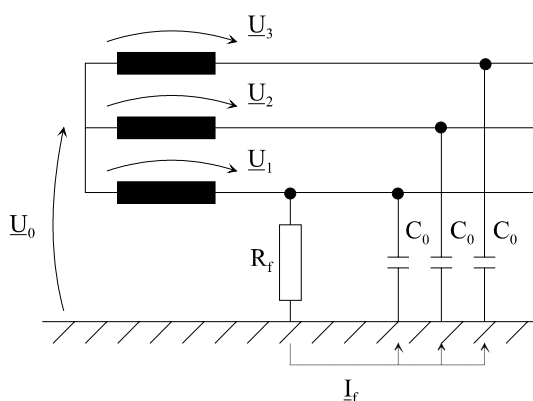


Figure 5.2: An earth fault in an isolated network.

The above figure is similar to Figure 5.1. The only difference is that the neutral point of the network is left floating. This causes a neutral voltage between the star point and ground, which is marked in the figure as U_0 . The fault current I_f flows through the earth capacitances (C_0).

An earth fault in an isolated network does not necessarily cause any disturbance to the power supply. During an earth fault, the potential of the neutral point moves towards the phase voltage. The earth fault lowers the voltage in the faulted phase and raises the voltages in the other phases. Because the voltage across the fault location decreases at the same time, the fault current is not always large, especially when the network is large or its fault resistance is high. The phase-to-phase voltages remain the same during the fault. The voltage vectors during an earth fault are presented in Figure 5.3.

The phase voltages during normal operation are marked with voltage vectors U_1 , U_2 and U_3 . During an earth fault, the potential of the neutral point changes, which

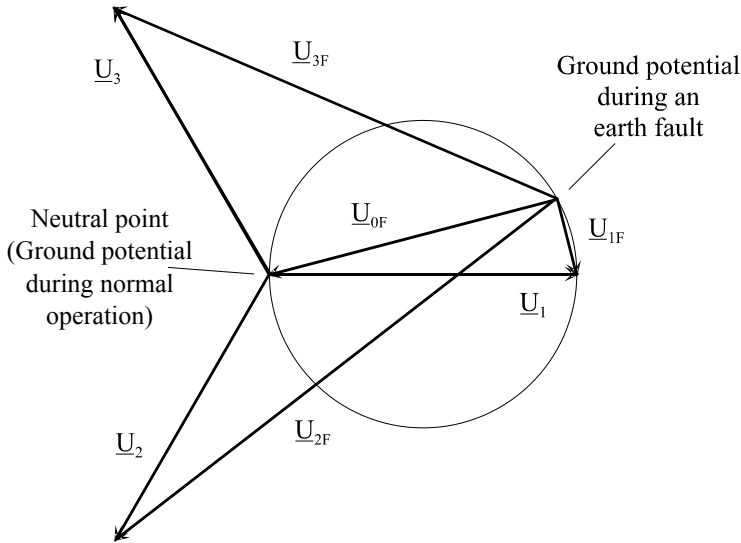


Figure 5.3: Voltage vectors during an earth fault.

causes a neutral voltage, \underline{U}_{0F} . Phase voltages during an earth fault are marked with \underline{U}_{1F} , \underline{U}_{2F} and \underline{U}_{3F} . The voltage vector \underline{U}_{0F} forms a circle as a function of fault resistance. This is mainly because the voltage vector \underline{U}_{0F} caused by the capacitive current is perpendicular to the voltage vector \underline{U}_{1F} , mainly caused by the resistive current.

Although keeping the network isolated reduces the number of interruptions in the distribution of electricity, it also puts more stress on the network. Voltages in healthy phases increase during an earth fault, which can cause more faults in the immediate future, such as a two-phase earth fault or a short circuit fault. This is also one reason why isolated networks are not so popular outside Scandinavia. [Nikander, 2002]

Equivalent circuit [Lehtonen and Hakola, 1996]

An equivalent circuit of an isolated network during an earth fault in phase 1 is depicted in Figure 5.4. When an earth fault occurs, the fault current flows through the earth capacitances (C_0), and the fault resistance (R_f), because there is no other route for the current. During the fault, the earth capacitances are connected in parallel so they can be added together. If the fault resistance is zero, the fault current (\underline{I}_e) can be calculated from (5.1), where $\omega_N = 2\pi f$ is the angular frequency of the network.

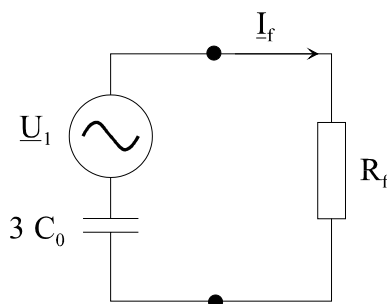


Figure 5.4: An equivalent circuit of an isolated network during an earth fault.

The amplitudes of the vectors \underline{U}_1 and \underline{I}_e are marked with scalars U_1 and I_e . The same notation is used throughout the thesis.

$$I_e = 3\omega_N C_0 U_1 \quad (5.1)$$

If the fault resistance differs from zero, the fault current is reduced. The reduced fault current (\underline{I}_e) can be calculated with (5.2).

$$I_f = \frac{I_e}{\sqrt{1 + \left(\frac{I_e}{U_1} R_f\right)^2}} \quad (5.2)$$

The neutral voltage (\underline{U}_0) measured by the protection and control IED is the voltage \underline{I}_f caused when it flows through earth capacitances, which is presented in (5.3). Therefore, the ratio between the amplitudes of the neutral voltage and the phase voltage during an earth fault can be calculated with (5.4).

$$U_0 = \frac{1}{3\omega_N C_0} I_f \quad (5.3)$$

$$\frac{U_0}{U_1} = \frac{1}{\sqrt{1 + (3\omega_N C_0 R_f)^2}} \quad (5.4)$$

(5.4) shows the same thing as Figure 5.3: when the fault resistance is very small the neutral voltage can rise as high as \underline{U}_1 . That also raises the voltages in the healthy phases, where the phase voltages can rise to phase-to-phase voltage. The highest voltage value of the healthy phases is about 1.05 times the phase-to-phase voltage, which is achieved when the fault resistance is about 37 percent of the impedance of the earth capacitances (see vector \underline{U}_{2F} in Figure 5.3). [Nikander, 2002]

Because the fault current is not necessarily high during earth faults, it is also difficult to detect and locate. Detection with overcurrent relays is not normally possible. The most reliable way to recognize an earth fault is by monitoring the neutral voltage \underline{U}_0 [Nikander, 2002]. However monitoring the absolute value of \underline{U}_0 is not sufficient. There is always some asymmetry in the network, and sometimes with high resistance faults an earth fault can even reduce \underline{U}_0 . That is because an earth fault changes the symmetry of the system, and by chance this change can be "towards symmetry". Sometimes the change can also be greater in its angle than in its amplitude. The best method is, therefore, to monitor the change in \underline{U}_0 .

5.1.3 Compensated network

The network is compensated if the neutral point of the network is connected to the ground via inductance. The main idea of this is to compensate the imaginary part of the fault current caused by earth capacitance in power lines. Compensation is normally done with so-called Petersen coils, and it can be either centralized (at one point) or distributed to many points in the network [Mörsky, 1993]. Sometimes, a resistor is also connected in parallel with the coil. Figure 5.5 presents an earth fault in a compensated network.

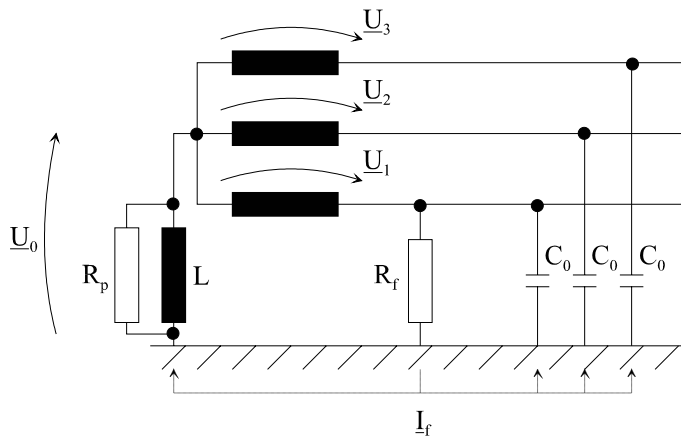


Figure 5.5: An earth fault in a compensated network.

As with the previous figures, \underline{U}_0 , \underline{U}_1 , \underline{U}_2 and \underline{U}_3 represent the neutral voltage and the phase voltages respectively. C_0 is the phase-to-earth capacitance and \underline{I}_f the fault

5.1. Earth fault in the distribution network

current caused by fault resistance R_f . The inductance of the Petersen coil is marked with L , and the resistance connected in parallel with it, R_p .

When an earth fault occurs, the inductance connected to the neutral point compensates the capacitive current due to the earth capacitances (phase-difference is 180 degrees). The fault current decreases considerably, which decreases protective earthing costs. The change in voltages during an earth fault is shown in Figure 5.6.

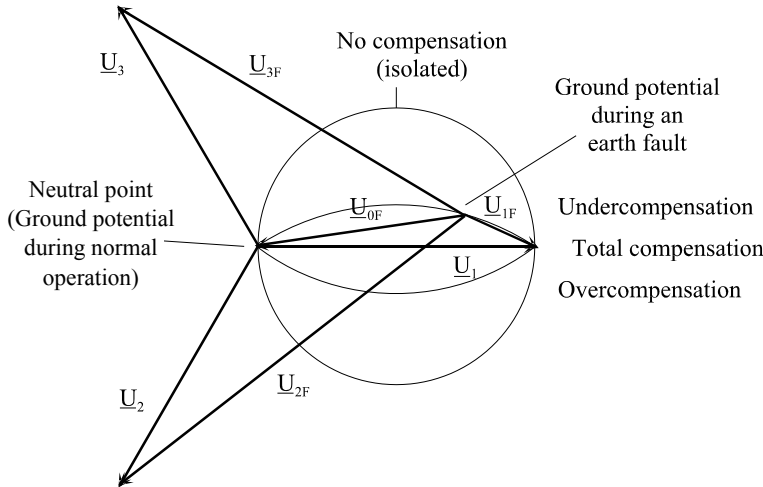


Figure 5.6: An earth fault in a compensated network (vector representation).

This figure is similar to Figure 5.3. Voltages during symmetrical operation are marked with \underline{U}_1 , \underline{U}_2 and \underline{U}_3 , and the voltages during an earth fault with \underline{U}_{1F} , \underline{U}_{2F} and \underline{U}_{3F} , respectively. The current that causes neutral voltage \underline{U}_{0F} is no longer entirely capacitive, and the angle between \underline{U}_{0F} and \underline{U}_{1F} is greater than 90 degrees. Therefore the potential of the star point doesn't form a circle, but a curve closer to an ellipsoid.

If the Petersen coil fully compensates the capacitive current, the network is said to be self-extinguishing. If an earth fault is only temporary, the network will extinguish a possible electrical arc automatically. The Petersen coil also smooths the changes in the neutral voltage, which prevents the fault recurring after the arc has been extinguished. Often, total compensation is not desirable, in which case detecting permanent earth faults becomes very difficult. An efficient compensation also increases the asymmetry during normal operation. In most cases, the coil is tuned so that the network is under- or over-compensated. Then, the fault current remains

large enough to be detected. Sometimes, a resistor is also connected in parallel with the Petersen coil, in order to increase the fault current during permanent earth faults. Such a resistor was also depicted in Figure 5.5. [Mörsky, 1993]

Equivalent circuit [Lehtonen and Hakola, 1996]

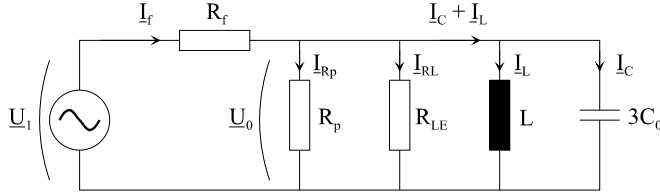


Figure 5.7: An equivalent circuit of a compensated network during an earth fault.

An equivalent circuit of a compensated network during an earth fault in phase 1 is depicted in Figure 5.7. In this case, the fault current has many routes. The capacitive current (I_C) flows through the earth capacitances ($3C_0$, because all three are connected in parallel), and the inductive current (I_L) through the Petersen coil (L). If the compensation is total, $I_L + I_C = 0$ and the fault current (I_f) only has a resistive component. The resistive component consists of the fault resistance (R_f), the leakage resistance of the coils and cables (R_{LE}) and a possible resistor connected in parallel with the Petersen coils (R_p). From the equivalent circuit the amplitude of the fault current (I_f) can be calculated with (5.5).

$$I_f = \frac{U_1 \sqrt{1 + R_{LE}^2 (3\omega_N C_0 - \frac{1}{\omega_N L})^2}}{\sqrt{(R_f + R_{LE})^2 + R_f^2 R_{LE}^2 (3\omega_N C_0 - \frac{1}{\omega_N L})^2}} \quad (5.5)$$

In the equation, ω_N represents the angular frequency of the network. If the network is self-extinguishing, the inductive current fully compensates for the capacitive current, and (5.5) can be simplified to (5.6).

$$I_f = \frac{U_1}{R_{LE} + R_f} \quad (5.6)$$

The amplitude of the neutral voltage (U_0) affecting across the parallel-connected capacitances, inductances and resistances can be calculated with (5.7).

$$I_0 = \frac{I_f}{\sqrt{\left(\frac{1}{R_{LE}}\right)^2 + \left(3\omega_N C_0 - \frac{1}{\omega_N L}\right)^2}} \quad (5.7)$$

As with previous equations, this is also simplified if the compensation is total. The total reactance drops to zero, and the ratio between the neutral voltage and the phase voltage can be calculated with (5.8).

$$\frac{U_0}{U_1} = \frac{R_{LE}}{R_{LE} - R_f} \quad (5.8)$$

For the equations (5.5) to (5.8) above, it was assumed that there was no resistor in parallel with the Petersen coil ($R_p = 0$). If a resistor is used, its effect can be taken into account by replacing R_{LE} by the parallel coupling of R_p and R_{LE} . As with isolated networks, the amplitude of the neutral voltage (U_0) can rise as high as the phase voltage (U_1).

5.1.4 Initial transients

When an earth fault occurs in an isolated or compensated network, there is always a fast transition, i.e. a transient. When the voltages on the phases change, the charge in them has to change too. During the transient, there is a current flowing from one phase to another which compensates for the change in the network. When the charge of the supply lines reaches the new equilibrium, the transient slowly decays. Utilization of these transients in protection and control IEDs has been rare, due to the high 10kHz sampling frequency requirements for the detection of the transients [Lehtonen, 1992].

The voltage transient due to an earth fault is shown in Figure 5.8. It also shows, how the voltages change during a low resistance earth fault - the voltage of the faulted phase drops close to zero whereas the voltages of the healthy phases rise to phase-to-phase voltage.

The transient consists mainly of two components - which are called the discharge component and the charge component. In addition, there are interline compensating components, whose function is to equalize the voltages of parallel lines at their sub-station terminals. In compensated networks there is also a decaying DC-component (Direct Current), which is due to the Petersen coil. [Lehtonen, 1992]

The discharge component results from the decrement of the voltage in the faulted phase. When the voltage in the faulted phase decreases, the energy stored in the

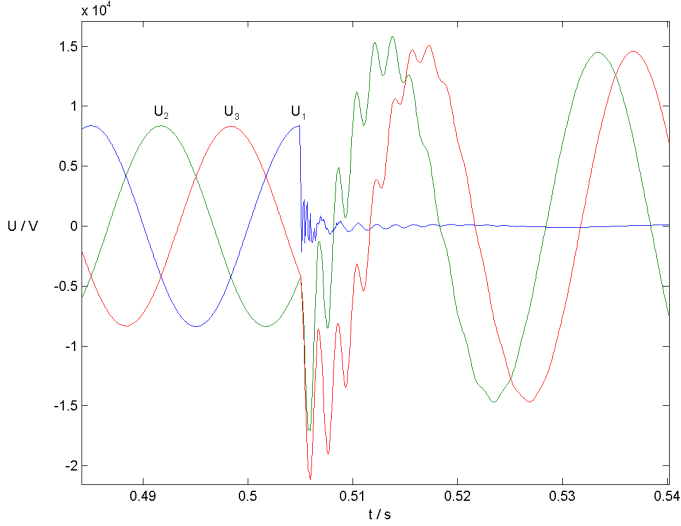


Figure 5.8: A simulated example, an earth fault in phase 1, transient components visible in phase voltages.

capacitances of the cabling has to decrease as well. Simultaneously, the voltages in the healthy phases rise, and these cables can reserve more energy. This appears in the phase voltage as a higher-frequency charge component. Because the charge component flows through a transformer, its frequency is much lower than that of the discharge component. The frequency of the discharge component is normally 500...2500 Hz and that of the charge component 100...800 Hz [Lehtonen and Hakola, 1996]. The amplitude of the charge component dominates the transient, which makes it more suitable for relaying purposes.

The charge transient can be modeled with the equivalent circuit presented in Figure 5.9. When an earth fault occurs at the substation, the angular frequency of the charge transient (ω_C) can be calculated with (5.9), (5.10) and (5.11) [Hänninen, 2001]:

$$\omega_C = \frac{1}{\sqrt{L_{eq}C_{eq}}} = \frac{1}{\sqrt{3L_T(C_0 + C_{pp})}} \quad (5.9)$$

$$L_{eq} = 1.5L_T \quad (5.10)$$

$$C_{eq} = 2(C_0 + C_{pp}) \quad (5.11)$$

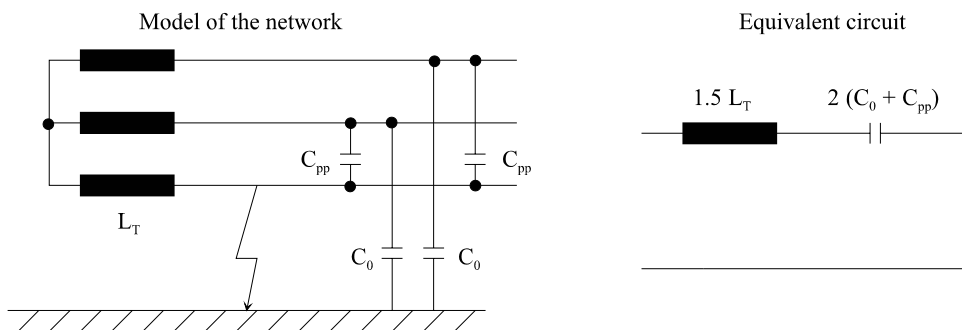


Figure 5.9: Network model and equivalent circuit used for modeling the charge transient, fault resistance 0Ω .

C_{eq} and L_{eq} correspond to the respective equivalent capacitance and inductance of the network. During an earth fault, the phase-to-phase capacitances (C_{pp}) and the earth capacitances (C_0) are connected in parallel, as are two of the transformer phase inductances (L_T). This causes the equivalent quantities to be as shown in (5.10) and (5.11).

The amplitude of the transient is also dependent on the phase of the fundamental frequency. If the fault occurs during the fundamental maximum, the transient amplitude (\hat{i}_{Ch}) is largest and can be calculated with (5.12) [Lehtonen and Hakola, 1996],

$$\hat{i}_{Ch} = \frac{C_{eq}\omega_C}{3C_0\omega_N} I_e \quad (5.12)$$

where ω_N corresponds to the angular frequency of the network, and \underline{I}_e to the amplitude of the uncompensated, steady-state earth fault current. The fault resistance in (5.12) is zero. At values close to fundamental zero, (the amplitude of the fundamental 50Hz or 60Hz component is zero) the amplitude is smallest, and in fact sometimes the transient might not be visible at all. Normally, the fault occurs during the fundamental maximum (i.e. amplitude of the fundamental 50Hz or 60Hz component has its maximum value), which is also the best case for calculations.

As noted from (5.12), the transient amplitude is linearly dependent on the transient frequency. In practice, it can be up to 10-15 times the fundamental component of the

earth fault current I_e . The fault resistance also has a significant influence on the charge transient. This not only has an effect on the earth fault current (I_e), but it also dampens the transient. The limit when the transient becomes overdamped in overhead lines is considered to be 50 - 200 Ω [Lehtonen and Hakola, 1996]. The greater the distance to the fault location, the greater the equivalent inductance will be, which lowers the transient frequency.

When an earth fault occurs in larger networks, the transients do not only flow from the faulty phase to the healthy ones, but also from the faulty feeder to the healthy feeders. The total change in the charge of a feeder is clearly visible in the neutral (summation) current I_0 of the feeder. An example is shown in Figure 5.10, which is a simulation result from the model presented later on, in section 5.3.2

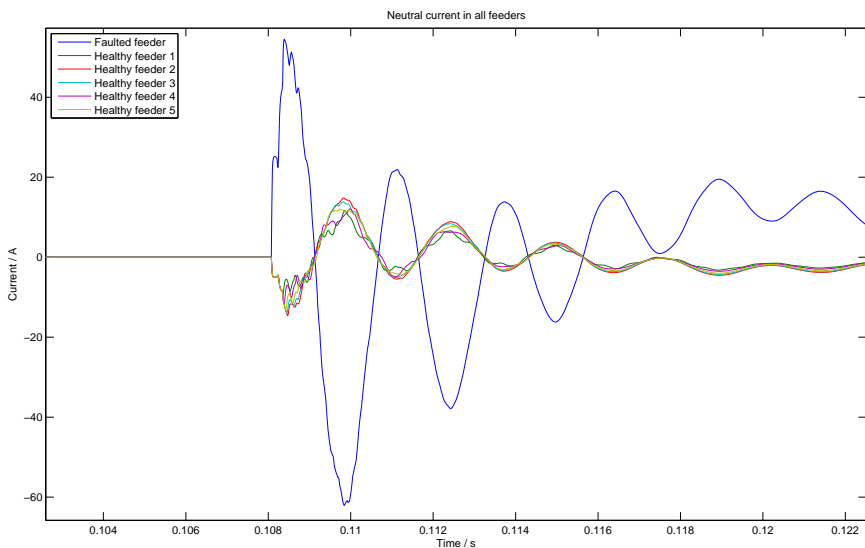


Figure 5.10: Neutral current in all feeders during an earth fault in one feeder, 6 feeders in the simulated example.

5.1.5 Measured fault resistances during earth faults

Fault impedance is normally purely resistive [Lehtonen and Hakola, 1996]. The fault reactance can thus be neglected, and only the fault resistance need be considered. As

5.1. Earth fault in the distribution network

explained in the previous sub-section, the charge transient normally becomes over-damped when the fault resistance is 50 - 200 Ω [Lehtonen and Hakola, 1996]. This means that earth contact has to be direct.

The resistance of a tree depends on many factors: the soil, humidity, season, type of tree, etc. Fault resistance measurements on an experimental 12 kV bare conductor line with an earthed neutral are reported in [Aro, 1993]. In summer, the resistance of unseasoned wood with a moisture-free surface was about 20 k Ω . In the spring, the resistance was 36...58 k Ω , and in winter, with frosty air and frozen soil, it was 2..3 M Ω . These values are much larger than 200 Ω , so in practice, charge or discharge transients during earth faults caused by fallen trees are too damped for relaying purposes.

Fault resistance is almost never zero, especially with overhead lines. In reference [Hänninen and Lehtonen, 1998], a study was made in order to determine most normal fault resistances in real-life situations. Figures 5.11 and 5.12 present the diagrams of the different fault resistances evaluated in the study.

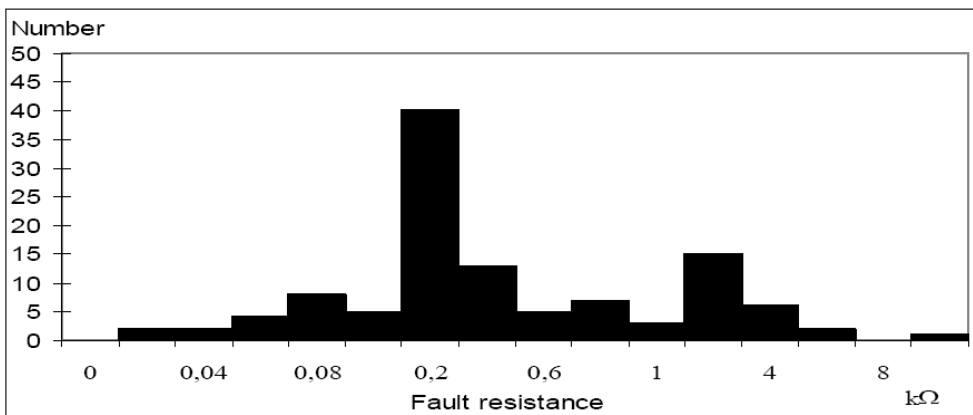


Figure 5.11: The division of the fault resistances in a compensated network [Hänninen and Lehtonen, 1998].

The study shows that there are clearly two categories of fault resistances. In the first category, the resistance is below a few hundred ohms. When the resistance is below a few hundred ohms, there is an actual galvanic connection to the ground, and the faulted part has to be disconnected from the network. In the other category, the fault resistance is several kilo-ohms. These situations correspond to cases when, say,

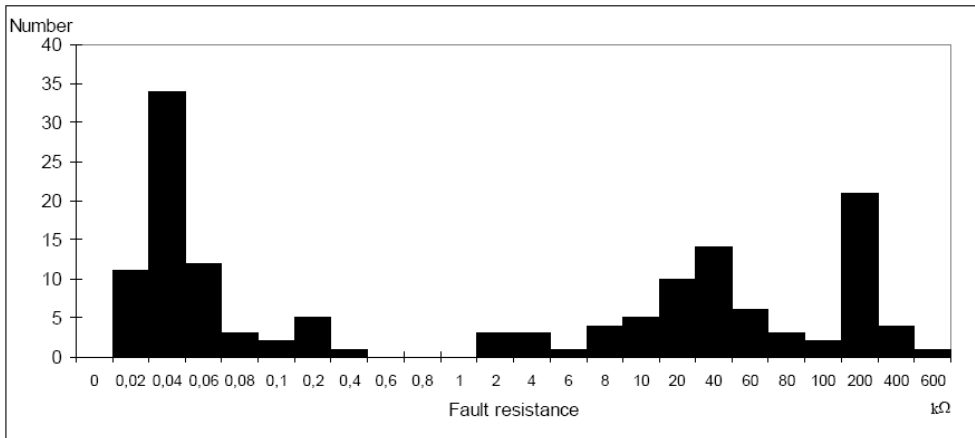


Figure 5.12: The division of the fault resistances in a isolated network [Hänninen and Lehtonen, 1998].

a tree forms the contact. The fault current is normally low, and normal operation is not threatened. These faults can, however, develop into low-resistance faults and/or short circuits if they are not detected in time.

5.2 Earth fault location methods

The indication and location of earth faults has proved to be a very challenging task. Fault resistances can vary greatly, as can the electrical capabilities of supply lines. Currents and voltages also vary considerably due to changes in the weather, or in the load. Connecting or disconnecting different electrical equipment can cause changes in electrical quantities that are very similar to earth faults.

In an isolated or compensated network, a single-phase earth fault always disturbs the symmetry of the network. The neutral voltage then changes abruptly, and this is normally the best method of recognizing an earth fault. Analyzing the changes that occur in current and voltage measurements helps in determining the fault location. The main objective has been to calculate the impedance between the IED and fault location. Cables have a known impedance per kilometer. If the impedance to the fault location can be estimated accurately, that data can be used to derive the distance to the fault.

The fault resistance can also vary according to the nature of the fault. If the cable

breaks, and the supply end of the cable touches the ground, the fault resistance can be close to zero. On the other hand, if the supply end stays in the air, the fault resistance can be several $M\Omega$. The resistance of a tree can also be several $k\Omega$. In practice, the fault resistance is never zero.

Therefore, merely calculating the fault resistance is not an adequate method for determining the distance to the fault location. Because the fault reactance is normally close to zero (fault impedance is normally only resistive), a much more reliable method is to calculate the inductance of the network.

5.2.1 Earth fault location methods based on initial transients

Much research has focused on calculating the distance from initial transients at the occurrence of an earth fault. As stated above, the current charge transient of the fault has a relatively low frequency and high amplitude in comparison with the other transient components, which makes it eminently suitable for earth fault location methods. The goal has been to estimate the inductance of the faulted phase from the transient. The distance can then be calculated from the inductance, assuming that the inductance per kilometer is known. The equations presented in section 5.1.4 were for those cases when the fault occurs at the substation. When the fault occurs further away in the network, the inductance of the line must also be taken into consideration.

Connecting a Petersen coil to the neutral point of a voltage transformer does not affect the amplitude of the charge transient, since the transient frequency is significantly higher than the fundamental frequency. The inductive reactance of a Petersen coil is therefore fairly large in the frequency area of the charge transient and it can be compared with isolation [Lehtonen, 1992]. For this reason, the transient method works on both isolated and compensated networks.

A method based on current and voltage transients measured from the incoming feeder was studied in [Hänninen and Lehtonen, 2002b]. Calculation of the distance from the transient took up a fairly large amount of the processor time. Several filters and a DFT (Discrete Fourier Transform) analysis had to be used before the result was achieved. The algorithm also used a large amount of memory, since the data from a relatively long period has to be processed. Furthermore, the references implied that the sampling frequency has to be relatively high, > 10 kHz for a reliable earth fault location, which is not possible with present-day protection and control IEDs. New earth fault location algorithms which have been proposed require even higher

sampling frequencies, up to 100 kHz [Ma et al., 2010].

Using sampling frequencies of less than 10 kHz creates an additional error in the estimates of the distance of the fault [Valtari, 2004]. The frequency of the charge transient is only 100...800 Hz, so based on the Nyquist-Shannon theorem, 2 kHz should be sufficient for the calculations [Phadke and Thorp, 1990]. The theorem does not fully apply to this case, since the measured transient is so short that only a few data points are used for the whole analysis [Lehtonen and Hakola, 1996].

Other drawbacks with the presented algorithm are based on the amount of data [Hänninen and Lehtonen, 2002b]. Since the whole analysis is made with the data from the beginning of the fault, there is only one dataset available from the fault transient. If the transient is not suitable for analysis because of other, concurrent changes in the voltages, the fault location can not be determined. Furthermore, the transient becomes overdamped when the fault resistance is 50...200 Ω [Lehtonen and Hakola, 1996].

Two different methods have been explored and tested for the calculation in [Hänninen and Lehtonen, 2002a]. The first one, called "the differential equation method", calculates the inductance in the time domain with the help of a trapezoidal rule [Schegner, 1989]. Another method has been studied, which uses wavelet transformation instead of the trapezoidal rule [Hänninen et al., 1999]. This method calculates the inductance in the frequency domain. The results with the differential equations have been slightly better, especially in an isolated network, which makes this a more recommendable implementation. The method for increasing the sampling frequency presented in Chapter 3 also presents the possibility of testing the performance of the algorithm without a 10 kHz sampling frequency, and this will be presented later on in this chapter.

Transient-based methods have also been used to indicate the faulted feeder in a substation. As described earlier in this chapter, in the case of a larger substation an earth fault causes the overall charges of different feeders to change, which can be observed from the neutral current. A method proposed in [Abdel-Fattah and Lehtonen, 2009] uses this phenomenon for detecting the faulted feeder. The neutral current transient flowing from the faulted feeder towards the substation equals the sum of the neutral currents of all the other feeders flowing away from the substation. A combination of a transient-based earth fault location algorithm with a faulted feeder, and faulted phase detection, provides complete earth fault location functionality in a substation, provided that the fault resistance is low enough.

5.2.2 Other algorithms for earth fault location

As stated, the algorithm presented above, which is based on the initial charge transient, suffers from the fact that it requires a sufficient number of samples from the duration of the transient. If the inductance could be calculated from the network states (before and after the fault) instead of the transition between them, accuracy could be greatly improved. This would allow the algorithm to repeat calculations and thus increase the accuracy of fault location by averaging the various consequent values. Promising results have been achieved, but fault location, especially in compensated networks, is still a challenging issue [Hänninen and Lehtonen, 2002a] [Wahlroos and Altonen, 2011].

MV networks are normally meshed in order to ensure energy distribution in fault situations. However, normally a network has radial operation, because it is simpler to control. Operating MV networks with a meshed rather than a radial topology would enable the utilization of new methods for earth fault location [Nikander, 2002]. Comparing the fault currents from two IEDs connected to the same faulted phase would provide more information about the fault. If the fault is between the IEDs, the ratio of the fault currents is inversely proportional to the ratio of the fault distances. There are also other methods for calculating the fault distance using the data from two IEDs. However, one drawback to this is that connecting a faulted part of the network into a closed ring might give rise to other dangerous situations, even if it were only for a short time.

The use of artificial neural networks (ANN) is also an interesting area for earth fault location algorithms [Eberl et al., 2000]. The objective is to teach the system the difference between the healthy state and the faulted state of a power line, and the differences in electrical quantities when the distance to the fault location changes. However, with current technology, the training period of the algorithm is long. Furthermore, the solution is not generic, but dependent on the environment. The algorithm has to be constantly adapted to new environments, which decreases the independence of the algorithm. Therefore, current ANN technology is not yet advanced enough for this purpose, although the situation may well change in the future.

Some algorithms use a model of the network to calculate the fault location [Saha et al., 2001]. Given adequate information about the network topology, it might be easier to determine the location of a fault. However, the need for a network topology increases the implementation costs and makes the IEDs less independent.

The use of specific cable radar is not, in itself, another algorithm, but is rather a separate device which calculates the distance to the fault location. It uses specific impulses, which it sends to the faulted power line. When the pulse reaches the fault location, there is a sudden change in the impedance. From this point a part of the signal impulse is reflected back to the radar. Analyzing the time interval between the transmitted and the returned impulse helps in determining the fault location. Cable radar is the most accurate method for detecting the fault. The drawback with this method is that it needs a separate device for the analysis. Furthermore, voltages have to be disconnected while the measurements are taken. In urban areas, where the cables are mostly underground, this method is still the only reasonable choice. Digging up part of a cable is such an expensive project that fault location has to be precise. [Mörsky, 1993]

5.3 Test results for the impact of sampling frequency on transient-based earth fault location

In order to test the performance of the method for increasing the sampling frequency of current and voltage measurements (as proposed in Chapter 3), the method was applied to a transient-based earth fault location algorithm. The method is presented below, in section 5.3.1 and the results are analyzed in section 5.3.2.

5.3.1 Description of the algorithm

The algorithm studied here is based on the research carried out during a Tekes research project in 2002 [Hänninen and Lehtonen, 2002b], and initially tested in [Valtari, 2004]. The basic concept of the algorithm comes from previous studies [Schegner, 1989], and only small modifications have been made. Using the trapezoidal rule [Phadke and Thorp, 1990] to solve the differential equation, and a current correction algorithm before the differential equation improved the accuracy. The algorithm uses voltage and current values measured from one feeder, so one algorithm per substation is sufficient, which is in line with the results in Chapter 3. In order to determine in which feeder the fault occurs, the location algorithm presented in [Abdel-Fattah and Lehtonen, 2009] was used. The inputs and outputs of the algorithm are presented in Table 5.1. The flow chart of the algorithm is presented in Figure 5.13.

In Figure 5.13 the components of the function were also introduced. The name

5.3. Test results for the impact of sampling frequency on transient-based earth fault location

Table 5.1: Inputs and outputs of the earth fault location algorithm

Type	Signal	Description
Inputs	U1, U2, U3, I1, I2, I3	Phase voltages and currents
	U0	Neutral Voltage
	Limit	Trigger level of neutral voltage
	C _{pp}	Phase-to-phase capacitance
	L _{tf}	Phase inductance of the voltage transformer
	L _{km}	Inductance of the power lines per kilometer
Outputs	LEFA	Low resistance earth fault alarm
	Distance	Distance to the fault location
	Deviation	Deviation of the calculated distance

of each component is written next to the corresponding flow chart element in italics, and the different components are explained more accurately below.

DetectTransient_A

The component DetectTransient_A keeps a buffer of phase voltages and currents from the previous 30 ms. Every 5 ms it checks the buffer and searches for a possible earth fault. The fault is detected by monitoring the neutral voltage. If the network has compensation capacitors, their influence has to be reduced in the data. After detecting a fault, the indication and the corresponding voltage and current buffers are fed to the next component.

Here, the faulted feeder is also detected with the method presented in [Abdel-Fattah and Lehtonen, 2009]. The average value of the neutral current for each feeder is calculated over the time-span of the first transient half cycle (from the beginning of the transient to the first zero crossing), see (5.13).

$$I_0 = \frac{\sum_{k=1}^N i_{0,k}}{N} \quad (5.13)$$

where:

$i_{r,k}$ is the instantaneous neutral current at sample k , and

N is the number of samples in the transient window.

The determination of the faulted feeder is then made by calculating the K value according to (5.14)

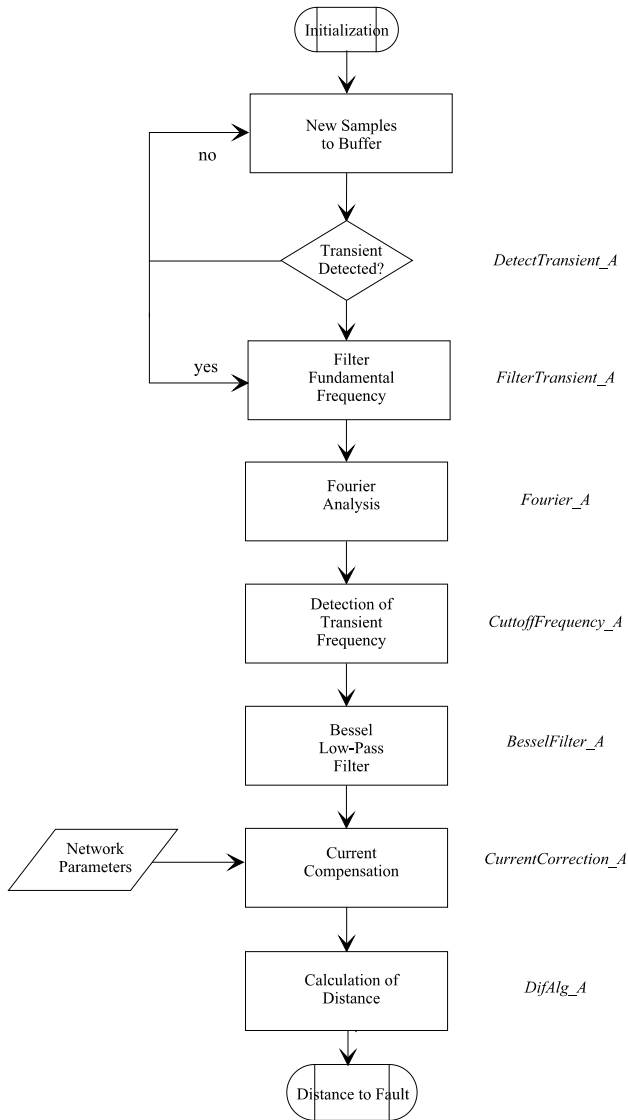


Figure 5.13: Flow chart of the differential equation algorithm and corresponding components.

$$K = \frac{|I_0 - I_{0,others}|}{I_{0,all}} * 100\% \quad (5.14)$$

where

5.3. Test results for the impact of sampling frequency on transient-based earth fault location

$$I_{0,other\,s} = \sum I_0 \text{ (for other feeders) and}$$

$$I_{0,all} = \sum |I_0| \text{ (for all feeders).}$$

This calculation gives K=100% for the faulted feeder and a value close to 0% for all the other feeders.

FilterTransient_A

FilterTransient_A removes the fundamental frequency from the transient with a comb filter; see (5.15) [Lehtonen, 1992]. It also determines the beginning of the transient before delivering data arrays to the next component. The most accurate analysis can be made from the first transient wavelength, so finding this is essential.

$$g(t) = f(t) - f(t + T) \tag{5.15}$$

In (5.15) $f(t)$ is the original and $g(t)$ the filtered signal. T is the period of fundamental frequency.

Fourier_A

Fourier_A performs a DFT analysis of the transient. Its purpose is to determine the transient frequency, so that higher frequencies can be filtered out. It calculates the amplitudes of the frequency components between the frequencies of 100 Hz and 1 kHz, and delivers them to the next component.

CutoffFrequency_A

After receiving the data from the Fourier analysis, CutoffFrequency_A calculates which frequency component has the largest amplitude. This frequency component is the transient frequency. The cut-off frequency for the following low-pass filter is set at 50 Hz higher than the transient frequency. [Hänninen and Lehtonen, 2002b]

BesselFilter_A

BesselFilter_A includes a second degree Bessel low-pass filter. Since the most accurate analysis can be made from the charge transient, the discharge transient and other high-frequency components are removed with this filter.

CurrentCorrection_A

When the calculations are made with the charge component, the effect of the transformer has to be taken into account. Part of the charge component flows through the transformer windings and part of it is delivered via phase-to-phase capacitances. These changes have to be compensated before the distance to the fault location can be calculated. This compensation is made with CurrentCorrection_A.

DifAlg_A

DifAlg_A includes the differential equation, which finally calculates the inductance of the faulted line, and through that the distance to the fault location. The calculation is done with the help of the trapezoidal rule, (5.16) [Phadke and Thorp, 1990]:

$$L = \frac{\Delta t}{2} \left[\frac{(i_{k+1} + i_k)(u_{k+2} + u_{k+1}) - (i_{k+2} + i_{k+1})(u_{k+1} + u_k)}{(i_{k+1} + i_k)(i_{k+2} - i_{k+1}) - (i_{k+2} + i_{k+1})(i_{k+1} - i_k)} \right] \quad (5.16)$$

In the rule, L is the inductance of the faulted phase, t the time interval between two consecutive samples, and i_k and u_k the respective current and voltage values at instant k . This rule can be used for all situations where the current and voltage fulfill the following differential equation of the first order (5.17).

$$u(t) = Ri(t) + L \frac{di(t)}{dt} \quad (5.17)$$

The above trapezoidal rule calculates local estimates from only three samples. As a result there will be an array with many different inductance values. The most likely real inductance value is determined with local variance [Schegner, 1989]. The algorithm calculates the variance of a certain number of consecutive inductance values. If the variance is small, the inductance value only changes a little. The period during which the smallest variance occurs is considered to be the best for calculations. The average inductance value of that period is the most-likely real value.

After that, both the distance and the distance deviation can be calculated from the inductance and the variance. For these calculations, the algorithm needs only the approximated inductance per km of the transmission cable.

5.3.2 Analyzing the simulation results

The algorithm was tested with simulated data. The model and the results from the different cases are presented in this section. The main focus of these cases was to evaluate the performance of the method for increasing current and voltage measurements presented in Chapter 3. The tests were performed in a simulation model with seven feeders (one incoming, six outgoing) under three different scenarios:

A) Single measurement with the full sampling frequency

B) Seven different sample streams, merged to full sampling frequency, as presented in Chapter 3. The voltage measurements are merged according to section 3.3.2 and the current measurements according to section 3.3.3.

C) Single measurement with one seventh of a full sampling frequency

The anti-alias filters of the individual IEDs were not taken into account in the simulation, as the target was only to focus on the effect of different sampling frequencies, and especially on the differences between cases B) and C) which would both have the same anti-alias filter.

Fault location accuracy is defined in [IEEE, 2004] according to (5.18), and is also often expressed as a percentage value instead of a per unit one.

$$e(\text{error}) = \frac{(\text{instrument reading} - \text{exact distance to the fault})}{\text{total line length}} \quad (5.18)$$

The required accuracy for fault location depends greatly on the type of network. For a rural overhead-line network, the main purpose is to locate the right control zone, i.e. which section of the network should be disconnected. Normally, an accuracy of 10% of the line length is considered sufficient for this [Wahlroos and Altonen, 2011], [Manner et al., 2011].

Simulation model

The simulation model used to test the algorithm and the measurement method was created with the alternative transient program ATP/EMTP, which is a popular simulation software package mainly intended for transient analysis applications. The model is presented below in Figure 5.14

More detailed information about the model is presented below, and the faults were simulated in Feeder 1.

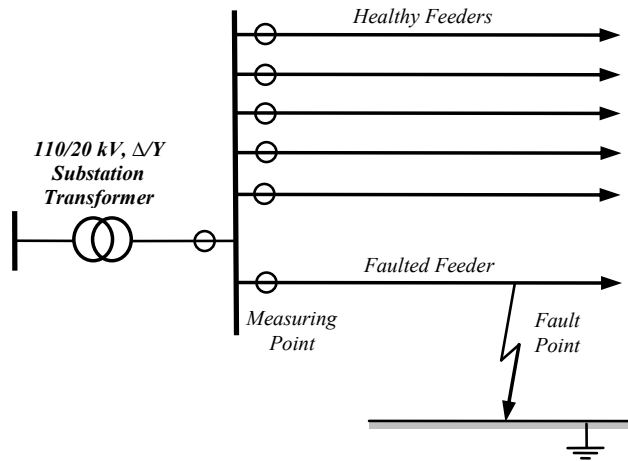


Figure 5.14: Simulation model used for testing.

- Substation transformers: 10 MVA, 110/20 kV. Six outgoing feeders, of total length = 244 km
- Feeder 1: 40 km, LV transformers (20/0.4 kV)= 1 MVA, Load = 900 kW
- Feeder 2: 33 km, LV transformers (20/0.4 kV)= 0.8 MVA, Load = 720 kW
- Feeder 3: 47 km, LV transformers (20/0.4 kV)= 1.25 MVA, Load = 1063 kW
- Feeder 4: 45 km, LV transformers (20/0.4 kV)= 0.8 MVA, Load = 800 kW
- Feeder 5: 37 km, LV transformers (20/0.4 kV)= 1.25 MVA, Load = 1125 kW
- Feeder 6: 42 km, LV transformers (20/0.4 kV)= 1 MVA, Load = 900 kW

Isolated network, $R_f = 10 \Omega$, sampling frequency varied

Figures 5.15 to 5.17 present the error of the algorithm, as well as the calculated deviation of the network set-up with three different sampling rates. In this set-up, the fault resistance (R_f) was 10Ω and the network had an isolated neutral. The network had six outgoing feeders in addition to the incoming one. The fault distance was varied from 0.8 km to 39.2 km.

5.3. Test results for the impact of sampling frequency on transient-based earth fault location

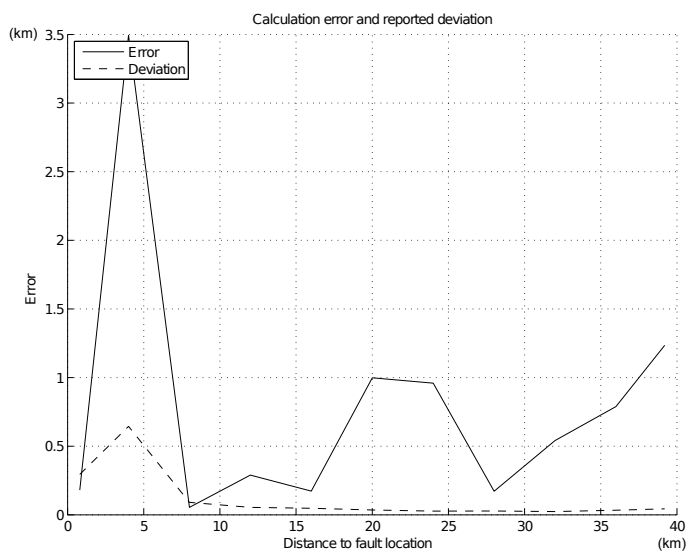


Figure 5.15: Results with sampling frequency of 16 kHz, $R_f = 10 \Omega$.

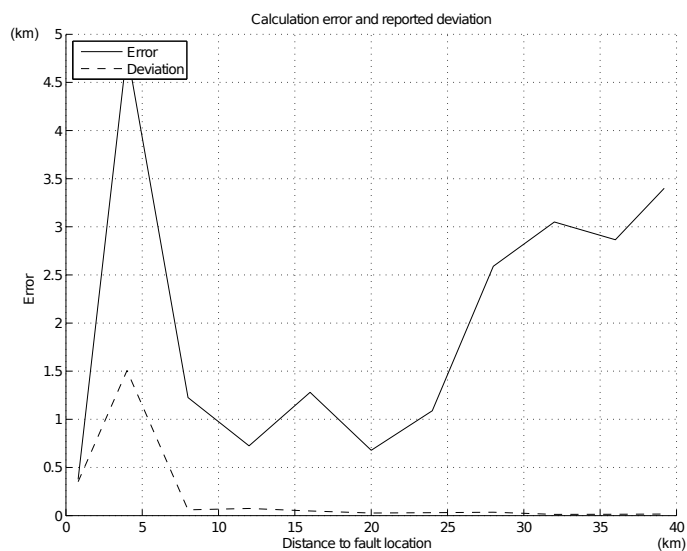


Figure 5.16: Results with seven different sample streams, combining to 16 kHz when processed as in Chapter 3, $R_f = 10 \Omega$.

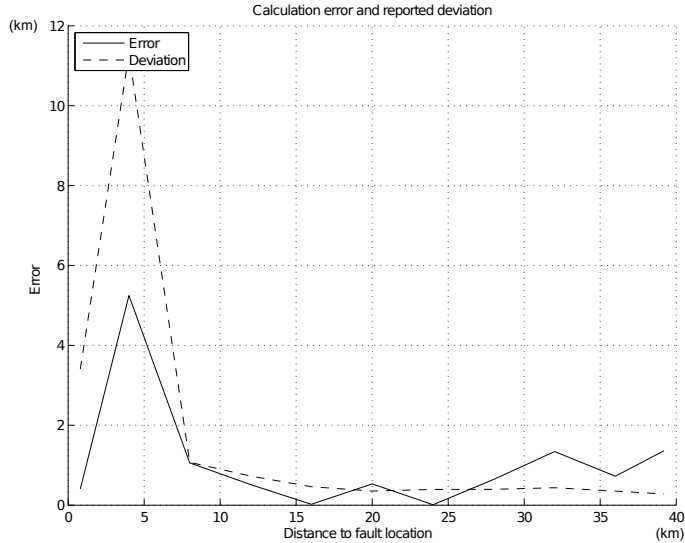


Figure 5.17: Results a sample frequency of $16 \text{ kHz} / 7 = 2.29 \text{ kHz}$, $R_f = 10 \Omega$.

The results do not reveal any large differences between the different sampling arrangements. As was expected, although the arrangement with a single, low sampling rate IED without measurement merging in Figure 5.17 does not perform as well as the method with measurement merging in Figure 5.16, or with the one single high sampling frequency measurement in Figure 5.15, the difference is not great. All the cases fulfill the criteria of 10% accuracy (4km in a 40km network), when the fault distance is over 5km.

The individual sampling frequency of 2.29 kHz does not correspond to a real case of protection and control IEDs, where the sampling frequency is a round number such as 2 kHz (which would result in a total sampling frequency of $7 * 2 \text{ kHz} = 14 \text{ kHz}$). An overall sampling frequency of 16 kHz instead of 14 kHz was used in order simplify the simulation arrangements (16 kHz means a sample time of $62.5 \mu\text{s}$).

Frequency and amplitude of the charge transient, $R_f = 10 \Omega$

One interesting point is to investigate how the transient behaves with different fault distances, because that is the only source of information in the algorithm. Viewing the frequency and amplitude of the transient with a function of fault distance gives us some idea about the behavior. Now we can also compare it to the theory from section

5.1. The derived transient frequencies and corresponding amplitudes of the Fourier component with different fault distances are presented in Figure 5.18.

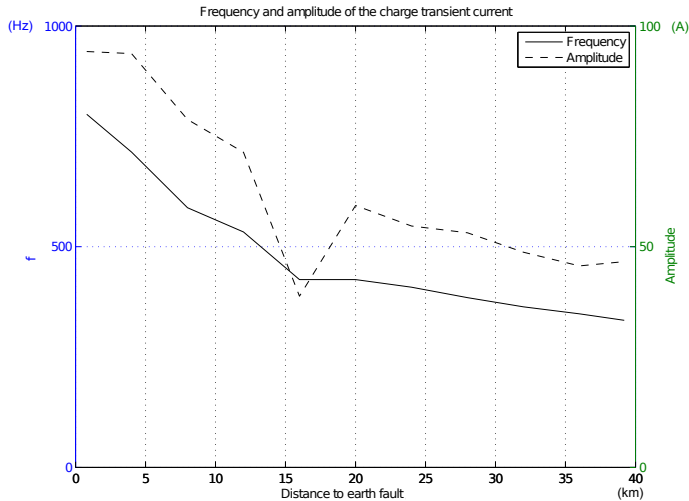


Figure 5.18: Transient frequency and amplitude with $R_f = 10 \Omega$.

Figure 5.18 supports the theory. When the distance between the fault location and the IED increases, the inductance also increases. This reduces both the frequency and the amplitude of the charge transient. The transient frequency is in the frequency area predicted by the references, and the amplitude varies from 90 A to 40 A.

Isolated network, $R_f = 80 \Omega$, sampling frequency varied

Figures 5.19 to 5.21 present the same information when the fault resistance is increased to 80Ω .

Here, the differences between the different sampling arrangements is clear. When the fault resistance increases, the transient becomes smaller and the analysis must be made from much smaller current and voltage variations. In this case, only the results with one single high frequency measurement are below the required 10% (or 4 km), see Figure 5.19. The results from the measurement merging method in Figure 5.20 are below 10% when the fault distance is between 8 km and 28 km. At the beginning of the feeder, the error in the algorithm is 30% and at the end of the feeder it is 15% of the feeder length. The results from the single low sampling frequency, Figure 5.21, are the worst, the maximum error being over 150%.

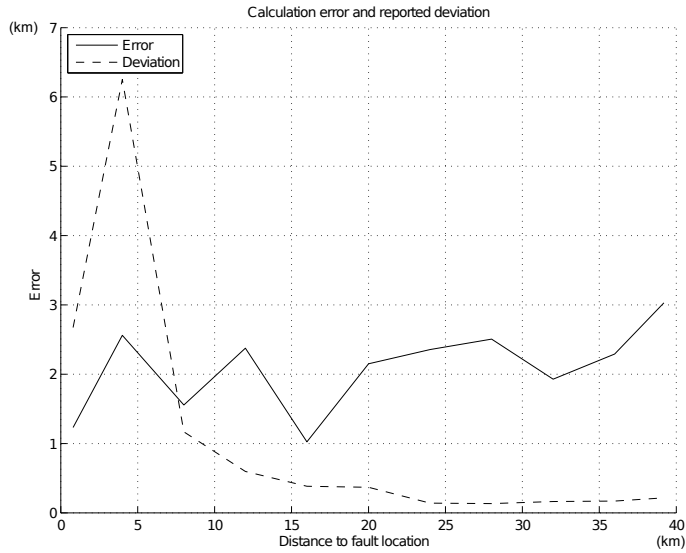


Figure 5.19: Results with sampling frequency of 16 kHz, $R_f = 80 \Omega$.

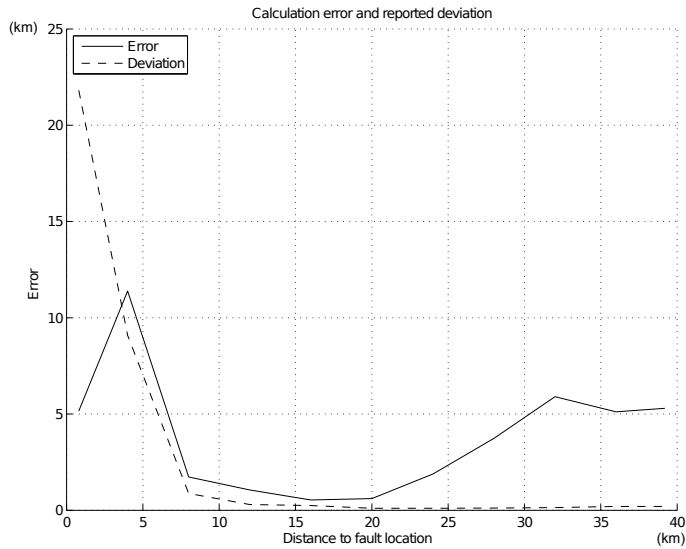


Figure 5.20: Results with seven different sample streams, combining to 16 kHz when processed as in Chapter 3, $R_f = 80 \Omega$.

5.3. Test results for the impact of sampling frequency on transient-based earth fault location

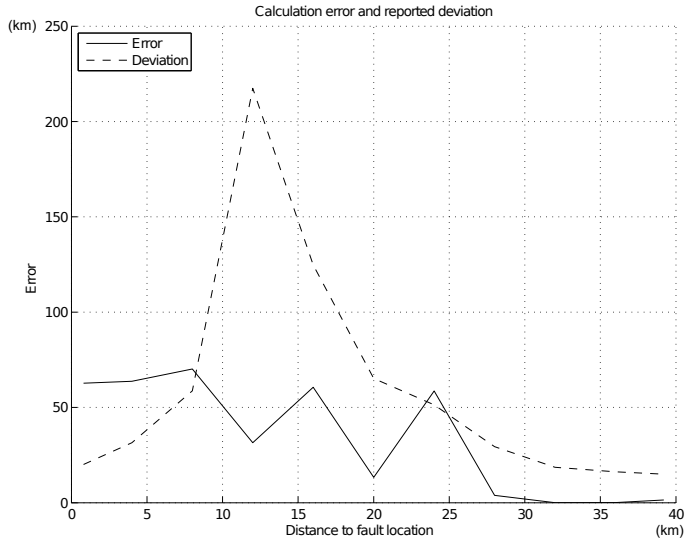


Figure 5.21: Results a sample frequency of $16 \text{ kHz} / 7 = 2.29 \text{ kHz}$, $R_f = 80 \Omega$.

Frequency and amplitude of the charge transient, $R_f = 80 \Omega$

As stated in section 5.1.4, the greater the distance to the fault location, the greater the equivalent inductance will be, which lowers the transient frequency. Furthermore, the transient amplitude is linearly dependent on the transient frequency. The fault resistance also dampens the transient, and with 80Ω fault resistance it is only around 30-40 A, which is one major reason for the errors of over 150% of the line length in Figure 5.21

Overall performance

The tests were repeated with different sampling frequencies. The aim was to compare three different arrangements. First, a case where the measurements are received from a single measurement device with a high sampling frequency was evaluated. Then the method presented in Chapter 3 was tried out, where the same sampling frequency was derived from multiple lower sampling frequency devices (7 in this case). Finally, for comparison, the measurement from one such device (without measurement merging) was used for fault distance calculation. These three cases with two different fault resistances resulted in six different cases, which are shown in Table 5.2.

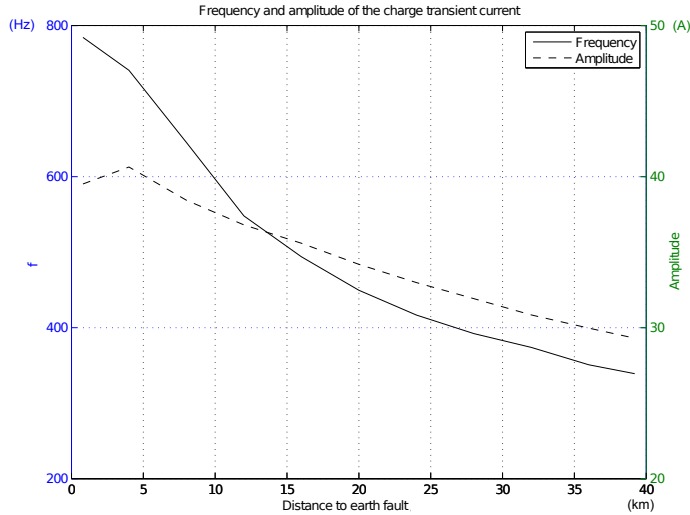


Figure 5.22: Transient frequency and amplitude with $R_f = 80 \Omega$.

Table 5.2: Different measurement cases

Abbr	Function
1	$R_f = 10 \Omega$, single measurement with the full sampling frequency
2	$R_f = 10 \Omega$, seven different sample streams, merged to full sampling frequency (as in Chapter 3)
3	$R_f = 10 \Omega$, single measurement with the one seventh of a full sampling frequency
4	$R_f = 80 \Omega$, single measurement with the full sampling frequency
5	$R_f = 80 \Omega$, seven different sample streams, merged to full sampling frequency (as in Chapter 3)
6	$R_f = 80 \Omega$, single measurement with the one seventh of a full sampling frequency

In order to make a more detailed evaluation, these six cases were repeated with three different sampling frequencies, 20 kHz (one IED 20 kHz / 7 = 2.86 kHz), 16 kHz (one IED 16 kHz / 7 = 2.29 kHz) and 10 kHz (one IED 10 kHz / 7 = 1.43 kHz). The fault distance has an influence on the transient, and therefore also on the

5.3. Test results for the impact of sampling frequency on transient-based earth fault location

accuracy of the estimation of the distance to the fault. Therefore, each network set-up was divided into three parts, with different distances to the fault location. The mean errors of the calculations with different sampling arrangements and fault distances are presented in Figures 5.23 to 5.25.

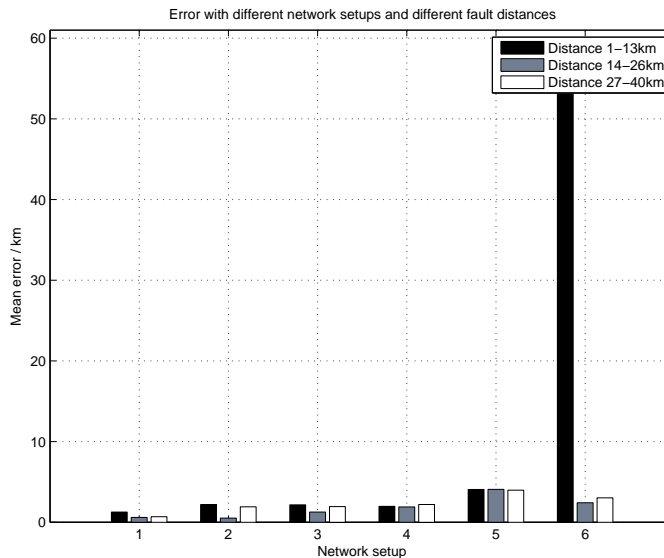


Figure 5.23: Mean errors with different sampling set-ups and fault distances, $f_s = 20$ kHz.

With a sampling frequency of 20 kHz, the differences between the different cases are not major when the fault resistance is 10Ω (Cases 1-3 in Figure 5.23). All three sampling frequency set-ups have a fault location error below 10% of the feeder length. When the fault resistance increases to 80Ω , the deficiencies of the lower sampling frequencies become more apparent (Cases 4-6 in Figure 5.23). With one single low sampling frequency measurement (Case 6 in Figure 5.23), the average error in fault location with fault distances from 1-13 km is nearly 150% of the feeder length. The other two cases still fulfill the 10% error requirement for the fault location, so fault location estimation within 10% error limits was achieved with IEDs operating with less than 3 KHz sampling frequency, when they were synchronized according to the concept presented in Chapter 3.

When the overall sampling frequency decreases, the performance of the measurement method proposed in Chapter 3 becomes more apparent. With an overall sam-

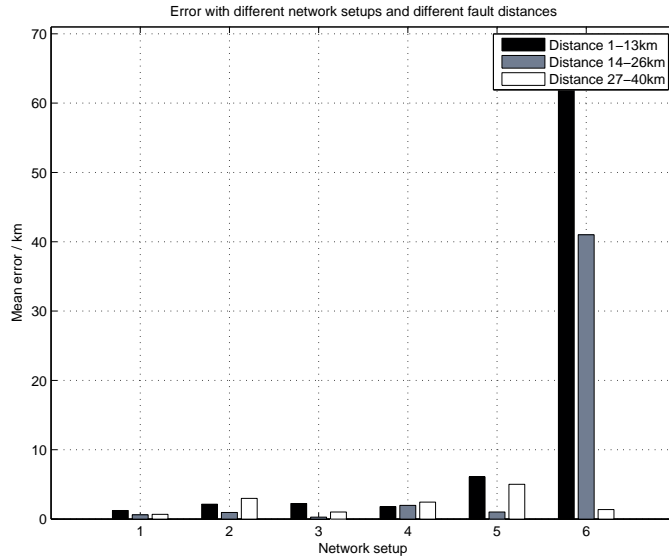


Figure 5.24: Mean errors with different sampling set-ups and fault distances, $f_s = 16$ kHz.

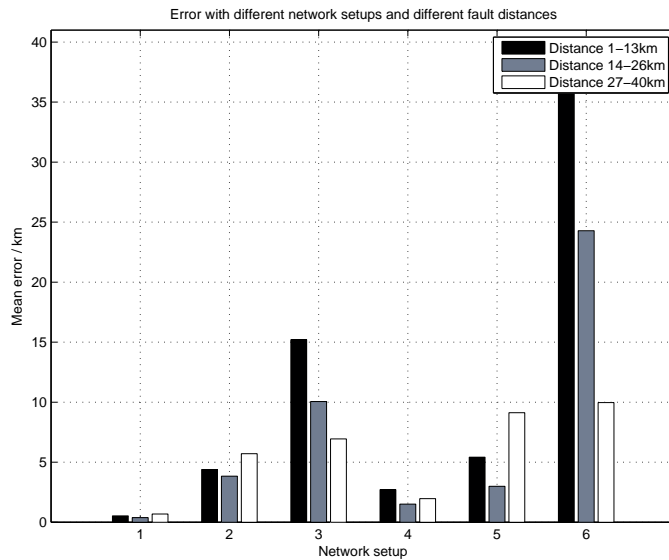


Figure 5.25: Mean errors with different sampling set-ups and fault distances, $f_s = 10$ kHz.

pling frequency of 16 kHz, fault distances can no longer be calculated without merging the measurements from different bays (see Figure 5.24). Case 6, with one single lower sampling frequency measurement introduces errors of over 100% in fault location estimation. The measurement merging method does not fulfill the 10% criteria either, as when the fault distance is below 14 km, the error is around 15%.

The simulation data shows that the measurement method presented in Chapter 3 also makes it possible to use transient-based methods when the sampling frequency of one IED is below 3 KHz, remembering that the sampling frequency limit earlier proposed was 10 kHz [Hänninen and Lehtonen, 2002a] [Abdel-Fattah and Lehtonen, 2009]. This was apparent from the voltage measurement, as the TI-ADC set-up from ADC design principles can be directly applied. However, it also brings benefits to the current measurements, which are clearly visible in this fault distance calculation algorithm, dependent on accurate current measurements.

The tests in this thesis were only performed on a simulation model. Unfortunately, the time frame of this thesis did not allow for a pilot implementation of the proposed measurement method to be performed on an IED, and neither was it possible to conduct field tests with the IEDs. Practical field tests always yield less satisfactory results than simulations, which are made with ideal signals. Re-evaluating the simulation results against field test results is a future research topic.

New fault location algorithms requiring even higher sampling frequencies, up to 100 kHz [Ma et al., 2010], have not been tested in this thesis. The research in this thesis was done utilizing the sampling frequency available with present-day IEDs, which is below 10kHz. A possible future research topic would be to test the latest methods (e.g. [Ma et al., 2010]) for increasing the sampling frequency with the set-up presented in Chapter 3, by utilizing, for example, multiple 10 kHz measurements, assuming that such IEDs will become available in the future.

5.4 Chapter summary

The set-up presented in the thesis can be used for transient-based, distance-to-fault calculation during low ohmic faults (below 100 Ω). This method can even be applied to modern protection and control IEDs with sampling frequencies below 3kHz, if they are synchronized according to the TI-ADC methodology.

This chapter also demonstrated the combination of the topics presented in this

thesis, i.e. the new, centralized, station-level data processing, re-allocation of functionality from the bay-level devices and the measurement method for increasing the accuracy of the measurements. After this initial and encouraging example, more research can be carried out with other functions.

Chapter 6

Summary

This thesis focused on the new challenges facing electricity distribution substations. New legislative requirements, changes in the business landscape or simply the more stringent day-to-day needs to improve processes have increased the stress on life-cycle costing. It seems very likely that the functional life cycle of bay-level protection and control IEDs is getting shorter. Even though the physical device itself might have a relatively long life cycle of 15-20 years, future roadmaps presented in various professional publications often have 5-10 year implementation steps. This means that the utilities must pay special attention to the overall architecture of the secondary system of a distribution substation, so that future updates can be carried out in a cost-efficient manner.

The centralized architecture evaluated in this thesis provides a basis for further development of the secondary system. It combines the bay-level devices with a target life-span of 15-20 years with a station-level computer with 2-year upgrade interval. The proposed architecture allows the primary functionality in the bay-level devices to remain unchanged, while enabling updates to be made to the station computer. The calculations show that the larger the substation, the more likely it is that the architecture presented here will be the most cost-efficient solution.

This centralized architecture can be implemented by utilizing the existing power utility standards. IEC 61850 provides the means for modeling the environment, and also for handling the communication. The process bus IEC 61850-9-2 allows all the station measurements to be available locally, and the latencies are short enough even for protection functionality, as long as the time synchronization is properly handled, with, for example, IEEE 1588. The recent additions to IEC 61850 with regard to the

engineering processes also support the centralized architecture.

The introduction of a station-level protection and control device also calls for a rethink of the functionality in the substation. As the architecture allows having both fixed, invariant functions, and flexible, adaptive functions, the functions required in the substation need to be reallocated. The functionality classification method proposed in this thesis takes a new view of a substation's functionality and provides the means for utilizing the new architecture in an optimal way.

In addition to re-allocating the old functionality, the new architecture also enables the utilization of totally new methods and functions. One such method, related to the measurement chain in a substation, is presented and tested here. When the measurements of the substation are synchronized in the way proposed here, the total sampling frequency of the station-level measurements can be increased.

All these aspects were tested on the platform of a transient-based earth fault location algorithm. Earlier studies had shown that transient-based methods are not feasible in bay-level IEDs, because the sampling frequency was too low. When the new measurement method was applied at the station level, the simulation results showed that transient-based methods are feasible, without the need to increase sampling frequency at the IED level. The architecture is also tested out in one practical, real-life pilot project.

6.1 Contribution of the thesis

The main contributions of the thesis can be divided into two categories - top/concept-level contributions and feature/application-specific contributions.

The concept-level contributions of the thesis are:

- New architectures for the secondary system of a distribution substation are summarized and evaluated. The most critical elements affecting the overall life-cycle costs are identified. A method is proposed for determining the optimal architecture for the automation of a substation, depending on its size. According to the results of this study, a substation with more than 5 feeders should utilize the centralized architecture proposed in this thesis.
- A method is provided for dividing the functionality of a substation, utilizing both substation-level and bay-level devices. Based on this method, the functional scope of both levels is presented, indicating which functions should be

implemented at the station level, and which at the bay level. The method is applied to a set of functions commonly used in a Finnish distribution substation.

The feature and application-level contributions of the thesis are:

- A new way of handling substation-wide measurements is provided, which can be used to increase the sampling frequency of the measurement chain without increasing the sampling frequency of the individual IEDs. The proposed method can be implemented with existing technology, and with the existing time synchronization method of IEEE 1588. A patent application has also been submitted for the principle [Valtari, 2012]. The patent has been allowed and is about to be granted.
- A transient-based earth fault location algorithm has been enhanced, utilizing the proposed measurement method. With this enhanced measurement method it was possible to achieve 10 % fault location accuracy with multiple IED measurements with 3 kHz sampling frequency, which compares well with the 10 kHz required in previous research.

6.2 Evaluation of the thesis

The strength of this thesis lies in the way it addresses many different aspects of the centralized architecture. As well as evaluating the top/concept-level issues, it also gives detailed specifications for issues such as measurement methods and individual functions. The measurement method, for which a patent application has been submitted, gives a clear indication of how the new architecture creates an innovative environment for new ideas on many levels. Furthermore, the way the measurement method was directly applied to a practical fault location algorithm adds value to the results.

The deficiencies in the thesis are in the evaluation of the financial impact of individual functions. The available statistics were not detailed enough to carry out an accurate financial analysis. Chapter 2 showed that the value of the increased reliability is more important than other elements in the life-cycle cost, but there were no statistics available for evaluating the financial benefit of a particular function. For this reason, the results from both Chapters 2 and 4 are more important in terms of the methods used to derive the results, rather than the actual values themselves.

6.3 Future research

The research into substation-level centralized functionality will continue after the submission of this thesis, particularly at the application level. The thesis proved that the architecture is cost-efficient and provides an environment which allows updates on a 2-year cycle while keeping the life-cycle costs below those of a set-up consisting of only bay-level IEDs. Future research will now focus on the applications allocated to the station level, as discussed in Chapter 4. During 2011 a laboratory environment was set up in cooperation with Tampere University of Technology, including an RTDS[®] realtime simulation environment modeling the network and sending all the data via IEC 61850 station and process buses. The first applications to be researched in this laboratory environment are algorithms for detecting high-impedance earth faults and double earth faults. In fact, the first results of tests conducted on high-impedance earth fault detection have already been published [Nikander et al., 2012]. The next target is also to conduct field tests with pilot installations, in order to confirm the results from both [Nikander et al., 2012] and from Chapters 3 and 5 of this thesis.

References

- ABB Ltd. *Teknisiä tietoja ja taulukoita*. ABB Ltd., 2000. in Finnish.
- ABB Ltd. *Relion Protection and Control 615 series Technical Manual*, 2.0 edition, 2009.
- ABB Ltd. *Relion Protection and Control 615 series Technical Manual*, 3.0 edition, 2010.
- M.F. Abdel-Fattah and M. Lehtonen. A Novel Transient Current-Based Differential Algorithm for Earth Fault Detection in Medium Voltage Distribution Networks. In *International Conference on Power Systems Transients (IPST)*, 2009.
- G.G. Angel. Maintenance Strategies for M.V. and H.V. Substations. In *The 17th International Conference and Exhibition on Electricity Distribution (CIRED)*, 2003.
- A. Apostolov and B. Vandiver. IEC 61850 GOOSE applications to distribution protection schemes . In *64th Annual Conference for Protective Relay Engineers*, 2011.
- A. Apostolov, D. Tholomier, and A. Edwards. Advanced Load-Shedding Functions in Distribution Protection Relays. In *The 19th International Conference and Exhibition on Electricity Distribution (CIRED)*, 2007.
- M. Aro. Pas-johtoon syntyneen vian ilmaiseminen sähköasemalla. Technical report, Helsinki University of Technology, Espoo, Finland, 1993. in Finnish.
- F. Baldinger, T. Jansen, M. van Riet, F. Volberda, F. van Erp, M. Dorgelo, and W. van Buijtenen. Advanced secondary technology to evoke the power of simplicity. In *The 9th International Conference on Developments in Power System Protection (DPSP)*, 2008.

- W.C. Black and D.A. Hodges. Time-interleaved Converter Arrays. *IEEE Journal of Solid-State Circuits*, SC-15(6):1022–1029, 1980.
- J. Castallenos. Engineering guidelines for IEC61850 based substation automation systems. In *Cigre Working Group B5.12*, 2009.
- G. Eberl, S. Hänninen, M. Lehtonen, and P. Schegner. Comparison of Artificial Neural Networks and Conventional Algorithms in Ground Fault Distance Computation. In *IEEE PES Winter Meeting, The Institute of Electrical and Electronics Engineers Power Engineering Society Winter Meeting, Singapore*, volume 3, pages 1991–1996, 2000.
- EC. *Communication from the Commission to the European Parliament, the Council, the European Economic and Social Committee and the Committee of the Regions - 20 20 by 2020 - Europe's climate change opportunity*. European Commission, 2008a.
- EC. *Communication from the Commission to the European Parliament, the Council, the European Economic and Social Committee and the Committee of the Regions - Energy 2020, A strategy for competitive, sustainable and secure energy*. European Commission, 2008b.
- J. Elovaara and Y. Laiho. *Sähkölaitostekniikan perusteet*. Otatiето Oy, Helsinki, Finland, 2004. in Finnish.
- EMV. *Electricity Market Act - Sähkömarkkinalaki - 386/1995*. Energy Market Authority, Finland, 1995. in Finnish.
- EMV. *Sähkön jakeluverkkotoiminnan ja suurjännitteisen jakeluverkkotoiminnan hinnoittelun kohtuullisuuden valvontamenetelmien suuntaviivat vuosille 2012-2015*. Energy Market Authority, Finland, 2011. in Finnish.
- Energiäteollisuus. *Keskeytystilasto 2005-2010 (Outage statistics 2005-2010)*. Finnish Energy Industries, Energiäteollisuus ry, Helsinki, 2005-2010. in Finnish.
- P. Ferrari, A. Flammini, S. Rinaldi, and G. Prytz. Time Synchronization Concerns in Substation Automation System. In *IEEE International Workshop on Applied Measurements for Power Systems (AMPS)*, 2011.

- Fortum. Fortum ulkoistaa sähköverkkopalvelunsa Eltel Networksille ja Empowerille Suomessa, October 2010. URL <http://www.tekniikkatalous.fi/energia/fortum+ulkoistaa+sahkoverkkopalvelunsa+suomessa/a514251>. in Finnish.
- F. Gorgette, O. Devaux, and J-L. Fraisse. Possible Roadmaps for New Requirements for French Distribution Control and Automation. In *The 19th International Conference and Exhibition on Electricity Distribution (CIRED)*, 2007.
- L. L. Grigsby. *The Electric Power Engineering Handbook*. CRC Press, 2000.
- GSMA. *European Mobile Industry Observatory 2011*. The GSM Association, 2012.
- S. Hänninen. *Single phase earth faults in high impedance grounded networks - Characteristics, indication and location*. PhD thesis, Helsinki University of Technology, Finland, 2001.
- S. Hänninen and M. Lehtonen. Characteristics of Earth Faults in Electrical Distribution Networks with High Impedance Earthing. *Electric Power Systems Research*, 44(3):155–161, 1998.
- S. Hänninen and M. Lehtonen. Earth Fault Distance Computation with Fundamental Frequency Signals Based on Measurements in Substation Supply Bay. Technical report, VTT Technical Research Centre of Finland, VTT research notes 2153, 2002a.
- S. Hänninen and M. Lehtonen. Maasulkujen etäisyyden laskenta syöttökennomittauksista. Technical report, VTT Technical Research Centre of Finland, TESLA Report 57/2002, 2002b. in Finnish.
- S. Hänninen, M. Lehtonen, T. Hakola, and R. Rantanen. Comparison of Wavelet and Differential Equation Algorithms in Earth Fault Distance Computation. In *13th Power Systems Computations Conference, Trondheim, Norway*, volume 2, pages 801–807, 1999.
- J. Heckel. Smart Substation and Feeder Automation for a Smart Distribution Grid. In *The 20th International Conference and Exhibition on Electricity Distribution (CIRED)*, 2009.

- M. Hinow, M. Waldron, L. Müller, and K. Pohlink H. Aeschbach and. Substation Life Cycle Cost Management Supported by Stochastic Optimization Algorithm. In *42nd General Session of CIGRE (International Council on Large Electric Systems)*, 2008.
- IEA. *World Energy Outlook*. International Energy Agency, 2009. Available at: <http://www.worldenergyoutlook.org/>.
- IEC. *International Electrotechnical Vocabulary, IEC Standard IEC 60050- 605-01-01*. The International Electrotechnical Commission, 1983.
- IEC. *Dependability Management. Part 3 Application guide - Section 3: Life Cycle Costing, IEC Standard 60300-3-6*. The International Electrotechnical Commission, 1997.
- IEC. *Standard for Communication Networks and Systems in Substations, IEC Standard 61850*. The International Electrotechnical Commission, 2005.
- IEC. *Standard for Communication Networks and Systems for Power Utility Automation, IEC Standard 61850-6 Edition 2*. The International Electrotechnical Commission, 2009.
- IEEE. *IEEE Guide for Safety in AC Substation Grounding, IEEE Standard 80-2000*. IEEE Power Engineering Society, 2000.
- IEEE. *IEEE Guide for Determining Fault Location on AC Transmission and Distribution Lines, IEEE Standard C37.114-2004*. IEEE Power Engineering Society, 2004.
- IEEE. *IEEE Standard Electrical Power System Device Function Numbers, Acronyms and Contact Designations C37.2-2008*. IEEE Power Engineering Society, 2008.
- IEEE. *Standard for a Precision Clock Synchronization Protocol for Networked Measurement and Control Systems, IEEE Standard 1588*. The Institute of Electrical and Electronics Engineers, 2009.
- IPCC. *IPCC Special Report on Renewable Energy Sources and Climate Change Mitigation*. Cambridge University Press, Cambridge, United Kingdom and New York, NY, USA, 2011.

- I. Jeromin, J. Backes, G. Balzer, and R. Huber. Life Cycle Cost Analysis of Transmission and Distribution Systems. In *The 20th International Conference and Exhibition on Electricity Distribution (CIRED)*, 2009.
- A. Johnson, J.E. Söderström, P. Norberg, and A. Fogelberg. Standard Platform for integrated soft protection and control. In *IEEE PES Conference on Innovative Smart Grid Technologies (ISGT 2010)*, 2010.
- K. Kauhaniemi, S. Voima, and H. Laaksonen. Adaptive Relay Protection Concept for Smart Grids. In *17th Power Systems Computation Conference (PSCC)*, 2011.
- E. Kettunen. Sähköasematietokoneen konfigurointi. Master's thesis, Tampere University of Technology, 2011. in Finnish.
- G.H. Kjølle, J. Heggset, B.T. Hjartsjø, and H. Engen. Protection System Faults 1999-2003 and the influence on the Reliability of Supply. In *Power Tech, IEEE Russia*, 2005.
- G.J. Klir and B. Yuan. *Fuzzy Sets and Fuzzy Logic: Theory and Applications*. Prentice Hall, 1995.
- P. Koponen. *Sparse Sampling Methods for Power Quality Monitoring*. PhD thesis, Tampere University of Technology, 2002.
- J. Laine. Sähköjaketuiverkon komponenttien pitoajat. Master's thesis, Lappeenranta University of Technology, 2005. in Finnish.
- E. Lakervi and E.J. Holmes. *Electricity Distribution Network Design*. The Institution of Engineering and Technology, 1996.
- E. Lakervi and J. Partanen. *Sähköjaketuteknikka*. Otatieto, Yliopistokustannus, 2008. in Finnish.
- J. Lassila, S. Viljanen, and J. Partanen. Investoinnit sähkön siirron hinnoittelussa. Technical report, Lappeenranta University of Technology, 2002. in Finnish.
- M. Lehtonen. *Transient Analysis for Ground Fault Distance Estimation in Electrical Distribution Networks*. VTT Technical Research Centre of Finland, VTT Publications 115, 1992.

- M. Lehtonen and T. Hakola. *Neutral Earthing and Power System Protection. Earthing Solutions and Protective Relaying in Medium Voltage Distribution Networks*. ABB Transmit Oy, Vaasa, Finland, 1996.
- B. Lundqvist. 100 Years of Relay Protection, the Swedish ABB Relay History. Technical report, ABB Automation Products, Sweden, 2010.
- S. Ma, B. Xu, G. Houlei, B. Zhiqian, and A. Kiimek. An improved differential equation method for earth fault location in non-effectively earthed system. In *The 10th International Conference on Developments in Power System Protection (DPSP)*, 2010.
- P. Manner, K. Koivuranta, A. Kostiainen, and G. Wiklund. Towards Self-Healing Power Distribution by Means of the Zone Concept. In *The 21st International Conference and Exhibition on Electricity Distribution (CIRED)*, 2011.
- M. Matikainen. Energiemarkkinaviraston Ajankohtaispäivät 2010, March 2011. URL http://www.energiemarkkinavirasto.fi/files/Matikainen_Mika_201003.pdf. in Finnish.
- F. Mekic, Z. Wang, V. Donde, F. Yang, and J. Stoupiš. Distributed Automation for Back-Feed Network Power Restoration. In *The 20th International Conference and Exhibition on Electricity Distribution (CIRED)*, 2009.
- S. Miyamoto, H. Ichihashi, and K. Honda. *Algorithms for Fuzzy Clustering: Methods in c-Means Clustering with Applications (Studies in Fuzziness and Soft Computing)*. Springer, 2008.
- J. Mörsky. *Relesuojaustekniikka*. Otatieto Oy, Helsinki, Finland, 1993. in Finnish.
- B. Nartman, T. BrandStetter, and K. Knorr. Cyber Security for Energy Automation Systems – New Challenges for Vendors. In *The 20th International Conference and Exhibition on Electricity Distribution (CIRED)*, 2009.
- A. Nikander. *Novel Methods for Earth Fault Management in Isolated or Compensated Medium Voltage Electricity Distribution Networks*. PhD thesis, Tampere University of Technology, 2002.
- A. Nikander, O. Raipala, J. Valtari, and E. Kettunen. Verifying The Method for Indication of High-Resistance Earth Faults in Developed RTDS Test Environment.

- In *The 10th Nordic Electricity Distribution and Asset Management Conference (NORDAC)*, 2012.
- J. O'Brien and A. Deronja. Use of Synchrophasor Measurements in Protective Relaying Applications. Technical report, IEEE Power System Relaying Committee Working Group C-14 Report, 2012.
- OSF. Consumer price index - appendix table 5. 2005=100, January 2011. URL http://www.stat.fi/til/khi/index_en.html.
- A. Oudalov, D. Ishchenko, J. Stoupis, and R. Cai. Re-Coordination of Protection Devices in Microgrids. In *The Electric Power System of the Future - CIGRE 2011 Bologna Symposium*, 2011.
- T. Pahkala, M. Hänninen, M. Matikainen, and L. Simola. Sähköverkkokomponenttien yksikköhintojen määrittäminen. Technical report, Empower, Energiamarkkinavirasto, 2010. in Finnish.
- J. Partanen, J. Lassila, T. Kaipia, M. Matikainen, P. Järventausta, P. Verho, A. Mäkinen, K. Kivikko, J. Pylvänäinen, and V-P Nurmi. Sähköjakaajaverkkoon soveltuvat toimitusvarmuuskriteerit ja niiden raja-arvojen sekä sähköjakaajaverkon toimitusvarmuudelle asetettavien toiminnallisten tavoitteiden kustannusvaikutukset. Technical report, Lappeenranta University of Technology, 2006. in Finnish.
- A.G. Phadke and J.S. Thorp. *Computer Relaying for Power Systems*. Research Studies Press Ltd, England, 1990.
- K.S. Rasmunssen. A Real Case of Self Healing Distribution Network. In *The 20th International Conference and Exhibition on Electricity Distribution (CIRED)*, 2009.
- O. Rintamäki and K. Kauhaniemi. Applying Modern Communication Technology to Loss-of-Mains Protection. In *The 20th International Conference and Exhibition on Electricity Distribution (CIRED)*, 2009.
- M.M. Saha, F. Provoost, and E. Rosolowski. Fault Location Method for MV Cable Network. In *The 7th International Conference on Developments in Power System Protection (DPSP)*, pages 323–326, 2001.
- P. Schegner. *Digitaler Erdschlussuniversalschutz. Konzept und erste Realisierung*. PhD thesis, Universität des Saarlandes, Germany, 1989. in German.

- M. Soudan and R. Farrell. Impact of Time-interleaved Analog-to-Digital Converter Mismatch on Digital Receivers. In *IEEE International Conference on Electronics, Circuits and Systems*, 2008.
- J. Starck, A. Hakala-Ranta, and M. Stefanka. Switchgear optimization Using IEC 61850-9-2 and Non-conventional Measurements. In *PAC World Conference*, 2012.
- J. Tengdin. High impedance fault detection technology. Technical report, IEEE Power System Relaying Committee Working Group D15, 1996. <http://www.pes-psrc.org/>.
- V. Terzija, G. Valverde, D. Cai, P. Regulski, V. Madani, J. Fitch, S. Skok, M. Begovic, and A. Phadke. Wide Area Monitoring, Protection and Control of Future Electric Power Networks. *Proceedings of the IEEE*, 99(1):80–93, 2011.
- Texas Instruments Inc. *Application Note 1728 IEEE 1588 Precision Time Protocol Time, Synchronization Performance*, 2007.
- J. Valtari. Development of Earth Fault Location Algorithm in Medium Voltage Network Protection Terminal. Master’s thesis, Tampere University of Technology, 2004.
- J. Valtari. *Method and System for Measuring Electrical Quantity in Electrical Network*. Patent Application WO2012110418 (A1), 2012.
- J. Valtari and P. Verho. Efficient Secondary System Configuration Process Utilizing Centralized Substation Functions. In *PAC World Conference*, 2011a.
- J. Valtari and P. Verho. Requirements and Proposed Solutions for Future Smart Distribution Substations. *Journal of Energy and Power Engineering (JEPE)*, 5(8): 766–775, 2011b.
- J. Valtari and P. Verho. Method to Increase Sampling Frequency by Merging Multiple Measurements . In *IEEE International Workshop on Applied Measurements for Power Systems (AMPS)*, 2012.
- J. Valtari, P. Verho, A. Hakala-Ranta, and J.Saarinen. Increasing Cost-Efficiency of Substation Automation Systems by Centralised Protection Functions. In *The 20th International Conference and Exhibition on Electricity Distribution (CIRED)*, 2009a.

- J. Valtari, P. Verho, A. Hakala-Ranta, and J. Saarinen. Increasing Cost-Efficiency of Substation Automation Systems by Centralised Protection Functions. *Indian Journal of Power and River Valley Development*, 1(1):1–4, 2009b.
- J. Valtari, T. Hakola, and P. Verho. Station Level Functionality in Future Smart Substations. In *The 9th Nordic Electricity Distribution and Asset Management Conference (NORDAC)*, 2010.
- M.J.M. van Riet, F.L. Baldinger, and W.M. van Buijtenen. Alternative Approach for a Total Integrated Secondary Installation in MV Substations Covering All Possible and Required Functions. In *The 18th International Conference and Exhibition on Electricity Distribution (CIRED)*, 2005.
- ViolaSystems. Case Vattenfall: Automating the Distribution Network, October 2011. URL <http://www.violasystems.com/sites/default/files/Vattenfall%20case.pdf>. in Finnish.
- C. Vogel. The Impact of Combined Channel Mismatch Effects in Time-Interleaved ADCs. *IEEE Transactions on Instrumentation and Measurement*, 54(1):415–427, 2005.
- F. Volberda, M. van Riet, and A. Pikkert. The Power of Simplicity. In *The 19th International Conference and Exhibition on Electricity Distribution (CIRED)*, 2007.
- A. Wahlroos and J. Altonen. Advancements in Earth Fault Location in Compensated MV Networks. In *The 21st International Conference and Exhibition on Electricity Distribution (CIRED)*, 2011.

Tampereen teknillinen yliopisto
PL 527
33101 Tampere

Tampere University of Technology
P.O.B. 527
FI-33101 Tampere, Finland

ISBN 978-952-15-3044-9
ISSN 1459-2045